Modelling the light competition between crops and weeds

Vom Fachbereich Gartenbau

der Universität Hannover

zur Erlangung des akademischen Grades eines

Doktors der Gartenbauwissenschaften

- Dr. rer. hort. -

genehmigte

Dissertation

von

Dipl.-Ing. agr. Manfred Röhrig

geboren am 01.09.1966 in Wiesbaden

1999

Referent: Prof. Dr. H. Stützel

Korreferent: Prof. Dr. P. C. Struik

Tag der Promotion: 10. Mai 1999

Kurzfassung

Manfred Röhrig: Modelling the light competition between crops and weeds
Keywords: Lichtkonkurrenz, Simulationsmodell, Blumenkohl, *Chenopodium album*

Der gezielte Einsatz von Unkrautregulierungsmaßnahmen erfordert eine möglichst genaue Abschätzung der zu erwartenden Schadwirkung. Bislang stehen hierfür nur sehr grobe, die spezifische Produktionssituation nicht berücksichtigende Methoden zur Verfügung. Ziel der vorliegenden Arbeit war die Untersuchung der Lichtkonkurrenz zwischen Unkräutern und Kulturpflanzen sowie die Quantifizierung der zugrundeliegenden Beziehungen. Darauf aufbauend sollte ein mechanistisches Simulationsmodell entwickelt werden.

In Feldversuchen wurden die Auswirkungen der Lichtkonkurrenz durch *Chenopodium album* L. auf die Kulturarten Blumenkohl (*Brassica oleracea* L. convar. *botrytis* var. *botrytis* L.) und Fababohne (*Vicia faba* L.) untersucht. Die Pflanzdichte von *C. album* variierte hierbei in zwei Stufen, die sowohl in Rein- als auch in Mischbeständen angelegt wurden. Für alle Arten wurde die Gesamttrockenmasse und deren Verteilung auf die einzelnen Pflanzenorgane sowie Höhe und Durchmesser der Gesamtpflanze gemessen. Die Systemanalyse der ermittelten Daten konzentrierte sich auf folgende Fragestellungen:

Vorhandene Modellierungsansätze zur **Lichtaufnahme in inhomogenen Pflanzenbeständen** sind entweder beschränkt auf spezielle Bestandesarchitekturen oder lassen sich aufgrund komplexer Berechnungen nur schwer ändern. Daher sollte ein dreidimensionales Modell entwickelt werden, das die Lichtaufnahme in heterogenen Bestandesstrukturen mit vergleichsweise einfachen Formulierungen beschreibt. Im Modell wird der gesamte Bestandesraum in würfelförmige Einheiten unterteilt, die entweder leer oder mit Blattfläche gefüllt sind. Die Blattfläche kann in einem frei wählbaren geometrischen Körper verteilt werden, der sich an einer beliebigen Position im Modellraum befindet. Die Lichttransmission wird berechnet, indem der Weg einzelner Lichtstrahlen von der Oberfläche des Bestandes bis zum Boden reproduziert wird. Die tägliche Lichtaufnahme wird für direkte und diffuse Strahlung getrennt geschätzt. Mit nur wenigen leicht meßbaren Parametern war das Modell in der Lage, die gemessene Transmission eines Blumenkohlbestandes mit hoher Genauigkeit zu abzubilden. Es soll daher zur Identifikation von Vereinfachungsmöglichkeiten bei der Quantifizierung der Lichtaufnahme in heterogenen Beständen dienen.

Die für die Lichtkonkurrenz entscheidenden Eigenschaften einer Pflanzenart sind die Wuchshöhe und die Verteilung der Blattfläche im Bestand. Schattenmeidende Unkrautarten wie *C.*

album sind in der Lage, ihren Habitus in Abhängigkeit von der Lichtqualität anzupassen. Daher wurde ein einfaches Modell zur **Bestandesentwicklung von *C. album* in Rein- und Mischbeständen** entwickelt. Die morphologische Anpassung wird durch die Änderung des Hellrot:Dunkelrot Verhältnisses im Bestand initiiert. Es wurde angenommen, daß die Blattfläche an den noch wachsenden Internodien diese Verschiebung verursacht. Aus den Daten wurde ein Schätzwert für diese ‚effektive' Blattfläche abgeleitet und in Beziehung zur Sproßstreckungsrate gesetzt. Dies ergab eine gute Beschreibung des potentiellen Höhenwachstums, das jedoch von *C. album* Pflanzen in einem geschlossenen Fababohnenbestand nicht erreicht wurde. Mit dem Konzept der ‚maximalen spezifischen Stengellänge' wurde eine Rückkopplung der Assimilatversorgung mit dem Höhenwachstum erreicht. Eine hinreichend genaue Simulation des Pflanzendurchmessers wurde durch eine Funktion von Temperatursumme und Pflanzdichte erreicht. Zusammen mit einer von den Konkurrenzbedingungen unbeeinflußten vertikalen Blattflächenverteilung ist es damit möglich, die räumliche Anordnung der Blattfläche von *C. album* zu jedem Zeitpunkt zu prognostizieren.

Über die **Stoffproduktion und -verteilung von *C. album*** ist bislang nur wenig bekannt. Diese Prozesse wurden daher vor allem auf den Einfluß der Lichtkonkurrenz untersucht. Zunächst wurde eine enge Beziehung zwischen der Transmission der photosynthetisch aktiven Strahlung (PAR) und dem Blattflächenindex gefunden. Die Gesamttrockenmasse war linear korreliert mit der kumulativ aufgenommenen PAR, die Ursachen einer jahreszeitlichen Variation der Lichtnutzungseffizienz konnten jedoch nicht vollends geklärt werden. Das Wurzel:Sproß Verhältnis blieb durch die Konkurrenz unbeeinflußt, die Verteilung zwischen Blättern und Stengel wurde jedoch durch Pflanzdichte und Bestandeszusammensetzung leicht verändert. Es konnte gezeigt werden, daß einfache allometrische Beziehungen zur Beschreibung der Stoffverteilung unter den Bedingungen des Feldgemüsebaus eingesetzt werden können.

Die gefundenen Beziehungen wurden zusammen mit Annahmen über unbekannte Größen und Prozesse in ein **Simulationsmodell** integriert. Bei der Kalibration des Modells traten Widersprüche in der Beschreibung des Wachstums von *C. album* auf. Des weiteren reagierte das Modell sensitiv auf eine ungenaue Schätzung der Blattflächenentwicklung. Mit dem gemessenen Blattflächenindex von *C. album* als Eingabegröße stimmten simulierte und beobachtete Ertragsverluste bei Blumenkohl gut überein. Eine erste Evaluation des Modells mit einem unabhängigen Datensatz ergab ebenfalls eine zufriedenstellende Beschreibung. Trotz der genannten Einschränkungen ermöglicht das Modell einen Einblick in die der Lichtkonkurrenz zugrundeliegenden Beziehungen.

Abstract

Manfred Röhrig: Modelling the light competition between crops and weeds
Keywords: light competition, simulation model, cauliflower, *Chenopodium album*

Weed management in plant production is based on a prediction of the impact of weeds on crop yield. Hitherto, only crude methods are available that neglect the influence of the specific production situation. The objective of this study was to analyse the competition for light between crops and weeds to quantify the underlying relationships and to develop a mechanistic simulation model.

In field trials, the effects of interspecific light competition were examined using *Chenopodium album* L. planted at two densities in pure and mixed stands with either faba bean (*Vicia faba* L.) or cauliflower (*Brassica oleracea* L. convar. *botrytis* var. *botrytis* L.). Data on total plant biomass and its allocation to the various plant organs as well as plant height and diameter were obtained for all species. The system analysis of the observational data focussed on the following topics:

Numerous approaches exist to calculate the **light interception in heterogeneous canopies**, but these are either limited to specific leaf area distributions or comprise complex and inflexible calculations. A three-dimensional model was developed that gives details on the light absorption in heterogeneous canopy architectures with comparatively simple routines. In the model, the complete canopy volume is divided into cubic subunits, which are either empty or filled with leaf area. Leaf area can be distributed in an arbitrarily chosen geometric solid positioned anywhere in the model domain. Transmission is calculated by following the path of solar rays from the top of the canopy to ground level. Daily canopy absorption is predicted separately for direct and diffuse radiation. With only few readily obtainable parameter, the model was able to accurately predict the canopy transmission measured in a cauliflower crop. It is thus useful as a heuristic tool to identify possible simplifications in the quantification of light interception by heterogeneous crops.

With respect to light, plant height and leaf area distribution are the main determinants of the competitiveness of a plant species. Shade-avoiding weed species such as *C. album* adapt their habit to the competitive environment. A simple model was constructed to estimate the **canopy development of *C. album* in pure and mixed stands**. Assumed to be mainly responsible for

the modulation of plant height, the leaf area around extending internodes was estimated. Relating this 'effective' leaf area to the stem extension rate yielded an accurate prediction of potential plant height growth. Since this potential was not realised under low light conditions in a faba bean canopy, the 'maximum specific stem length' was estimated to obtain a feedback of assimilate shortage on height growth. Plant diameter was sufficiently accurate predicted as a function of thermal time and plant density. As the vertical leaf area distribution did not change, it is concluded that leaf area of *C. album* can be predicted at every point in time and space from a given total leaf area and plant density.

Little information exist on the **dry matter production and partitioning of *C. album***. These processes were therefore systematically analysed, in particular to which extent they are modified by light competition. A close correlation between the transmission of photosynthetically active radiation (PAR) and the leaf area index was found. Biomass production was linearly related to cumulative intercepted PAR, but a seasonal variation of the light-use efficiency could not entirely be explained. The root:shoot ratio was unaffected by competition, whereas planting density and canopy composition slightly changed the distribution pattern between stem and leaves. It could be shown that in field vegetable production with an abundant water and nutrient supply simple allometric relationships for dry matter distribution are adequate.

An integrative **model for light competition** was developed, based on the analytical results and assumptions made for unknown variables and processes. Calibration runs revealed uncertainties predicting the growth of *C. album* and a high sensitivity on the leaf area development. With the LAI of *C. album* as input a good correspondence between simulated and observed yield loss of cauliflower was found. A first evaluation with an independent data set likewise gave an acceptable prediction. Nevertheless, the model proposes to be an effective tool to gain insight into the mechanisms of light competition.

Contents

List of main symbols

Variable	Description	Units
dl	edge length of cubes	m
d_p, w_p	distances and weights of the Gaussian integration algorithm	-
l	fraction of leaf area index	-
l_x, l_y	extent of the model domain in width and length	m
p_c	pathlength correction for paths other than vertical	-
q	relative light intensity, indices see below	-
rgc	relative ground cover	-
r_t	translocation rate	$°C^{-1}$
t	(thermal) time	h, d, °Cd
D	plant diameter	m
DL	daylength	h
F	fraction of radiation averaged over the plot, indices see below	-
H	plant height, internode length	m
I	light intensity, indices see below	$W\ m^{-2}$
J	cumulative intercepted PAR	$MJ\ m^{-2}$
K	light extinction coefficient	-
L	leaf area index, LAI	$m^2\ m^{-2}$
L_d	leaf area density of the canopy	$m^2\ m^{-3}$
LUE	light-use efficiency	$g\ MJ^{-1}$
O_{av}	average projection of leaves	-
PAR	photosynthetically active radiation ('light')	$MJ\ m^{-2}$
PC	phyllochron interval	°Cd
PD	plant density	m^{-2}
SLA	specific leaf area	$m^2\ g^{-1}$
SSL	specific stem length	$m\ g^{-1}$ stem plant^{-1}
T	relative light transmission	-
T_{av}	daily mean temperature	°C
TS	temperature sum	°Cd
$TSER$	potential thermal stem extension rate	$mm\ °C^{-1}$
V	volume of the canopy	m^3
W_x	plant dry weight	$g\ m^{-2}$

for x:

G	generative shoot		Sh	shoot
L	leaf		T	total plant
R	root		V	vegetative shoot
S	stem (including petioles)			

Variable	Description	Units
α, β	solar azimuth angle and solar elevation angle	rad
ε	stepwidth along the path of a solar ray	-
ρ_{sph}	reflection coefficient for a spherical leaf angle distribution	-
σ	scattering coefficient for visible light	-

Index	Description
0	on a horizontal surface above the canopy / cube
a	absorbed
c	related to a cube
f	diffuse radiation
r	direct beam
i	intercepted
s	scattered
t	transmitted

Names and units of auxiliary variables are specified in the text.

1. Introduction

'Science is concerned with prediction' (THORNLEY & JOHNSON, 1990). But the real world is infinitely complex making it impossible to anticipate all cause and effect interactions in their entirety. It is therefore necessary to structure this complexity and define manageable parts of reality. These systems are determined by boundaries, some kind of input and output as well as interacting components. The system behaviour is observed in experiments and the scientific effort is to predict the interrelation of the system elements and thus the system response to external variables.

Based on observational data, every scientist develops a theory of how the system examined is presumed to work. Generally, such concepts do not include all but only the governing processes, resulting in an abstracted view of reality. Since data rarely explain the hypotheses as a whole but frequently raise further questions, more experimentation is needed to bridge knowledge gaps. This traditional way of research tries to explain 'what happens', but if the objective is 'how much happens' (THORNLEY, 1976), the scientist has to put his conceptual scheme in concrete terms by means of mathematical formulations. This can be achieved empirically by relating the system input to its observed output, essentially resulting in a direct description of observational data. An empirical approach is especially useful when summarising larger systems, but it does not have an explanatory value since no insight is given into the processes involved. The description of the system response by quantification of functional relationships between system components is realised in mechanistic approaches. As a general rule, simplifying assumptions have to be made for processes not well understood, but at the same time indicate possible fields for further investigations. Incorporating the system mechanism into a mathematical simulation model may result in a better prediction of the system response and the identification of its determinants. The final touchstone of a model should always be its potential to describe measured data of the real system, indicating the applicability of the implemented relationships. If sufficiently evaluated, such an explanatory model can then be used to extrapolate the simulation results beyond the scope of the underlying experimental data and give information on the system behaviour in other situations.

In plant ecology, various levels of differentiation can be classified according to the system size. Mechanistic models are generally used to explain phenomena found on a higher level by

integrating knowledge of a lower level. Thus, the system response on a canopy scale – as in the present study – may be explained by the properties of individual plants. Due to the infinite number of sublevels (plant organ, tissue, cells, cell components, molecules etc.) the abstraction level used for a simulation model has to be adapted to the intended purpose. Calculation of the behaviour of a plant canopy on the basis of molecular processes, for instance, does not only imply the risk of an addition of inaccuracies, but also unduly increases the research effort to analyse the system. It is thus inevitable to limit the system boundaries of a model by focussing on the main aspects of a problem. This necessarily involves the implementation of summary and simplifying relationships for processes on lower levels of abstraction.

In recent years, the ecological consequences of modern plant production have repeatedly been in the public discussion. Weed management and in particular the chemical weed control was critically perceived and political action was demanded. Consequently, the admission of a number of herbicides was withdrawn and the introduction of new agents was aggravated. An accurate prediction of the impact of weed infestations on crop yield was always the basis of weed management decisions, but this estimation gets vital in the present situation to minimise ecological damages and economical losses. In vegetable production, only crude measures such as 'critical periods' are available, defining the time interval in which a crop has to be kept weed-free to achieve the potential yield (NIETO ET AL., 1968; ROBERTS, 1976). As this concept ignores the specific production situation, it has to be investigated if a dynamic simulation model remedies these deficits to come to a more adequate method for decision support in weed control. The objective of the present study is to analyse the competition for light between crops and weeds, to derive and quantify the functional relationships determining the outcome of these interactions and to develop an integrative simulation model. The observational data come from field trials, where *Chenopodium album* L. was grown with either faba bean (*Vicia faba* L.) or cauliflower (*Brassica oleracea* L. convar. *botrytis* var. *botrytis* L.). The crop-weed system analysed here is evidently only a part of the intricate competitive situation found in the field. But a successful quantification is only feasible, if the effects of competition can be assigned to one cause only. The system is therefore defined by

- the focus on one growth factor,

- a canopy comprising two species and

- a limitation to one crop growth cycle.

The system input are weather data and the target value is the crop yield. Other external variables such as nutrients and water as well as biotic and abiotic factors have an impact on the system. Their effects on crop yield, however, were minimised as far as possible in the field experiments and could thus be excluded from the system under consideration and its analysis.

Crop yield is considered to be a result of dry matter production and distribution (growth, Fig. 1) and the morphological differentiation (development). The amount of radiation energy available for absorption is calculated first according to the actual distribution of leaf area in the canopy. Growth is described as a function of absorbed light and the efficiency to convert
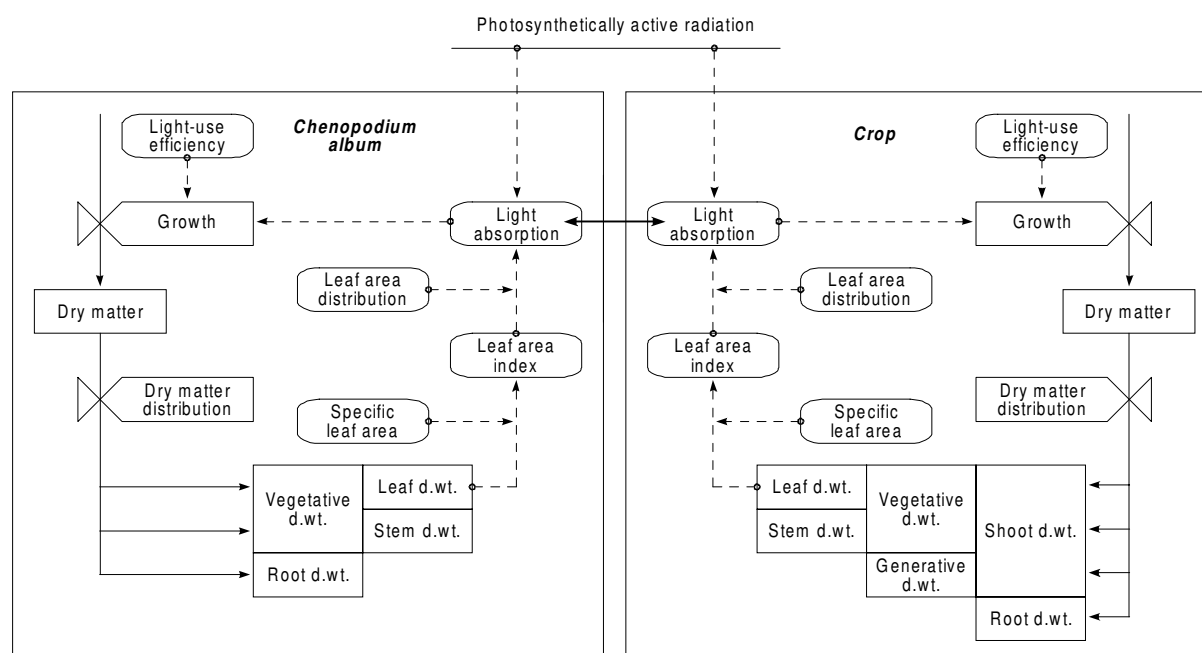

Fig. 1. Schematic diagram of the growth processes in the crop-weed system.

this energy to biomass. The total dry matter increase is allocated to root and shoot. In crops, the above-ground dry matter (including retranslocation) is partitioned into generative and vegetative organs, whereas seed production in *C. album* is neglected. The vegetative shoot dry matter is partitioned into two compartments according to their main function of light interception (leaf) or structural stability (stem, petioles). The leaf area index is calculated from leaf dry matter and is distributed in the canopy dependent on the spatial expansion of the plants. The developmental processes are direct functions of temperature.

Plants competing for light mutually reduce the amount of radiation available for growth. It has been shown in many field and simulation studies hitherto that with respect to light competition the distribution of leaf area in the canopy is of utmost importance (e.g. LAWSON, 1972; FRIESEN, 1979; JOENJE & KROPFF, 1987; KINIRY ET AL., 1992). Thus, special attention was drawn to this fact in the present study because existing light interception models are either not able to cope with a leaf area distribution that is heterogeneous in all dimensions (MONSI & SAEKI, 1953; GIJZEN & GOUDRIAAN, 1989) or comprise inflexible and complicated geometrical calculations (NORMAN & WELLES, 1983). Hence, the light interception of a spatially heterogeneous plant canopy has to be analysed (Chapter 3). Many weed species of arable land are able to react to shading with an increased height growth. Since *C. album* is a characteristic exponent of this plant type, the morphological properties of *C. album* should be quantified dependent on the competitive situation (Chapter 4). This extends approaches proposed hitherto that describe height development as a function of temperature only (SPITTERS & AERTS, 1983; WILES & WILKERSON, 1991). Dry matter production and partitioning of weeds are commonly analysed in lesser detail than those of the competing crop species (KROPFF & SPITTERS, 1992). A closer look into the growth processes of *C. album* is therefore necessary, in particular to which extent they are modified by light competition (Chapter 5). Subsequently, an integrative simulation model is proposed based on the analytical results and assumptions made for unknown variables and processes. The validity of the implied relationships and their interactions is to be assessed by comparing the model output to measured data (Chapter 6). Thereafter, the model will finally be discussed with respect to its assumptions and limitations as well as to suggestions on future developments (Chapter 7).

This present study is intended to be another step towards a realistic description of crop-weed interactions. Progress is made, if it helps to gain more insight into the underlying mechanisms and to indicate 'white spots' in our knowledge of light competition between plant species.

2. Material and Methods

Effects of interspecific light competition between *Chenopodium album* L. and either faba bean (*Vicia faba* L. cv. Scirocco, NPZ, Hohenlieth, Germany) or cauliflower (*Brassica oleracea* L. convar. *botrytis* var. *botrytis* L. cv. Fremont, Royal Sluis, Neustadt, Germany) were examined in field trials in 1994 and 1995. The experiments were conducted on a silty loam soil (80% silt, 10% sand, 10% clay, pH 6.5) at the experimental station in Ruthe (52°15' N, 9°50' E, 73 m a.s.l.) near Hanover, Germany.

2.1. Experiments

Field trials in 1994

To achieve different degrees of competition, the plant density of *C. album* was varied at two levels. Due to the contrasting morphology and competitiveness of cauliflower and faba bean *C. album* densities were selected crop-specifically to obtain similar relative yield effects in both crops. In addition to mixed stands, plots with *C. album* in monoculture were planted at the same densities. The plots were laid out in completely randomised blocks with four replications. Within each plot four subsections were used for successive harvests throughout the growing period (Table 1).

Cultivation. One week after sowing into peat-filled seed pans the germinated cauliflower seedlings were pricked into peat blocks and put into a propagation greenhouse. At least one week prior to planting the transplants were hardened off in a cold frame. In the field the plants were arranged in a rectangular pattern and gaps due to losses were filled with spare plants up to two weeks after planting. Soil samples were taken shortly before (0-30 cm) and four weeks after transplanting (0-60 cm) to analyse the mineral soil nitrogen content (N_{min}) using a 0.1M CaCl for extraction. The N_{min} supply in the field was then replenished with calcium ammonium nitrate to 130 kg N ha^{-1} at the first and to 270 kg N ha^{-1} of mineral soil nitrogen at the second application. The calculation of the latter was based on N_{min} values obtained from mixed stands at high weed density in order to provide for maximum demand. All plots were well watered with rotary sprinklers to avoid water limitations, thus ensuring that the observed effects can be attributed to light competition. *C. album* was sown by hand directly to the field. After a germination test, a quantity of seeds appropriate to obtain target densities was mixed

Table 1. Details of experimental design, crop husbandry and measurements in the 1994 field experiments with C. album *and either cauliflower or faba bean.*

	Cauliflower	Faba bean
Sowing date	18 February	7 April
Planting date	18 April	
Harvest dates	16 May	18 May
	31 May	4 July
	20 June	25 July
	1 July[†]	15 August
Planting pattern (m)	0.5×0.6	0.3×0.08
Plant density (m^{-2})	3.3	40
Plot size (m)	8.4×4.0	7.0×2.0
Plants per harvest	10	20
Chenopodium album		
Sowing date(s)		
early	19 April	15 April
late	-	6 May
Plant density (m^{-2})		
low (target / emerged)	25 / 24	100 / 110
high (target / emerged)	50 / 41	200 / 150
Plants per harvest	5 or 3 (early or late growth stages, respectively)	

[†] no dry matter measurements

with quartz sand and spread out uniformly over the plot. Faba bean was drilled with a precision seed drill and no nitrogen fertilisation or irrigation water was applied. To examine the effects of the time of weed emergence, the faba bean experiment included two *C. album* sowing dates. In all experiments weeds emerging spontaneously were removed by hand; pests and insects were controlled chemically for both crops and weed.

Data collection. At four successive harvests 10 cauliflower, 20 faba bean and 3 to 5 *C. album* plants were taken from the designated subplots. Plants were dug out to a depth of about 20 cm to obtain the major proportion of the main and lateral roots; they were washed and separated from the shoots. Measurements of the shoot length from base to top and its greatest width gave the plant height and diameter, both with an accuracy of *c*. 5 mm. The shoots were divided into stems (including petioles), green leaves, senescent leaves and generative organs (crops only). In cauliflower, the generative organ is defined as the inflorescence without wrapper leaves, referred to as 'curd' in this study. All plant parts were dried for at least 3 days

at 100 °C and weighed. The area of green leaves was measured with a LI-COR 3100 Area Meter (LI-COR Inc., Lincoln, NE, USA).

Field trials in 1995

Since the basic cultivation methods mainly correspond to those of the preceding trials, only the modifications are given (Table 2).

Cultivation. The cauliflower experiments were carried out as a spring and a summer planting with identical layouts, using an isometric planting pattern. Due to a long juvenile phase the onset of competition between crop and *C. album* plants sown directly was notably delayed. To achieve early competition, the *C. album* plants were raised in peat-filled conetrays. Four to five seeds were laid into a cone of *c*. 10 cm^3 and singled after emergence. The seedlings were transplanted to the field at *c*. 200 °Cd after emergence, having about 3 nodes and an average

Table 2. Details of experimental design, crop husbandry and measurements in the 1995 field experiments with C. album *and cauliflower.*

	Experiment 1	Experiment 2
Sowing date	24 February	8 June
Planting date	24 April	18 July
Harvest dates	24 May	9 August
	9 June	23 August
	28 June	13 September
	10 July	9 October
Transmission measurements	31 May	1 August
	15 June	15 August
Planting pattern (m)	0.45 × 0.52	
Plant density (m^{-2})	4.3	
Plot size (m)	7.3 × 2.0	
Plants per harvest	4	
Chenopodium album		
Sowing date	3 April	27 June
Planting date	3 May	20 July
Plant density (m^{-2})		
low (mixed / pure)	12.8 / 17.1	
high (mixed / pure)	38.5 / 42.7	
Plants per harvest	5 or 3 (early or late growth stages, respectively)	

height of 3 cm. The weed densities were achieved by placing one or three *C. album* between two cauliflower plants for low and high density plots, respectively. In pure weed stands the same pattern was used, except that the position of the crop was filled by another weed.

Data collection. The size of the cauliflower plots was reduced, thus only 4 crop plants were taken at four successive harvests. To get more detailed information about the spatial distribution of dry matter and leaf area of *C. album* plants, the shoots were dissected horizontally in 20 cm segments from the base upwards. From each segment stems and green leaves were separated and the number of nodes was recorded.

The leaf area index of cauliflower in weed-free plots was determined with a LI-COR LAI-2000 Canopy Analyzer twice in each experiment. Measurements were made along and across row direction on two transects each, with four measurements per transect as recommended for heterogeneous canopies (WELLES & NORMAN, 1991). Since the plots were only 2 m wide, a 45° view cap was used to block the sensor's field of vision from neighbouring plots. To meet the requirement of diffuse sky conditions, data were taken at early morning hours. If direct radiation was encountered, the part of the plot to be measured was shaded by a large plastic frame. At the same day around noon, light transmission was measured with a line quantum sensor (LI-COR LI-191 SA) below and a point sensor (LI-COR LI-190 SA) above the canopy. Ten measurements were taken per plot to obtain an average value. At the time of these measurements the cauliflower plants had no or only a small inflorescence.

Weather data

The experimental station is equipped with an on-site automatic weather station (Campbell Scientific, UK) that supplies hourly data of air temperature, global incoming radiation and relative humidity. The vapour pressure deficit was calculated according to STÖCKLE & KINIRY (1990) and the daily mean air temperature, T_{av}, is given by

$$T_{av} = \frac{T_{max} - T_{min}}{2} \tag{1}$$

where T_{max} and T_{min} are the maximum and minimum air temperature (°C), respectively. The general weather conditions during the experiments are shown in Fig. 2.
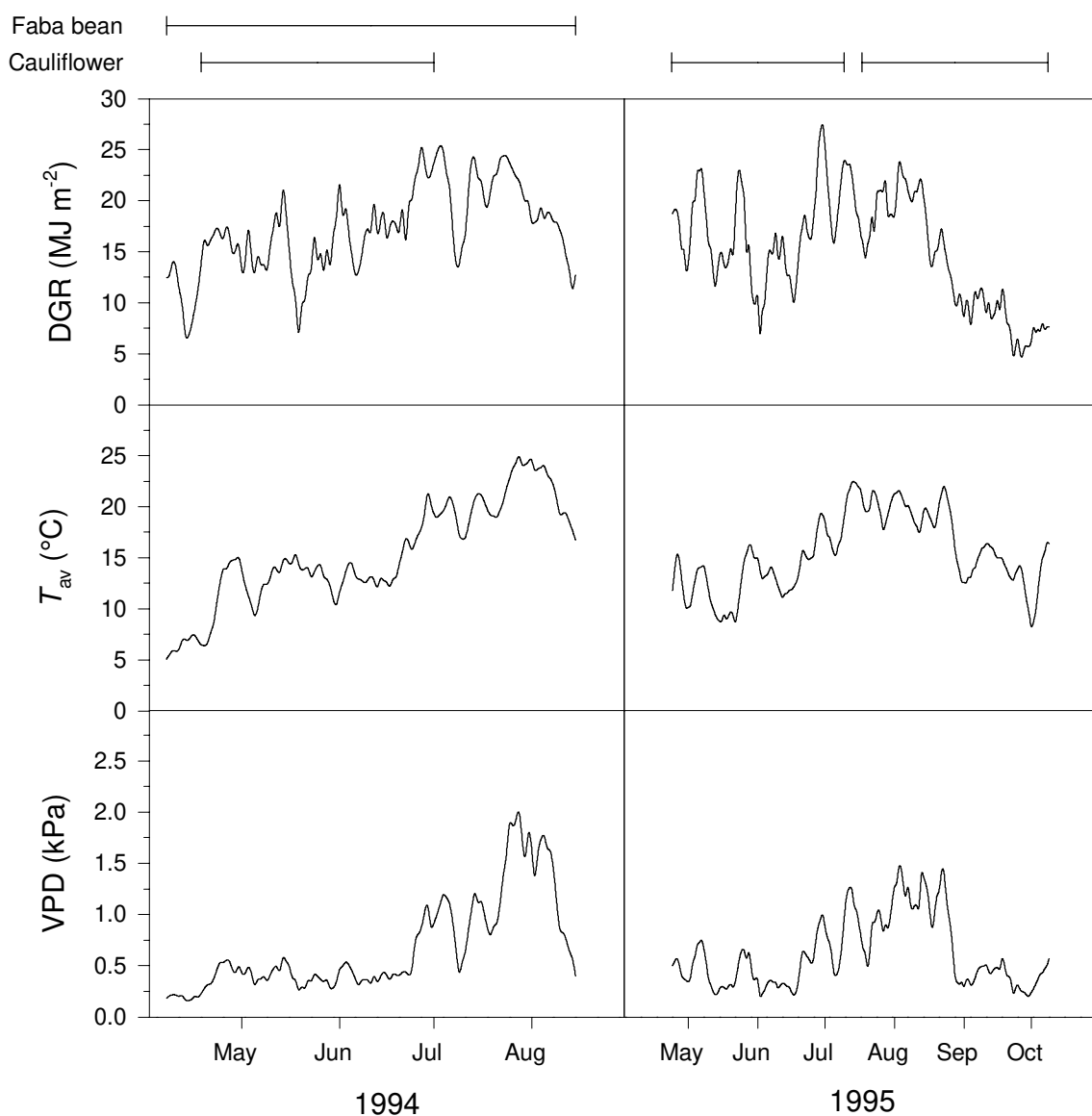
Fig. 2. Global radiation, DGR, mean temperature, T$_{av}$, and vapour pressure deficit, VPD, at the experimental station near Hanover, Germany. Data shown are running averages of five days. In addition, the growing period of faba bean and cauliflower in the experiments is depicted.

2.2. Calculations

Developmental processes are functions of the temperature sum, *TS*, calculated according to

$$TS = \sum \left(T_{av} - T_b \right) \tag{2}$$

where T_b is the base temperature which is assumed to be 0 °C for all species. Calculation of *TS* starts at planting for cauliflower and at the three-node stage for *C. album*. The term 'light'

in this study is used in the sense of photosynthetically active radiation (PAR), which is assumed to be 50% of the global incoming radiation (SZEICZ, 1974).

Statistical results were obtained by use of the SAS statistical package (SAS/STAT, 1990). Data subjected to analysis of variance (SAS procedure GLM) were tested for significant differences between the mean values by protected Fischer's LSD at a significance level of 0.05. Non-linear regression analyses in Chapter 4 were performed with the simulation environment ModelMaker (WALKER, 1997), which uses a Marquart optimisation algorithm (MARQUART, 1963) to minimise the residual sum of squares. The software also gives an uncertainty of parameter value (i.e. the square root of the diagonal elements of the covariance matrix), which is multiplied with the square root of the mean square of the residual to yield the asymptotic standard error of the coefficient (GALLANT, 1987).

The simulation model (Chapter 6) was coded in Object Pascal for Windows 32, using Borland Delphi 3.0. Model calculations were performed on an IBM-compatible personal computer equipped with 64MB RAM and a Pentium Pro processor.

2.3.   Data utilisation

For the sake of brevity, the cauliflower trials in 1995 are herein frequently referred to as 'experiment 1' and 'experiment 2' only; data from the 1994 cauliflower trials are always specified by the experimental year.

Chapter 3: Three-dimensional light interception model

Since no calibration to the model parameter were made, all measurements of canopy transmission and leaf area index made in the 1995 cauliflower experiments were used for evaluation.

Chapter 4: Canopy development of C. album

For the simulation of plant height development, data from the cauliflower trials in 1995 were taken to estimate the potential stem extension. Data from the 1994 experiment with faba bean were used to quantify the feedback of assimilate shortages on height growth. Calculation of plant diameter was performed using all data from the above-mentioned trials.

Chapter 5: Dry matter production and partitioning of C. album

The quantification of dry matter production of *C. album* was carried out with data from pure weed stands of the 1995 cauliflower experiments. Although the faba bean experiment in 1994 also comprised monospecific weed plots, the data basis was considered too weak: Due to a long juvenile phase, *C. album* plants of the early sowing date could only be collected in harvests 2 to 4; moreover, weed plants in harvest 2 were very small. Likewise *C. album* plants from the late sowing date were only sampled in harvests 3 and 4. Dry matter partitioning of *C. album* was analysed using data from all treatments of the 1994 faba bean trial and the 1995 cauliflower experiments.

Chapter 6: Light competition model

C. album infestations did not have an effect on the yield of faba bean. Therefore, the emphasis of the simulation model for light competition lies on the experiments with cauliflower. The model was calibrated with data from the 1995 experiments and evaluated with data from the 1994 trials.

3. A three-dimensional approach to modelling light interception in heterogeneous canopies

The accuracy of plant growth models depends strongly on a precise calculation of radiation uptake. Numerous approaches exist to estimate light absorption in spatially heterogeneous canopies, but these have either restrictions with respect to canopy structure or involve complex and inflexible calculations. The objective of this study was to develop a simulation tool to assess the radiation penetration into canopies that should (a) give details on the light absorption in heterogeneous canopy architectures and (b) comprise simple routines easily to adapt. In the model, the complete canopy volume is subdivided into cubic units being either empty or filled with leaf area. Leaf area can be distributed in an arbitrarily chosen geometric solid positioned anywhere in the model domain. Transmission through the cubes is calculated by following the path of solar rays from the top of the canopy to ground level. Daily canopy absorption is calculated separately for direct and diffuse radiation, taking reflection and scattering of the direct beam into account. Using only few readily obtainable parameters, a close agreement between simulated and measured canopy transmission of a cauliflower crop was found (r^2 = 0.97). Comparing different canopy structures ranging from single plant canopies to a 'closed canopy', gave detailed information on the absorption characteristics and the distribution of light absorption in individual plants. Results for 'closed canopies', and row crops tally with those of earlier models. It is thus useful as a reference model to identify possible simplifications in the quantification of light interception by heterogeneous crops.

3.1. Introduction

Modelling light penetration through a canopy and light absorption by foliage is crucial for the determination of plant photosynthesis in crop growth models. To reduce model complexity, usually a homogeneous distribution of foliage in the vertical and/or the horizontal direction (MONSI & SAEKI, 1953; DE WIT, 1965; DUNCAN ET AL., 1967) is assumed. This holds true for many agricultural crops after canopy closure, but overestimates radiation absorption in spatially heterogeneous canopies, where a substantial clumping of foliage is observed. To simulate light penetration in such canopies more realistically, it is necessary to estimate the amount of radiation (a) passing through the canopy being at least partially intercepted by foliage and (b) passing unobstructedly to ground level. For a given location, these amounts vary with diurnal and seasonal changes of the solar position as well as with canopy architecture.

In row crops foliage elements are clumped along parallel rows leaving gaps without ground cover. Different approaches to calculate light transmission and interception in row canopies have been proposed hitherto. One determines the proportion of foliage which is penetrated by a solar ray of selected origin (CHARLES-EDWARDS & THORPE, 1976; GIJZEN & GOUDRIAAN, 1989). Light transmission is defined by the light extinction coefficient of the crop, its leaf area density and the pathlength of a solar ray through the canopy foliage. This pathlength is

estimated primarily by determining the entry point of the ray into the foliage envelope. If this envelope has a given geometrical shape, the exit point is fixed and thus the pathlength of the ray travelling through foliage is determined. To simplify calculations, rows are defined to be a continuous in the longitudinal direction. In the model of CHARLES-EDWARDS & THORPE (1976), total incoming radiation is separated into the direct and diffuse component assuming a standard overcast sky. The pathlength of the direct beam is calculated based on the polar coordinates of the solar position, whereas the average pathlength of the diffuse radiation has to be integrated over all polar coordinates of the hemisphere above the canopy. Canopy geometry, which also influences the pathlength, is defined as an array of parallel rows of plants with an ellipsoidal cross section. Transmission profiles are then calculated for direct and diffuse radiation using numerical integration methods. The model presented by GIJZEN & GOUDRIAAN (1989) accounts likewise for the distribution and absorption of diffuse and direct light, but also incorporates reflection and multiple scattering of radiation. The fraction of diffuse light is estimated from the atmospheric transmissivity (defined as the ratio between actual global radiation and extra-terrestrial radiation, SPITTERS ET AL., 1986). The canopy consists of parallel rows with a rectangular cross section. Light attenuation is described similar to the procedure used by CHARLES-EDWARDS & THORPE (1976), but is modified by introducing scattering and reflection coefficients. Absorption of radiation coming from every direction of the hemisphere is calculated using the Gaussian integration method (GOUDRIAAN, 1986). JACKSON & PALMER (1979) proposed a model to assess the light penetration into a row crop based on the assumption that the intercepted radiation is proportional to the total ground area shaded by the plants. They separate the light transmitted through an orchard into two additive components: (1) the fraction of light travelling through plant foliage which is estimated by using the leaf area index based and shaded ground area and (2) the fraction of light passing unobstructedly between plants which is derived from measured canopy dimensions (JACKSON & PALMER, 1972). Canopies are classified into rows with a triangular or rectangular cross section and are continuous in row direction. THORNLEY ET AL. (1992) applied this model to a greenhouse cucumber crop, incorporating a modification for calculating leaf irradiance for a photosynthesis model (THORNLEY & JOHNSON, 1990).

The application of these models is limited to canopies where the foliage envelopes of individual plants overlap enough to be a continuous along the row direction. To account for individual plant geometry and row structure, MANN ET AL. (1980) assumed single plants to be ellipsoids randomly distributed in row direction. The shaded area of each plant is used to

calculate the probability that a randomly selected point of the soil surface is shielded from the sun by a distinct number of foliage envelopes. This probability is taken to weight the Beer's law transmission of direct solar radiation through the canopy. The region potentially shaded by the projection of foliage elements is similarly defined in a model proposed by WHITFIELD (1986). The canopy is assumed to consist of parallel rows with equally spaced plants. Since the planting pattern may not be strictly rectangular, the rows are randomly shifted against each other. An individual plant's foliage is confined to an ellipsoidal envelope, and all foliage is assumed to have the same light interception characteristics. Based on these assumptions, the area shaded by the canopy is estimated for direct beam only, using comparatively simple formulations for canopy transmission.

In row models specific restrictions with respect to canopy architecture apply. The canopy extent in the longitudinal direction has either to be described as a continuous block or as randomly distributed individuals, if plants are spaced. However, many horticultural field crops such as cauliflower, celery and kohlrabi are planted in strict rectangular or diagonal patterns. A model to describe this situation has to allow for an arbitrary stipulation of plant locations. This regularity implies a discontinuous leaf area distribution in all directions, not accounted for in row models (WHITFIELD, 1986). Three-dimensional light interception models remedy these shortcomings, but are inevitably more complex. NORMAN & WELLES (1983) gave a solution for the estimation of the total pathlength of direct solar beam within an array of subcanopies, without restriction on their spacing or shape. However, calculations become more complicated when exceeding simple geometric descriptions for the foliage envelope. GRACE ET AL. (1987) applied the model of NORMAN & WELLES (1983) to predict the interception of light in stands of *Pinus radiata*. To save computing time the model is run only for selected points in time to cover a representative range of radiation environments. Subsequently equations are developed to predict canopy interception from incoming radiation. WANG & JARVIS (1990) adapted the model to arrays of trees in a stand. As a simplification, a three-dimensional grid of 52 points is projected into a tree crown. Weighted values of absorbed radiation, photosynthesis and transpiration at these grid points are summed, yielding estimates for both the individual tree and the entire canopy.

In the model presented by RYEL ET AL. (1993) the geometry of a single plant is described as a cylinder. These cylinders are divided twice into concentric subsections and layers to allow for spatially differing plant characteristics such as orientation and density of foliage. Light interception is calculated within these subsections in a three-dimensional array of points, also

using the procedure of NORMAN & WELLES (1983) to calculate the pathlength of radiation. BEYSCHLAG ET AL. (1995) extended this approach from single-plant to canopy scale. The canopy can consist of monotypic plants or mixed species, simulating a competitive situation. Canopy structure is represented by an array of cylinders and light interception of a plant in the centre of the whole plot is calculated.

Another possibility to increase the spatial resolution is the subdivision of plant canopies into discrete ordinates. In optical remote sensing this approach is used in models for the interpretation of surface data from surveillance aircraft or satellites (KIMES, 1991; MYNENI ET AL., 1991). The theoretical principle underlying these models is the treatment of solar rays originating at a given point in the upper hemisphere as first-order vectors that travel through a cubically subdivided canopy volume. Within this volume a fraction of radiation energy is either absorbed, transmitted or reflected. The path of reflected radiation is tracked through the canopy resulting in second and higher-order vectors. Computations are halted if the radiation intensity falls below a threshold value or the ray leaves the system on the upper boundary. The exit coordinates of the ray are retained and thus the models give details on the spatial distribution of reflected radiation, which can be compared to remote sensing data allowing deductions on the observed vegetation (GOEL, 1988). In crop growth models, reflection and scattering are usually treated with summary coefficients. With this requisite, only the calculation of the first order vector through a geometrically dissected canopy volume is necessary. This was implemented in recent modelling efforts proposed for tree canopies (WILLIAMS, 1996; DE CASTRO & FETCHER, 1998).

The objective of this study was to develop a simple, flexible and generic model to analyse light absorption in heterogeneous canopies. It was evaluated with field data from two cauliflower experiments and was used to systematically analyse the effects of different canopy architectures on light absorption characteristics.

3.2. Model description

Geometry

In the model a domain is defined by width l_x, length l_y, and plant height H. The domain is completely subdivided into equal cubic units with an edge length dl. Within this volume the origins of foliage envelopes can be distributed arbitrarily. The shape of these envelopes can be

determined by any geometric solid. Currently, individual plants can be described by an ellipsoidal, half-ellipsoidal, conical or rectangular shape (Fig. 3) and by a 'closed canopy'. Since an ellipsoidal shape is frequently used as a description of the foliage envelope, the procedure for this situation is derived in the following.
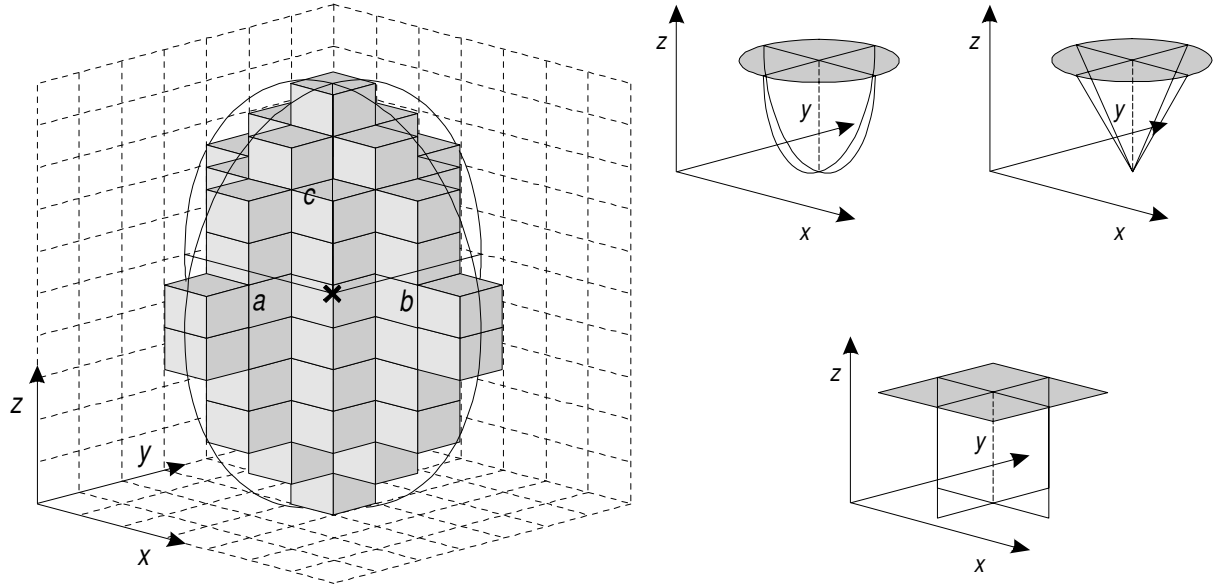

Fig. 3. Schematic representation of a subsection of the model domain (left). The semi-axes a*,* b *and* c *originating in the centre of the ellipsoid (×) define the solid in width, depth and height (*x*,* y*,* z*). The complete model domain is divided into cubic subunits, but only the cubes inside the foliage envelope are shown. Examples for geometrical descriptions of leaf area distribution (right): half-ellipsoidal, conical and rectangular. Drawn are the projection (greyed), the centre line (broken) and the diagonals in* x*- and* y*-direction.*

The canopy foliage is assumed to be completely filled by leaf area which is homogeneously distributed without an azimuthal preference. Leaf area density, L_d, is then calculated by

$$L_d = \frac{L\, l_x\, l_y}{V} \tag{3}$$

where L is the leaf area index and V the plant canopy volume. In an ellipsoidal spheroid with semi-axes a, b and c (m, Fig. 3), V is determined by summation of all cubes that meet the requirement

$$\frac{x^2 - x_n}{a^2} + \frac{y^2 - y_n}{b^2} + \frac{z^2 - H_n/2}{c^2} \leq 1 \tag{4}$$

where x, y and z (m) define the cube location, x_n and y_n (m) are the coordinates of the stem position and H_n is the height of plant n. This procedure is used rather than calculating the ellipsoidal volume geometrically to avoid errors when estimating leaf area density. The cubic subunits are thus either empty or occupied by a constant leaf area density. If foliage envelopes overlap, the leaf area density of the respective cubes is multiplied by the number of plants involved. Different geometric descriptions are obtained by simply changing eq. 4 to calculate the coordinates inside the respective solid.

Incoming radiation

Daily values of incoming global radiation (400-3000 nm, W m^{-2}) are input in the model. On the basis of the latitude of site and day of year, the diurnal distribution of global radiation is calculated first. For specified hours of day, the fractions of direct and diffuse radiation are then generated from the ratio between measured global radiation and extra-terrestrial radiation. These calculations were done according to GOUDRIAAN & VAN LAAR (1994), who use a slightly modified procedure of SPITTERS ET AL. (1986). The origin of the direct beam is the solar position, whereas diffuse light is considered to radiate uniformly from every direction of the hemisphere.

Light interception and transmission

A solar ray is considered a source vector that originates at a given position in the upper hemisphere and every cube in the top layer of the domain is irradiated by one ray. The entirety of these rays are tracked through the whole model domain until they reach ground level. It is therefore essential to obtain the coordinates of all cubes that contribute to the rays' path. If a beam is defined by the solar azimuth angle, α, and the solar elevation angle, β, it can be described as a straight line in three dimensions (Fig. 4A). Simple algebraic considerations (ALT, 1999, pers. comm.) lead to the form

$$\begin{pmatrix} x \\ y \\ z \end{pmatrix} = \begin{pmatrix} x_0 \\ y_0 \\ z_h \end{pmatrix} + \mu \begin{pmatrix} m_x \\ m_y \\ m_z \end{pmatrix} \quad \text{with} \quad m_x = \frac{\sin\alpha}{\tan\beta}, \quad m_y = \frac{\cos\alpha}{\tan\beta}, \quad m_z = -1 \tag{5}$$

with (x, y, z) being the Cartesian coordinates of a point hit by a beam travelling through (x_0, y_0, z_h) and μ being the variable parameter of the equation of the straight line. Beginning with the first cube entered ($i = 1$), the ray is followed stepwise to identify all cubes along the ray's
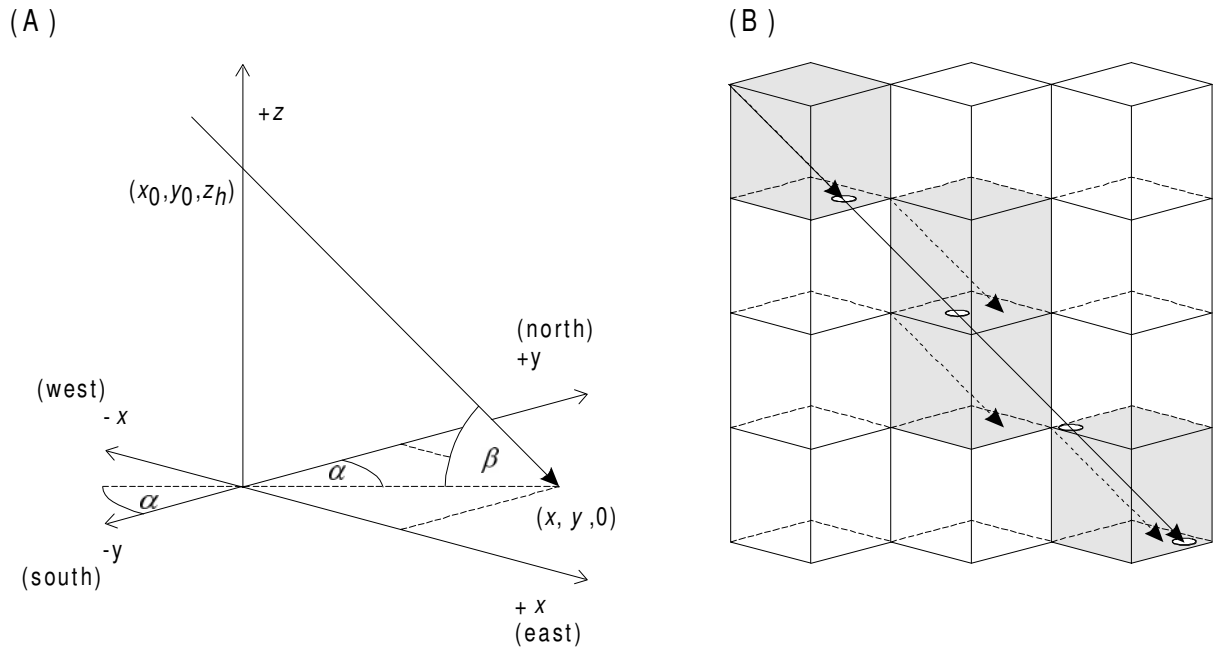
Fig. 4. Description of a beam ($\rightarrow$) with a solar elevation angle of $\beta = 45°$ and a solar azimuth angle of $\alpha = 45°$. (A) If the ray travels through point (x_0, y_0, z_h), it reaches ground level at point (x, y, 0). (B) Path of the ray through a plane of cubes. Shown are the actual pathway (solid line) and the approximation by the model (dotted lines). It starts off at top left cube and leaves the layers at the marked spots, whose (rounded) coordinates determine the position of next cube (greyed) that contributes to the path calculation.

path. Eq. 5 yields the coordinates of the next cube entered if μ is substituted by $i \cdot \varepsilon$ (Fig. 5), where ε is the stepwidth depending on α and β by

$$\varepsilon = \frac{1}{\max\left(\left|m_x\right|, \left|m_y\right|, \left|m_z\right|\right)} \tag{6}$$

Note that the absolute values are necessary because α may be negative. As the domain is subdivided into discrete units, the resulting coordinates have to be rounded to the next integer, giving a 'stepped' path of the solar ray (Fig. 4B). The pathlength through a cube equals dl, if the beam originates directly overhead ($\beta = 90°$). For any other solar elevation a dimensionless correction factor, p_c, (Fig. 5) has to be determined by

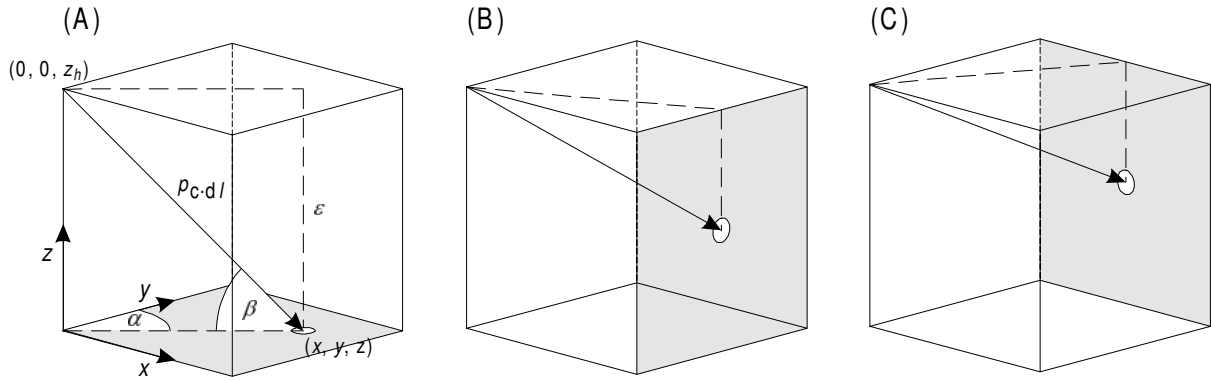$$p_c = \frac{\varepsilon}{\sin \beta} \qquad \text{for} \qquad 0° < \beta \leq 90° \tag{7}$$

Fig. 5. Identification of the adjacent cube reached by a solar ray (→) travelling through (0, 0, z_h). Greyed sides are penetrated by the ray at the exit point shown. The solar angles, the stepwidth ε (eq. 6) and the pathlength correction p_c *(eq. 7) are (A)* α = 45°, β = 45°, ε = 1, p_c = 1.41, *(B)* α = 63.43°, β = 24.09°, ε = 0.5, p_c = 1.22, *(C)* α = 26.57°, β = 24.09°, ε = 0.5, p_c = 1.22.

Direct radiation

In the following discussion relative light intensities, q_c, are related to a cube at the position (x, y, z), but for the sake of readability these subscripts are omitted.

If a solar ray travels through a cube filled with leaf area, part of the radiation is intercepted taking reflection into account. Intercepted radiation is either absorbed or scattered. The difference between incoming and intercepted light is then transmitted to the next cube. If a cube is empty, no radiation is intercepted and the complete incident radiation is transmitted deeper into the canopy.

The light extinction coefficient for non-transmitting, non-reflecting ('black') leaves, K_{bl}, is determined as in GOUDRIAAN (1977) by

$$K_{bl} = O_{av} \ p_c \tag{8}$$

where O_{av} is the average projection of the leaves which is 0.5 for a spherical leaf angle distribution. With a scattering coefficient, σ, of 0.2 for visible light (GOUDRIAAN, 1977), the fraction of absorbed radiation, $q_{c,a}$, according to Beer's law is

$$q_{c,a} = (1 - \sigma) \, q_{c,0} \left(1 - e^{-K_{bl} \, L_{c,d} \, \mathrm{d}l}\right) \tag{9}$$

where $q_{c,0}$ is the radiation incident on the cube surface and $L_{c,d}$ the leaf area density in the cube. For cubes in the top layer $q_{c,0}$ equals the relative light intensity above the canopy

(= 100 %). The leaf area density $L_{c,d}$ equals L_d (eq. 3) for singly occupied cubes. To obtain the leaf area index within the cube, the leaf area density is multiplied by the vertical dimension through a cube dl. The fraction of intercepted radiation, $q_{c,i}$, is given by

$$q_{c,i} = \left(1 - \rho_{sph}\right) q_{c,0} \left(1 - e^{-K_a L_{c,d} \, dl}\right) \tag{10}$$

where ρ_{sph} is the reflection coefficient for a spherical leaf angle distribution (GOUDRIAAN, 1988) and K_a is the apparent extinction coefficient (GOUDRIAAN, 1977), which are calculated by

$$\rho_{sph} = \frac{2}{1 + 1.6 \sin \beta} \frac{1 - \sqrt{1-\sigma}}{1 + \sqrt{1-\sigma}} \tag{11}$$

and

$$K_a = K_{bl} \sqrt{1-\sigma} \tag{12}$$

Finally, the fraction of scattered radiation, $q_{c,s}$, in a cube is calculated by

$$q_{c,s} = q_{c,i} - q_{c,a} \tag{13}$$

As an approximation, scattered radiation is assumed to behave like diffuse radiation. The path of scattered (and reflected) radiation is not traced further through the canopy resulting in a calculation of the downward flux only. The fraction of transmitted radiation, $q_{c,t}$, is then the remainder after the interception by leaf area in the cube

$$q_{c,t} = q_{c,0} - q_{c,i} \tag{14}$$

and is used as input radiation for the next cube ($q_{c+1,0}$). The average of $q_{c,a}$ and $q_{c,s}$ of all rays considered yields the relative amounts of absorbed, F_a, and scattered radiation, F_s, of the whole plot.

The model domain has periodic boundary conditions: radiation as well as foliage envelopes 'leaving' on one boundary re-enter on the opposite side. This eliminates (a) edge effects: the origin of a modelled plant does not influence its light absorption and it can be seen as located in the centre of a larger field and (b) energy losses: all incoming radiation is (after reflection) either intercepted or transmitted to ground level.

Diffuse radiation

The diffuse fraction of incoming radiation is assumed to be composed of an infinite number of solar rays originating from every part of the sky. To apply the routines described above, the diffuse radiation is integrated over fifteen angles of incidence (α, β) assuming a uniform overcast sky. The light extinction coefficient used is K_a (eq. 12) resulting in a relationship between the canopy light extinction coefficient for diffuse radiation and the leaf area index (GOUDRIAAN, 1977, eq. 2.41). Neglecting further scattering and reflection, the fraction of absorbed diffuse radiation in a cube is calculated by

$$q_{c,a} = q_{c,i} = q_{c,0} \left(1 - e^{-K_a L_{c,d} \, dl}\right) \tag{15}$$

The fraction of scattered direct beam is assumed to convert to diffuse radiation and to be absorbed accordingly.

Integration of light absorption

Especially at low solar elevations, a large number of cubes are hit by a beam. Hence calculations for a single solar ray can take up to several minutes, even on a powerful computer. If a complete growing period is to be simulated, the model tends to become cumbersome. To reduce calculations, the Gaussian integration method (GOUDRIAAN, 1986) is used, which has been successfully applied in crop growth modelling (KROPFF, 1993). Light absorption is computed only for selected points, p, located at defined distances, d_p, from the central point of the integration range and weighted, w_p, accordingly (Table 3). An algorithm based on three points can accurately integrate a polynomial up to fifth order, whereas a 5-point integration can handle polynomials up to seventh order (GOUDRIAAN, 1986). To minimise the numerical error due to the large integration range of α (2π), the 5-point method is chosen, whereas three points are sufficient for β and the diurnal course. For the latter three points in time, t_p, between midday and sunset are selected by

$$t_p = 12 + 0.5 \, DL \left(0.5 + d_{3p}\right) \quad \text{with} \quad p = [1..3] \tag{16}$$

where DL is the daylength. At these points the direct, $I_{0,r,tp}$, and the diffuse component, $I_{0,f,tp}$, of the global incoming radiation as well as the fraction of absorbed, $F_{a,r,tp}$, and scattered direct beam, $F_{s,r,tp}$, are determined.

Table 3. Distances and weights for the Gaussian integration.

Point p	3-point algorithm		5-point algorithm	
	Distance d_{3p}	Weight w_{3p}	Distance d_{5p}	Weight w_{5p}
1	-0.387298	0.277778	-0.453090	0.118463
2	0	0.444444	-0.269235	0.239314
3	0.387298	0.277778	0	0.284444
4			0.269235	0.239314
5			0.453090	0.118463

The amounts absorbed, $I_{a,r,tp}$, and scattered, $I_{s,r,tp}$, are then obtained by

$$I_{a,r,t_p} = I_{0,r,t_p} \ F_{a,r,t_p} \qquad \text{and} \qquad I_{s,r,t_p} = I_{0,r,t_p} \ F_{s,r,t_p} \tag{17}$$

The absorbed fraction of diffuse radiation is determined only once a day, but has to be integrated over the whole hemisphere. Thus five azimuth, α_p, and three elevation angles, β_p, are selected as the origin of diffuse radiation with

$$\alpha_p = 2\pi \left(0.5 + d_{5p}\right) - \pi \quad \text{for} \quad -\pi < \alpha \le \pi \quad \text{with} \quad p = [1..5]$$
$$\beta_p = \frac{\pi}{2}\left(0.5 + d_{3p}\right) \qquad \text{for} \quad 0 < \beta \le \frac{\pi}{2} \quad \text{with} \quad p = [1..3] \tag{18}$$

The absorbed fraction of diffuse radiation, $F_{a,f}$, is calculated from these fifteen angles of incidence and weighted according to

$$F_{a,f,\alpha} = 2\pi \sum_{p=1}^{5} F_{a,f,\alpha_p} \ w_{5p}$$
$$F_{a,f} = \frac{\pi}{2} \sum_{p=1}^{3} F_{a,f,\alpha,\beta_p} \ \sin\beta_p \ \cos\beta_p \ w_{3p} \tag{19}$$

Multiplication by $\sin\beta_p$ considers the fraction of radiation effective on a horizontal plane, and the factor $\cos\beta_p$ is needed when integrating the solid angles over the hemisphere. As the scattered direct beam is considered diffuse radiation, the amount of absorbed diffuse radiation, $I_{a,f,tp}$, at the selected points in time is

$$I_{a,f,t_p} = \left(I_{0,f,t_p} + I_{s,r,t_p}\right) F_{a,f} \tag{20}$$

Summation of the weighted values $I_{a,r}$ and $I_{a,f}$ yields the daily absorption of radiation, I_a

$$I_{a,r} = D \sum_{p=1}^{3} I_{a,r,t_p} \, w_{3p} \quad \text{and} \quad I_{a,f} = D \sum_{p=1}^{3} I_{a,f,t_p} \, w_{3p}$$

$$I_a = I_{a,r} + I_{a,f}$$

(21)

Model evaluation

Since plant dimensions were only measured at harvest, a sigmoid function was used to interpolate for the dates of transmission measurement. The canopy light transmission data were compared to simulated daily values using four different leaf area distributions and a 'closed canopy' situation. The radiation distribution for the respective day was estimated from measured global radiation. With plant positions and dimensions as well as the leaf area index given, no further calibrations to model parameters were made thus all field data was used for evaluation.

Model sensitivity analysis

To test the sensitivity of the model, several scenario calculations were conducted with model domain and canopy structures arbitrarily defined. The domain had a ground area of 1 m^2 with $l_x = l_y = 1$ m, and an upper limit at plant height H; the edge length of the cubes dl was 0.01 m. All plants were considered to be ellipsoids of revolution, resulting in $a = b$ in Fig. 3 and eq. 4. Four model canopies (A-D) of contrasting structure and light absorption characteristics and a 'closed canopy' situation were examined (Table 4). Plant height and diameter were chosen to obtain a constant leaf area density L_d of ~0.1 m^2 m^{-3}. In canopies A and B one plant is located in the centre of the plot, representing wide-spaced crops of different geometry. Row spacing and planting distance are equally 1 m because of the periodic boundary conditions. Canopy C idealises a wide-spaced row canopy with a south-north orientation. Within-row plant distance here is 0.25 m, whereas row spacing is 1 m. A more homogeneous leaf area distribution is realised in canopy D, which planting pattern is near-isometric. Row spacing and planting distance are both 0.5 m, with adjacent rows being shifted by 0.25 m.

Firstly, the absorption behaviour and transmission profiles were calculated for a single non-scattering solar ray with both solar angles at 45°, i.e., originating in south-west at a medium elevation (1 May at 14:00 h, Hanover, Germany). Canopies A to C were compared to the 'closed canopy' case.

Table 4. Properties of the model canopies in the scenario calculations. Relative groundcover denotes the fraction of shaded ground with the sun directly overhead. In canopy A to D all plants are assumed to have an ellipsoidal foliage envelope.

Canopy	Plants	Leaf area index	Plant height	Plant diameter	Relative groundcover	Position of plant main axis (x, y)
	m^{-2}	$m^2\ m^{-2}$	——— m ———		—— % ——	——— m ———
A[†]	1	1	0.71	0.51	20.53	(0.5, 0.5)
B[‡]	1	1	0.24	0.89	62.21	(0.5, 0.5)
C[§]	4	1	0.53	0.30	25.80	(0.5, 0.25) (0.5, 0.5) (0.5, 0.75) (0.5, 1)
D[¶]	4	1	0.53	0.30	28.27	(0.25, 0.25) (0.25, 0.75) (0.75, 0.5) (0.75, 1)
'closed canopy'	-	1	0.10	-	100	-

[†] Wide-spaced canopy, large gaps   [‡] Wide-spaced canopy, small gaps
[§] Wide-spaced row canopy   [¶] Near-isometric canopy

In another scenario calculation, the origin of a single non-scattering solar ray was modified to analyse the interdependence between the solar angles and canopy structure. The elevation angle ran from a low solar position (5°) to directly overhead (90°), whereas the azimuth angle spread from south (0°) to west (90°). The absorption characteristics of canopies A to C and the 'closed canopy' were calculated.

Finally, the effects of row orientation on light absorption on a specific day (21 June) were quantified for canopies C and D. In this analysis, the orientation of the canopies was varied from south-north to east-west in 10° steps. To additionally examine the significance of direct beam, the fraction of direct radiation was incrementally increased from 0 to 80 %.

3.3. Results and discussion

Model evaluation

For all leaf area distributions tested a close relationship was found between measured and simulated canopy light transmission in a cauliflower crop (Table 5). The slope is closest to the ideal value of 1.0 when assuming an ellipsoidal shape (Fig. 6). Larger slopes at other geometrical descriptions are caused by an inappropriate description of the heterogeneity in early crop growth stages where transmission is high. Although the intercept for the ellipsoidal foliage envelope is statistically significant, the numerical deviation from zero is small.

Table 5. Regression coefficients, their corresponding standard error (s.e.) and the coefficient of determination (r^2) of the comparison between measured and simulated light transmission in cauliflower. Four leaf area distributions (Fig. 3) as well as a 'closed canopy' situation were evaluated.

Leaf area distribution	slope	s.e.	intercept	s.e.	r^2
Ellipsoidal	1.14	0.052	-0.046[*]	0.028	0.97
Half-ellipsoidal	1.16	0.053	-0.055[n.s.]	0.028	0.97
Rectangular	1.17	0.056	-0.021[n.s.]	0.028	0.97
'Closed canopy'	1.22	0.065	-0.019[n.s.]	0.031	0.96
Conical	1.24	0.057	-0.16[*]	0.033	0.97

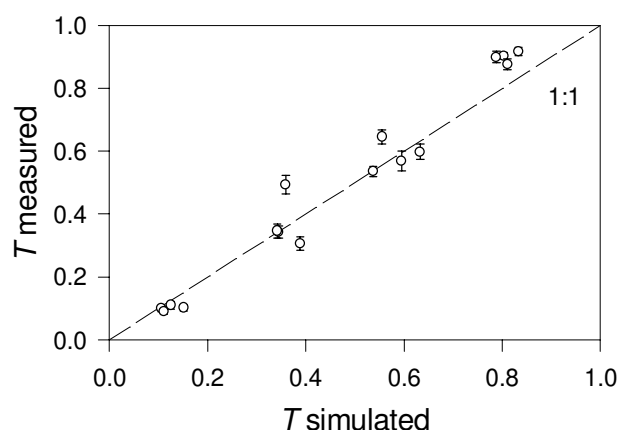[*] Significant at the 0.05 probability level   [n.s.] not significant

Fig. 6. Measured and simulated daily canopy transmission, T*, in cauliflower. Shown are the means (○) and s.e. (bars) of 10 repeated measurements in individual plots. Only the simulated results for an ellipsoidal leaf area distribution are given. For statistics see Table 5.*

A comparatively larger intercept is calculated for the conical distribution. This diversion is due to an substantial overestimation at full cover, i.e., low transmission.

The good correspondence of measured and simulated canopy transmission shows that the model gives quantitatively correct results for the situations tested. Using ellipsoidal foliage envelopes results in a much more realistic estimation of canopy transmission than the assumption of a 'closed canopy', but leads to an underestimation of light transmission in early growing periods. This indicates that more attention has to be drawn to the morphological changes during the development of a cauliflower plant. Since simple geometrical shapes should preferably be used, this would imply to switch for example from a conical to an ellipsoidal description at an appropriate developmental stage. The assumption of a spherical leaf angle distribution as a 'point of reference' (GOUDRIAAN, 1988) did not lead to erroneous results when simulating cauliflower. However, the model will have to be calibrated to plant canopies where the leaf angles substantially deviate from a spherical distribution or if the leaves have an azimuthal preference. Within a foliage envelope, leaf area is assumed to be homogeneously distributed. In later growth stages of cauliflower, the curd occupies a large fraction of the plant's volume and may affect the light interception characteristics. If substantial deviations between the field situation and simulation results occur, subregions could be defined inside the solid, describing the outer shape of the plant (NORMAN & WELLES, 1983; GRACE ET AL., 1987; RYEL ET AL., 1993). Within these subregions, varying leaf area densities as well as leaf angle distributions (GOUDRIAAN, 1988) could be considered.

Model sensitivity analysis

The different model canopies and their absorption characteristics are shown in Fig. 7. Canopy A absorbs 29 % of the total incoming energy, the maximum being shifted significantly towards the source of radiation. On the south western border the canopy absorbs more than twice the vertical irradiance due to a substantial amount of radiation reaching the foliage envelope laterally through large gaps between plants. The structure of canopy B approaches a closed canopy showing little response to changes of α. Light absorption on the side facing the ray's origin is only slightly higher than on the opposite side. It achieves a total relative absorption of 41 %. Having a comparable relative ground cover to canopy A, the row canopy C absorbs 33 % of the incoming energy. The four plants also show a notable peak of absorption in the south-west as an effect of the wide row spacing. The transmission profiles of
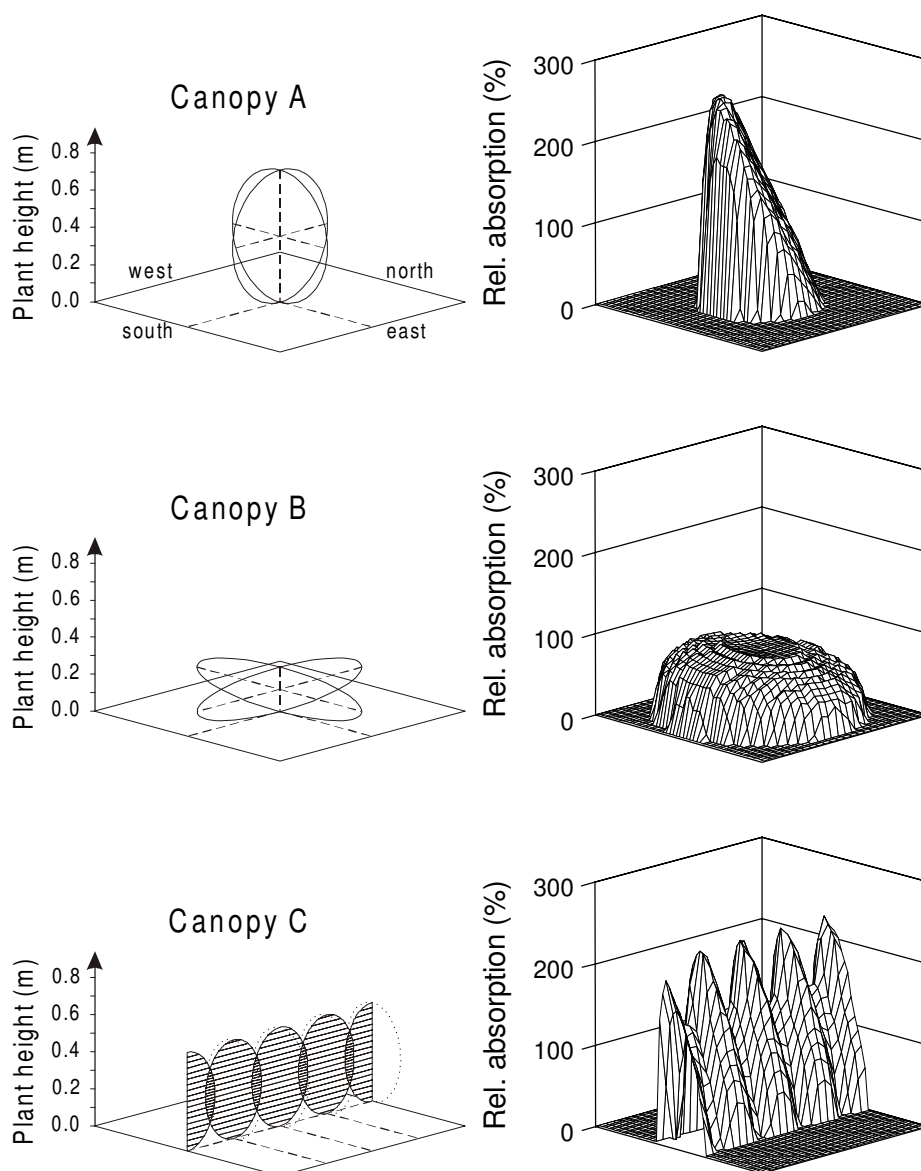
Fig. 7. Foliage envelopes of model canopies A, B and C (left) and simulated absorption of a single non-scattering solar ray (right) in relation to a horizontal plane above the crop. The beam originates in the south-west (α = 45°) with an elevation angle of β = 45° (see Fig. 4). Note that the foliage envelopes of canopy C overlap resulting in a doubled leaf area density in this region.

the canopies A to C (Fig. 8) show significantly different light transmission compared to a 'closed canopy' structure. Due to a high relative ground cover canopy B transmits only 10 % more of the incoming radiation, whereas this shift increases with spatial discontinuity to 17 % and 22 % for canopy C and A respectively.

Modifying the solar position in an adequate range results in the light absorption depicted in Fig. 9. Evidently all canopies show little response to changes of α when the sun is nearly
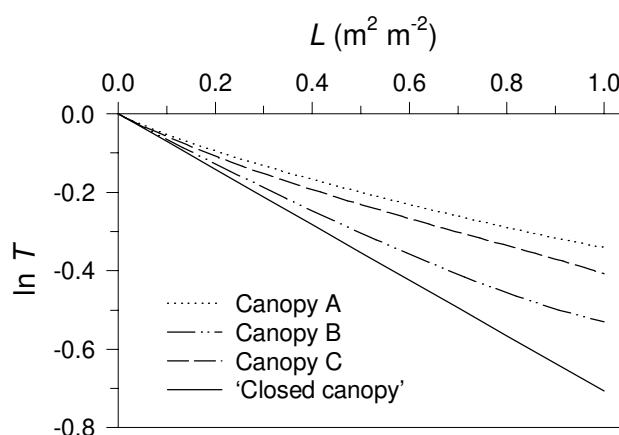
Fig. 8. Relationship between the simulated transmission, T, *for a single non-scattering solar ray (α = 45°, β = 45°) and the leaf area index,* L, *in different canopy architectures.*

overhead, but absorption increases substantially towards low elevation angles because the pathlength increases through the canopy. The latter effect varies with canopy structure: canopies A and B are solids of rotation, resulting in a reflection of the absorption contours by a line at $\alpha = 45°$, i.e. $F_{a,\alpha=0°} = F_{a,\alpha=90°}$. The single plant canopies, however, do not behave in the same way: as the gaps between plants maximise at $\alpha = 45°$, canopy A shows the least absorption due to a considerable amount of radiation reaching the ground surface unimpeded. In canopy B more radiation reaches the flank of plants, whereas absorption decreases at other α owing to mutual shading. But the effect is not as significant as in canopy A, confirming the above results that canopy B is hardly influenced by changes of α. Canopy C shows the least absorption at $\alpha = 0°$ when the solar position is in the south with radiation travelling parallel to the row direction. The absorption at low elevation angles increases towards an α of 45°, where the pathlength through the rows maximises.

In latitudes of northern Europe, a row crop planted in a south-north orientation absorbs more radiation than an east-west oriented crop (Fig. 10). This phenomenon, however, is dependent on the fraction of direct radiation: light absorption is independent on row orientation if all incoming PAR is diffuse. Inevitably, a canopy with a more homogeneous leaf area distribution is much less sensitive to a change in orientation. Under the given conditions, canopies with a near-isometric planting pattern absorb on average 5 % more radiation than a row crop.
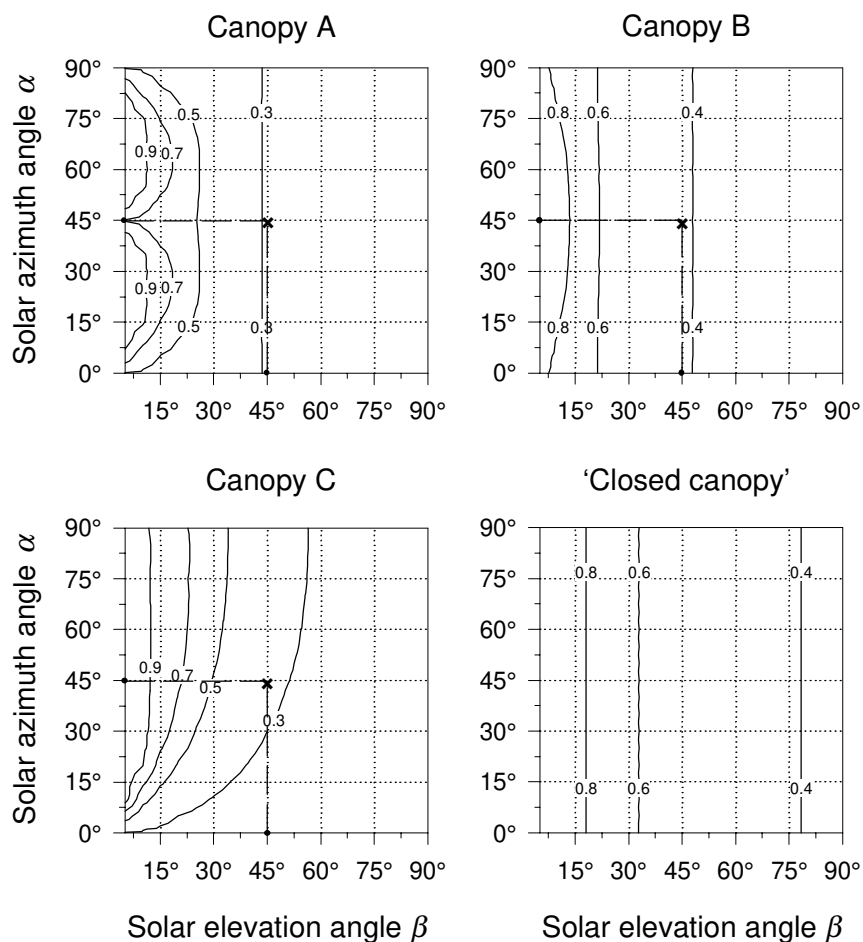
Fig. 9. Simulated lines of equal light absorption (numbers in graphs) of a non-scattering solar ray originating at an azimuth angle, α, and an elevation angle, β, in different canopy structures. The ✗ marks the situation shown in Fig. 7.

Simulation of light penetration into the four model canopies tally with earlier modelling efforts. The transmission profile in a 'closed canopy' resulted in a linear relationship between the leaf area index and the natural logarithm of the canopy transmission as postulated by Beer's law. A strong influence of the solar position, e.g., in the seasonal course, different radiation regimes and planting patterns on the light absorption in heterogeneous canopies was also found by DE CASTRO & FETCHER (1998). Calculation of the daily absorption of radiation in a row canopy gave qualitatively identical results to those of earlier row crop models (CHARLES-EDWARDS & THORPE, 1976; GIJZEN & GOUDRIAAN, 1989). The scenario calculations outline the capability of the model to analyse canopies ranging from a 'closed canopy' situation to individual plants. Especially in heterogeneous canopy architectures, the influence of a neighbouring plant varies with its distance and azimuthal orientation (BEYSCHLAG ET AL., 1995). Thus the model can give valuable information in situations where
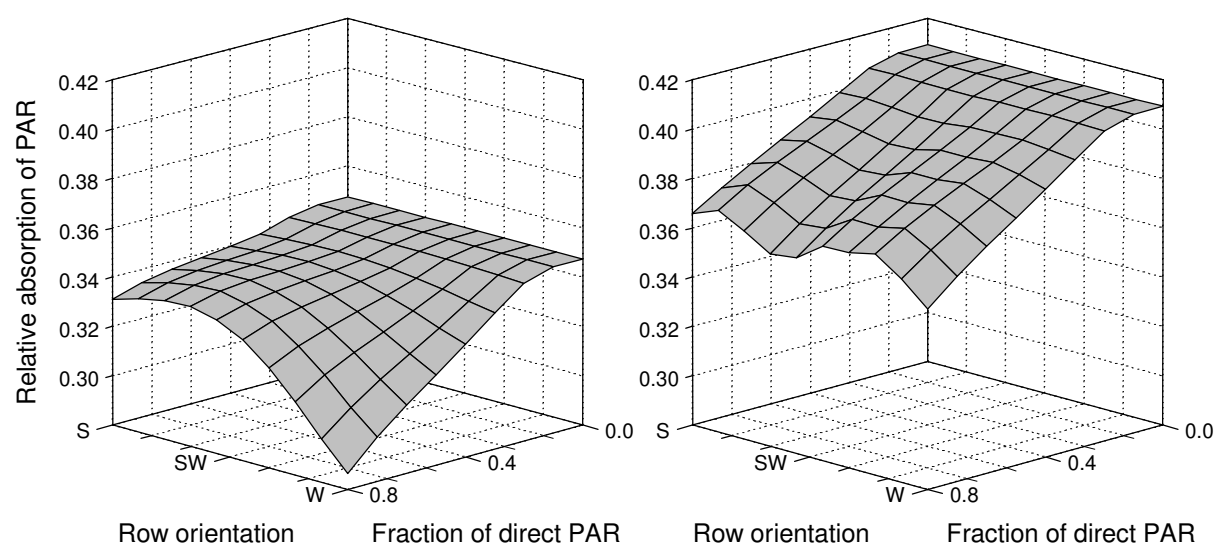
Fig. 10. Relative daily absorption of PAR on a mid-summer day (21 June) as a function of row orientation and the fraction of direct radiation. The graph shows the results for canopy C (row crop, left) and canopy D (near-isometrically planted crop, right) as defined in Table 4.

the light distribution within the canopy is important, such as the evaluation of different planting patterns or the estimation of light interception in a multispecies canopy.

Despite the simple relationships and optimised integration routines, the model implementation takes up relatively much computational resources due to a large number of repetitious calculations. It is thus primarily intended to work as a heuristic tool and should be used to identify possible simplifications for the assessment of light interception in heterogeneous canopy structures.

In conclusion, simulation results indicate that modelling light absorption has to allow for the spatial heterogeneity of the crop. The model presented here provides the opportunity to analyse canopy structures ranging from single individuals to homogeneous crops. Simulation results are consistent with earlier modelling approaches but the formulations can be modified and extended more easily. It is therefore a useful and flexible tool to calculate the effects of planting patterns or interspecific competition for light. Simulated transmission corresponds with measurements in cauliflower, suggesting that the heterogeneous leaf area distribution of this crop should not be ignored. The universality of the model has yet to be tested.

4. Canopy development of *Chenopodium album* in pure and mixed stands

Plant height and leaf area distribution in a multi-species canopy are the principal determinants of the competitiveness of a plant species. Shade-avoiding species show a habit adapted to the competitive environment. The objective of this study was to quantify the morphological plasticity of *C. album* in response to shading and to develop a simple simulation model from these relationships. Plant heights of *C. album* differed significantly between pure stands and mixed plots of cauliflower experiment 1, whereas density effects were not as marked. In the second cauliflower trial less variation was observed. Faba bean suppressed *C. album,* which was unable to overgrow the crop. Assumed to be mainly responsible for plant height modulation due to spectral changes, the leaf area around extending internodes was estimated. Relating this 'effective' leaf area to the stem extension rate yields an accurate prediction of potential plant height growth. Since this potential could not be realised under low light conditions in a faba bean canopy, the 'maximum specific stem length' was estimated to obtain a feedback of assimilate shortage on height growth. Simulation of plant diameter is most precise when based on thermal time and plant density. As the vertical leaf area distribution did not change, it is concluded that leaf area of *C. album* can be predicted at every point in time and space from a given total leaf area and plant density. This information is useful in models for light competition to improve the description of weed competition effects.

4.1. Introduction

Light competition in a plant community has a direct impact on growth and morphology of the individual plant. Whilst the light quantity influences the biomass production, the light quality induces plant specific responses to the competitive environment. A vegetation canopy absorbs light mainly in the blue and red spectral wavebands and almost totally transmits the far-red (HOLMES & SMITH, 1977). This shift in the red:far-red ratio (R:FR) as signal of shading is transduced by a family of phytochromes and leads especially in angiosperms to various responses summarised in the term 'shade avoidance syndrome' (SMITH & WHITELAM, 1997). Thus, individuals in a population can show physiological and morphological differences to plants growing isolated (BALLARÉ ET AL., 1995). One of the most prominent responses to spectral changes is an increased stem extension. More than 40 years ago, DOWNS ET AL. (1957) reported that *Phaseolus vulgaris* L. plants exposed to additional far-red radiation given at the end of the daily photoperiod showed a marked internode elongation in comparison to control plants. Similar results were obtained with *Cucumis sativus* L. (MEIJER, 1958) and *Lactuca sativa* L. plants (HENDRICKS ET AL., 1959).

In experiments with *C. album* a linear relationship was found between the logarithm of the stem extension rate and the phytochrome photoequilibrium (MORGAN & SMITH, 1976; 1978). The photostationary state of phytochrome again was related to the R:FR by a rectangular hyperbola (SMITH & HOLMES, 1977). SMITH (1986) reported experiments with *C. album* where a reduction of the R:FR increased plant height but affected neither fresh and dry weight

nor photosynthetic rates. It was concluded that the effects on stem extension were due to increased cell elongation as no changes in the rates of cell division or node formation were observed. It was shown subsequently that phytochrome can even perceive the quality of radiation reflecting from nearby foliage without direct shading (BALLARÉ ET AL., 1987; SMITH ET AL., 1990). This means that the amount of incident light does not primarily determine shade avoidance responses.

When modelling interspecific light competition it is essential to adequately quantify the space occupied by the plants involved. Under ample supply of nutrients and water, overgrowing and shading the crop foliage primarily determines the competitiveness of a weed (e.g. LAWSON, 1972; FRIESEN, 1979; QASEM, 1992). This stresses the importance of stem elongation and relative canopy height (FIVELAND, 1974; JOENJE & KROPFF, 1987; KINIRY ET AL., 1992b). KROPFF (1986) suggested to simulate morphological processes such as stem extension and branch formation explicitly dependent on environmental factors, because physiological models for light competition show a high sensitivity to relative height differences between competing plants (SPITTERS, 1984; KROPFF, 1986). In the models proposed hitherto height growth was related to temperature only: either directly (WILLIAMS ET AL., 1989) or to the developmental stage (SPITTERS & AERTS, 1983; SPITTERS, 1984; 1989; 1990; KROPFF, 1988; WILES & WILKERSON, 1991), which itself is a function of temperature. This neglects the plant's ability to react dynamically to the variation of light quality and quantity due to competition. By introduction of the specific stem length (*SSL*, height d.wt.$^{-1}$) the temperature-based approach was extended to integrate the effects of a shortage of assimilates due to reduced light intensity (KROPFF & LOTZ, 1992; KROPFF, 1993). If the maximum *SSL* (thinnest stem possible) for a species is reached and the amount of available assimilates does not cope with the requirements for the potential stem extension, height increase is assumed to cease. Whilst this approach allows for decreased plant height due to a deficiency of radiation, it does not provide for the promoting effects of qualitative changes in the light environment.

In addition to plant height, the vertical distribution of leaf area is a crucial factor determining the relative competitiveness of plants (BARNES ET AL., 1990; WILKERSON ET AL., 1990). As a first approximation SPITTERS & AERTS (1983) assumed a uniform vertical leaf area distribution. Their simplification setting the assimilation rates of the two competing species proportional to the light intensities at half of their heights was also used by KINIRY ET AL. (1992b). If the assumed uniformity, i.e. a rectangular leaf area distribution does not adequately reflect the field situation, the use of parabolic (SPITTERS, 1990) or triangular

distributions (NORMAN, 1979; PEREIRA & SHAW, 1980) was proposed. The latter was used by WILES & WILKERSON (1991) to simulate different profiles, as they found that under severe light competition plants tend to establish more leaf area in the upper regions of the canopy. But the assignment of a specific leaf area distribution is static, i.e. not altered by the varying degree of competition during the growing period.

The models of crop-weed interaction proposed so far are not able to explain the phenotypic plasticity induced by changes in light quality. At the same time, these models show a high sensitivity to plant height, a characteristic strongly influenced by the red:far-red ratio in the canopy. A successful quantification of the relationship between light quality and stem extension rates in *C. album* seedlings (HUGHES & WAGNER, 1987) makes it feasible to examine this dependence in subsequent developmental stages. Since growing stem tissues have been identified to perceive spectral changes (MORGAN ET AL., 1980), the leaf area around and above the zone of elongating internodes is assumed to be mainly responsible for increased plant heights. This fraction of canopy leaf area is called 'effective' in the following discussion.

The aim of this study was the quantification of the canopy development of *C. album* in response to different degrees of shading and the incorporation of these functional relationships into a simple simulation model.

4.2. Model description

To simulate the height growth of *C. album*, a relationship between the stem extension rate and the leaf area around and above actively growing internodes had to be established. In the following, this 'effective' LAI in pure and mixed stands is calculated. This estimate is related to the potential stem extension rate, thus modifying the temperature dependency of this plant characteristic for spectral changes. The approach of the specific stem length was applied as a feedback of assimilate shortages on the height growth rate. Finally, the development of the plant diameter is quantified as a function of temperature and planting density.

Henceforth, data and estimates of leaf area index, *L*, internode length, *H*, and plant diameter, *D*, refer to *C. album* only, but a subscript is omitted for the sake of readability.

Estimation of the 'effective' canopy LAI

Since spatially resolved data on plant height and LAI of *C. album* were only taken in the cauliflower crops, only this subset of available data is used for this analysis.

Due to the interdependence of leaf area and internode extension and owing to the difficulties of measuring internode extension in field experiments without disturbing the canopy, the 'effective' LAI had to be calculated in several steps (Fig. 11). On a node N, an internode with the length, H_N, and leaf area, L_N, is located. H_N and L_N develop towards final values $H_{N,f}$ and
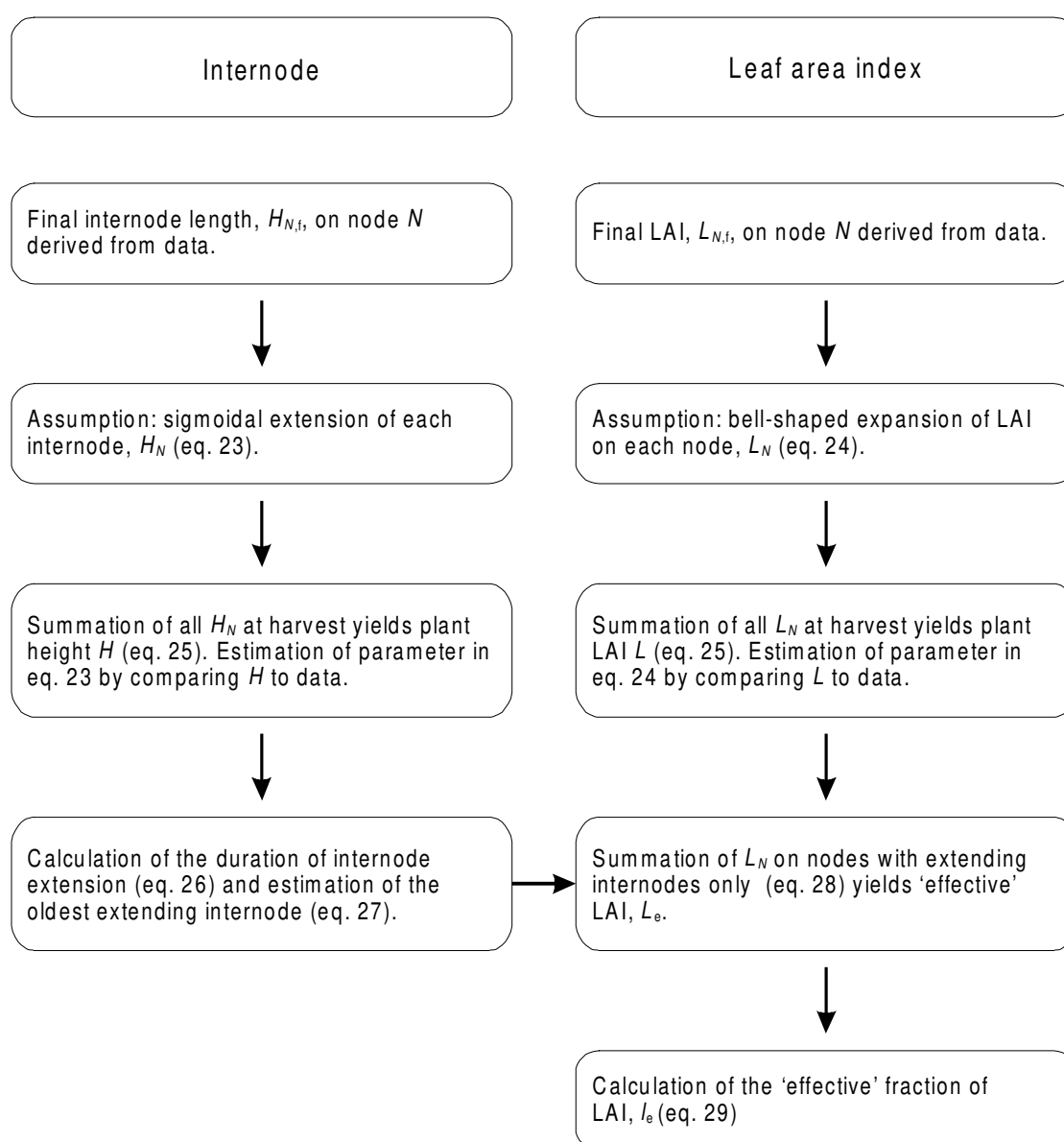

Fig. 11. Schematic diagram of the procedure to estimate the 'effective' fraction of LAI of C. album. *For details on the calculations see text.*

$L_{N,f}$, respectively, which are specific for each node. These final values were determined from measurements at the harvest, when either plant height or plant LAI reached their maximum. Confirmed by results found in faba bean (DENNETT ET AL., 1979) and sugar beet (MILFORD ET AL., 1985a;b), a linear relationship between the temperature sum after 3-node stage, TS, and the number of macroscopically visible nodes, N_v, is assumed

$$N_v = m\,TS + 3 \tag{22}$$

where m (°Cd^{-1}) is the reciprocal of the phyllochron interval, PC, which denotes the time between the appearance of consecutive nodes. The extension of individual internodes towards $H_{N,f}$ is assumed to follow a logistic course

$$H_N = \frac{p_0}{p_0 + (1 - p_0)\,\mathrm{e}^{-\mu\,t_N}}\,H_{N,f} \quad \text{with} \quad t_N = TS_h - (N - 1)\,PC \tag{23}$$

where $p_0\,H_{N,f}$ is the value of H_N at thermal time $t_N = 0$, μ (°Cd^{-1}) is the specific growth rate and TS_h is the temperature sum at harvest. The term t_N defines how long H_N has been extending at the time of TS_h. Similarly, the leaf area, L_N, on node N expands according to

$$L_N = \frac{p_0}{p_0 + (1 - p_0)\,\mathrm{e}^{-\mu\,t_N}}\,L_{N,f} \quad \text{with} \quad t_N = TS_r - \mathrm{abs}(TS_h - (N - 1)\,PC - TS_r) \tag{24}$$

where the term for t_N contains a temperature sum TS_r, after which the function declines symmetrically. In contrast to the sigmoidal course of H_N in eq. 23, the graph of eq. 24 is bell-shaped to allow for a decreasing leaf area due to senescence. Eqs. 23 and 24 were combined for all nodes

$$H = \sum_{N=1}^{N_h} H_N \quad \text{and} \quad L = \sum_{N=1}^{N_h} L_N \tag{25}$$

where H and L are measured plant height and LAI, respectively. N_h is the number of visible nodes at harvest which is defined by eq. 22 with $TS = TS_h$. Eq. 25 allowed to estimate the coefficients p_0 and μ (eq. 23) and TS_r (eq. 24) by non-linear least squares regression.

Subsequently, the duration of internode extension, $TS_{m,H}$, while internodes are sensitive to spectral changes, had to be determined. Since logistic functions reach their final value at infinity, $TS_{m,H}$ was defined as the intercept of the tangent at the point of inflexion with the

asymptote of the logistic function. This procedure results in a similar behaviour as a 3-line step function (SQUIRE, 1989; STEWART & DWYER, 1994) and is preferred to an arbitrary stipulation. $TS_{m,H}$ can be derived from the properties of the logistic growth function (for details see THORNLEY & JOHNSON, 1990, p. 78f)

$$TS_{m,H} = \frac{\ln\left(\frac{1-p_0}{p_0}\right) + 2}{\mu} \tag{26}$$

The oldest node, N_a, with an actively growing internode was determined

$$N_a = \begin{cases} N_h - \dfrac{TS_{m,H}}{PC} & \text{for } TS_h > TS_{m,H} \\ 1 & \text{for } TS_h \leq TS_{m,H} \end{cases} \tag{27}$$

i.e. all internodes on node N_a to N_h have not yet reached their maturity time $TS_{m,H}$. The 'effective' LAI, L_e, was then calculated as the sum of the leaf area on all growing internodes

$$L_e = \sum_{N=N_a}^{N_h} L_N \tag{28}$$

The 'effective' fraction of total leaf area, l_e, is given by

$$l_e = \frac{L_e}{L} \tag{29}$$

ranging from one in early to zero in later growth stages. If l_e is plotted against TS, it is readily interpolated by a logistic function.

Simulation of plant height and diameter of C. album

When *C. album* grows underneath a crop, a fraction of crop foliage contributes to the 'effective' canopy leaf area. Therefore the horizontal plane above which internodes of *C. album* are extending, H_g, is approximated

$$H_g = H\left(1 - l_e\right) \tag{30}$$

Eq. 30 defines the height of the oldest elongating internode. Only crop foliage located above this threshold represents the 'effective' fraction of crop leaf area, $l_{e,cr}$

$$l_{e,cr} = \begin{cases} 1 - \dfrac{H_g}{H_{cr}} & \text{for } H_g < H_{cr} \\ 0 & \text{for } H_g \geq H_{cr} \end{cases} \tag{31}$$

where H_{cr} is the plant height of the crop. Assuming that leaf area from different species does not vary in its effect on internode extension, the 'effective' canopy leaf area index, $L_{e,c}$, can be obtained

$$L_{e,c} = l_{e,cr} \; L_{cr} + l_e \; L \tag{32}$$

where L_{cr} and L are the leaf area indices of crop and *C. album*, respectively.

It is assumed that *C. album* in the cauliflower experiments was able to realise its potential height growth rate, i.e. no assimilate limitations occurred in these trials. The potential thermal stem extension rate, *TSER*, is defined as the total plant height increase of *C. album* per degree Celsius of average daily temperature. *TSER* was estimated by interpolating the relationship plant height vs. *TS* with logistic functions and dividing the resulting height growth rates by T_{av}. The function to describe the relationship between $L_{e,c}$ and *TSER* was constrained to (a) go through the origin and (b) to approach a maximum. A sufficiently accurate description was achieved by using a rectangular hyperbola of the form

$$TSER = \frac{TSER_{max} \; L_{e,c}}{c + L_{e,c}} \tag{33}$$

where $TSER_{max}$ is the maximum *TSER* and c is a dimensionless curvature coefficient. The parameter of eq. 33 were obtained by comparing simulated and calculated *TSER* for harvest dates. Assimilate availability, however, may affect height growth of *C. album* under low light conditions. To include this in the model, the maximum specific stem length, SSL_{max}, i.e. the thinnest stem possible (KROPFF & LOTZ, 1992; KROPFF, 1993), is estimated by

$$SSL_{max} = e^{-s_1 H + s_2} \tag{34}$$

where s_1 and s_2 are constants. In the model, the actual *SSL* is calculated by

$$SSL = \frac{H}{W_s / PD} \tag{35}$$

where W_S is the stem dry weight and PD is the planting density of *C. album*. The potential thermal stem extension rate is realised only if sufficient assimilates are available, otherwise the daily height increase is set to zero

$$\frac{\mathrm{d}\,H}{\mathrm{d}\,t} = \begin{cases} TSER\ T_{\mathrm{av}}\ 10^{-3} & \text{if} \quad SSL \le SSL_{\mathrm{max}} \\ 0 & \text{if} \quad SSL > SSL_{\mathrm{max}} \end{cases} \tag{36}$$

Plant diameter increases per day as a function of temperature sum and planting density according to

$$\frac{\mathrm{d}\,D}{\mathrm{d}\,t} = d_0\ \mathrm{e}^{-d_1\,TS - d_2\,PD}\ T_{\mathrm{av}}\ 10^{-3} \tag{37}$$

where d_0 (mm °C^{-1}) is the maximum thermal increase rate, d_1 (°Cd^{-1}) and d_2 (m^2) are the coefficients for the temperature sum and planting density, respectively. The parameter d_0 to d_2 were determined by integrating eq. 37 and comparing simulated to measured plant diameter. The factor 10^{-3} in eqs. 36 and 37 converts from millimetre to metre.

4.3. Results

Experiments

Significant plant height differences of *C. album* between mixed and pure stands were found in cauliflower experiment 1 (Fig. 12). Shading by crop plants increased height growth of *C. album*, when grown with cauliflower. In experiment 2, the plants were generally taller than those of the first trial. Plants in pure stands of *C. album* were able to build up a markedly higher LAI than in the same plots in spring. Thus, mutual shading stimulated height growth in these plots resulting in generally insignificant plant height differences between pure and mixed stands. Although sown only one week after the faba bean crop, *C. album* plants of the early sowing date were constantly shaded by the faba bean canopy, resulting in a significantly reduced plant height compared to monospecific weed plots. *C. album* sown into the faba bean crop three weeks later did not emerge adequately. The actual plant density fell markedly short of the target value, hence no results could be obtained from these plots. Generally, no significant differences in height between planting densities were found.
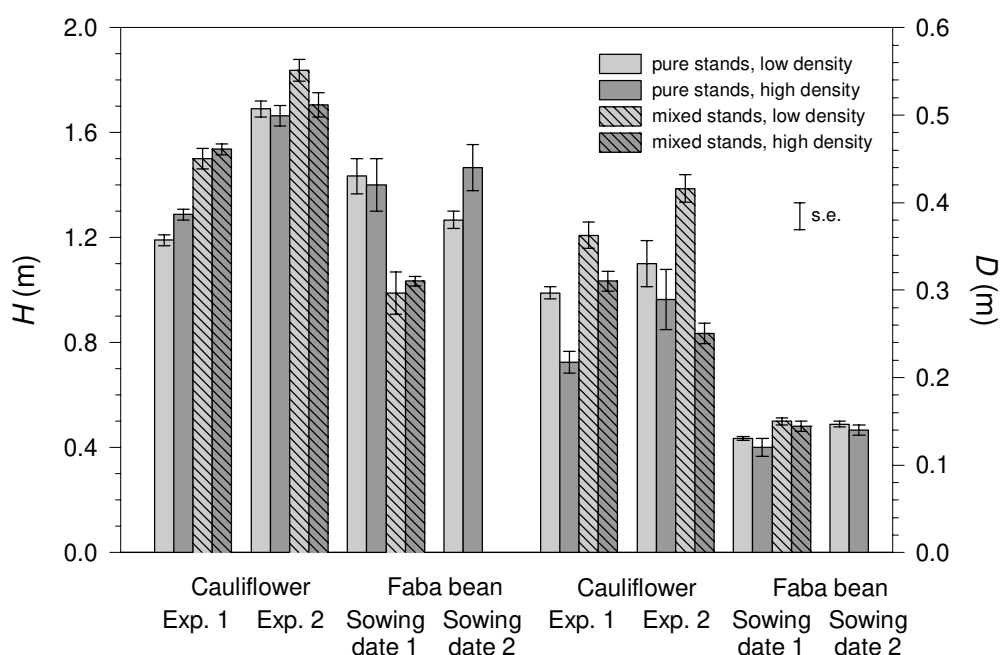
Fig. 12. Plant height, H, *and diameter,* D, *of* C. album *measured at last harvest of the respective treatment. The mixed plots of sowing date 2 in the faba bean experiment were not evaluated because* C. album *did not reach target densities due to inadequate emergence.*

Increased planting density, however, reduced plant diameter of *C. album* in both cauliflower experiments. In the faba bean experiment, *C. album* plants had a markedly smaller diameter compared to the cauliflower trials and less variation was observed.

In neither cauliflower experiment was the vertical leaf area distribution of *C. album* changed notably: the maximum leaf area density was found halfway up the plants.

Estimation of the 'effective' leaf area index

The final values $H_{N,f}$ and $L_{N,f}$ were obtained by Chanter growth equations (THORNLEY & JOHNSON, 1990, p. 83, eq. 3.6b) used to interpolate the relationships node number vs. plant height and node number vs. plant LAI (Fig. 13). Being a hybrid of a logistic and a Gompertz function, the Chanter equation was most flexible in describing the data: the coefficient of determination exceeded 0.995 in all cases. With $H_{N,f}$ and $L_{N,f}$ given, a set of estimates was obtained for the parameter in eqs. 23 and 24 (Table 6) yielding a close agreement between measured and estimated plant height and plant LAI of *C. album* (Fig. 14). From the estimates of eq. 23 a duration of internode extension, $TS_{m,H}$, of 310 °Cd was calculated. Using this value, the oldest node with a growing internode and thus the 'effective' LAI of *C. album* is
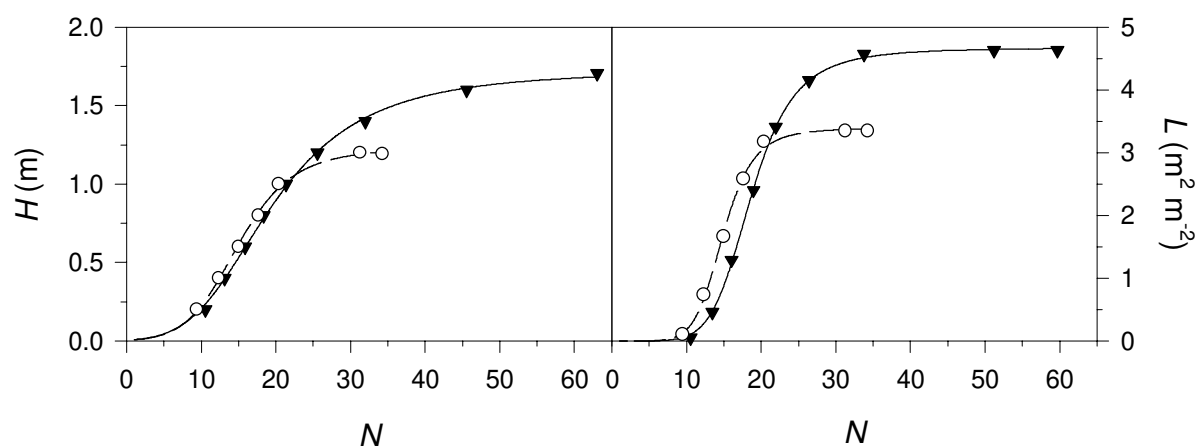
Fig. 13. Chanter growth equations used to interpolate measured plant height, H, *(left) and leaf area index,* L, *(right) of* C. album *as a function of node number,* N. *As an example, data from the pure* C. album *stand at low density in cauliflower experiment 1 (○) and the mixed stand at high density in cauliflower experiment 2 (▼) are shown.*

Table 6. Results of the non-linear least squares regression analyses. The coefficients are given for internode extension, H_N, *and leaf area expansion,* L_N, *on node N as well as for the relationship between the temperature sum after 3-node stage,* TS, *and the 'effective' fraction of LAI,* l_e, *of* C. album. *The asymptotic standard error of the estimates are given in parentheses.*

	Internode length H_N (eq. 23)	Leaf area index L_N (eq. 24)	'Effective' fraction of LAI l_e (eq. 38)
Start parameter, p_0	0.00276 (0.00716)	0.00234 (0.0145)	0.000445 (0.000232)
Specific growth rate, μ (°Cd^{-1})	0.0255 (0.0111)	0.0453 (0.0580)	0.0105 (0.00106)
Function declines at ... °Cd, TS_r	–	591 (9.5)	–
r^2	0.99	0.91	0.98
Maturity time TS_m (°Cd)	310	178	–

readily estimated. Plotting the 'effective' fraction of LAI against the temperature sum (Fig. 15) yields a response, which is interpolated by a modified logistic function

$$l_e = 1 - \frac{p_0}{p_0 + (1 - p_0)\,\mathrm{e}^{-\mu\,TS}} \tag{38}$$

accurately describing the gradual decline from one to zero (Table 6). Eq. 38 can be extrapolated to start from the time of emergence by replacing the thermal time after 3-node stage, *TS*, by *TS* – 200 °Cd and $l_e = 1$ for *TS* < 200 °Cd. This function is implemented in the model and is used to approximate the 'effective' canopy LAI, $L_{e,c}$.
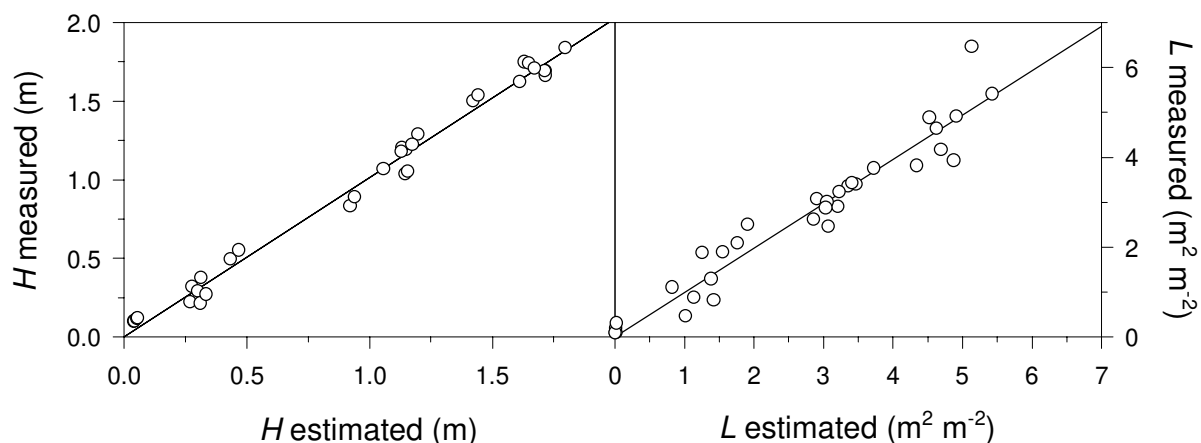

Fig. 14. Correlation between measured plant height, H, *(left) and leaf area index,* L, *(right) of* C. album *and an estimate from the extension of internodes and the expansion of leaf area (eq. 25) on consecutive nodes, respectively. Symbols represent calibration data from the 1995 cauliflower experiments and the lines depict linear regressions which were not significantly different from the bisecting line (α = 0.05). For the results of the parameter estimation see Table 6.*
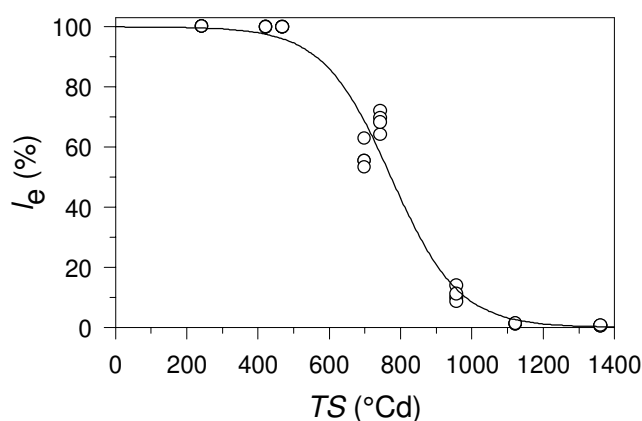

Fig. 15. Relationship between the 'effective' fraction of LAI of C. album, l_e, *and the temperature sum after 3-node stage,* TS. *The symbols represent data obtained by eq. 29 and the line depicts the modified logistic function used for interpolation (eq. 38). For the results of the parameter estimation see Table 6.*

Simulation of plant height and plant diameter of C. album

The thermal stem extension rate is adequately estimated from $L_{e,c}$ by the rectangular hyperbola

$$TSER = \frac{3.33\,(\pm 0.26)\,L_{e,c}}{1.04\,(\pm 0.21) + L_{e,c}} \qquad (\pm\,\text{s.e.}) \tag{39}$$

The variation explained by the function is 90% for the cauliflower data used for calibration and 78% for faba bean data (Fig. 16). *C. album* growing in mixed faba bean plots did not achieve the same height increase rates than plants in a cauliflower crop, although theoretically growing under a high 'effective' canopy LAI. Consequently, *TSER* and thus total height of *C.*
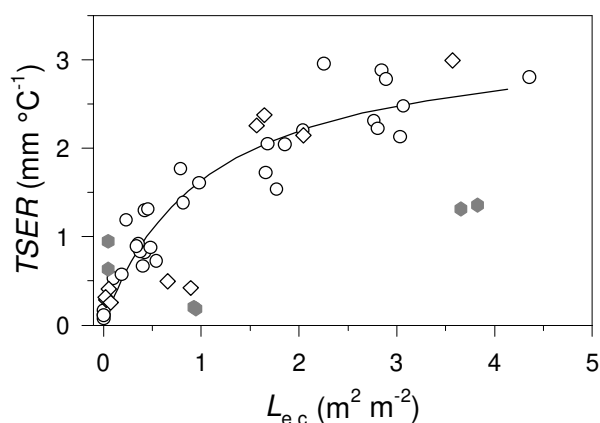

Fig. 16. Relationship between the thermal stem extension rate, TSER, *of* C. album *and the 'effective' canopy LAI,* $L_{e,c}$. *The solid line depicts the rectangular hyperbola* TSER = TSER$_{max}$ $L_{e,c}$ / (c + $L_{e,c}$). *Shown are data from the 1995 cauliflower experiments (○) used for calibration and the monospecific weed plots of the 1994 faba bean trial (◇). Data from* C. album *plants growing under a closed faba bean crop (⬤) are omitted in this analysis.*

album plants growing under a faba bean crop will be considerably overestimated by eq. 39. To account for this effect in the model, the maximum specific stem length was determined

$$SSL_{max} = e^{-2.4\,H + 1.7} \tag{40}$$

The parameters were estimated by eye since the line in Fig. 17 is supposed to be an upper limit enclosing all data points. This value is compared to the actual *SSL*, which is determined with values for stem dry weight obtained by non-linear interpolation between the harvests. Finally, the daily height increase is calculated according to eq. 36. Using all data available, a sufficient description for the plant diameter of *C. album* is achieved by
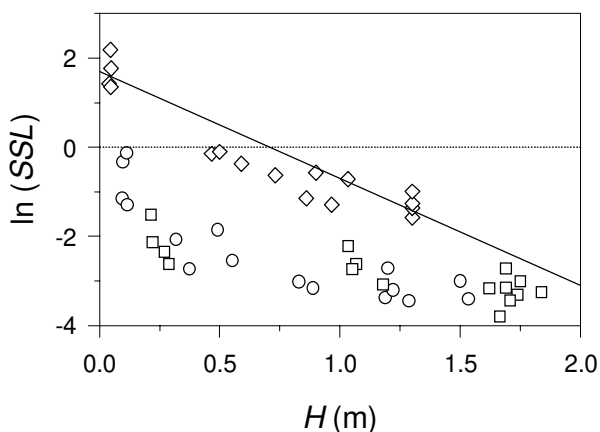
Fig. 17. Relationship between the specific stem length, SSL*, and plant height,* H*, of* C. album*. Symbols indicate data from cauliflower experiment 1 (○), experiment 2 (□) and the 1994 faba bean experiment (◇). The line represents the maximum* SSL *possible in relationship to height.*

$$\frac{\mathrm{d}D}{\mathrm{d}t} = 0.755 \left(\pm 1.16 \; 10^{-5}\right) e^{-0.00181 \left(\pm 6.65 \; 10^{-8}\right) TS - 0.00694 \left(\pm 8.32 \; 10^{-7}\right) PD} \; T_{av} \; 10^{-3} \qquad (\pm \text{s.e.}) \qquad (41)$$

Comparing measured and simulated plant height and plant diameter yielded a good prediction of the spatial development of *C. album* in all environments examined (Fig. 18, Table 7).
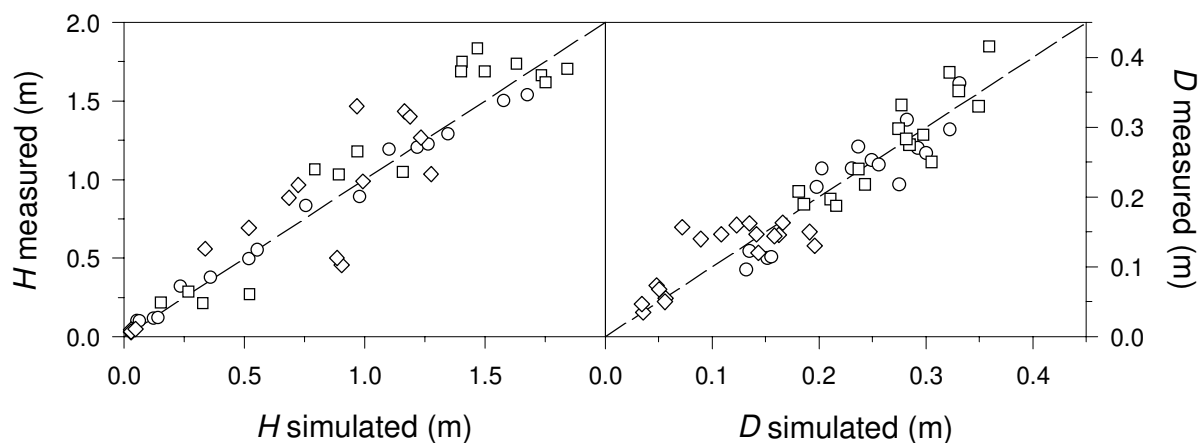
Fig. 18. Comparison between measurements and simulation. Symbols denote data from the cauliflower experiment 1 (○), experiment 2 (□) and the 1994 faba bean experiment (◇). Lines indicate perfect agreement. Left: plant height, H*, of* C. album *estimated as potential height growth corrected with the specific stem length (eq. 36). Right: plant diameter,* D*, of* C. album *simulated as a function of thermal time and plant density (eq. 37). For statistics of the regression see Table 7.*

Table 7. Statistics of the regression analysis measured vs. simulated plant height and plant diameter of C. album*. Shown are the value (± s.e.) of the slope and the intercept, the coefficient of determination and the number of observations. The parameters of all regressions were not significantly different from the properties of the bisecting line (slope = 1, intercept = 0, α = 0.05).*

Simulation of..	Data set	Slope	Intercept	r^2	N
Plant height	Cauliflower 1995	1.04 (± 0.047)	0.027 (± 0.050)	0.94	32
	Faba bean 1994	1.00 (± 0.12)	0.043 (± 0.093)	0.82	18
	All data	1.03 (± 0.047)	0.031 (± 0.045)	0.91	50
Plant diameter	All data	0.96 (± 0.052)	0.0091 (± 0.011)	0.88	50

4.4. Discussion

Data from the field experiments presented here support the findings that spectral changes caused by leaf area (SMITH, 1986) increase plant height growth of *C. album* (MORGAN & SMITH, 1976; 1978). In cauliflower experiment 1 low average temperatures retarded the leaf area development of *C. album* in pure stands. At the same time, the leaf area of cauliflower in mixed stands stimulated internode elongation of *C. album* resulting in significantly taller plants in the early cauliflower experiment. Since plant density did not cause height differences, a marked interspecific effect is assumed. Due to higher temperatures in cauliflower experiment 2, *C. album* was able to establish a larger LAI in pure stands compared to the equivalent treatment in the spring experiment. This distinction could not be observed in mixed stands where leaf area development of *C. album* in experiment 2 corresponded to that of the first trial. It is therefore concluded that in contrast to a temperature limitation in spring, the radiation uptake of *C. album* in mixed stands was reduced by cauliflower slowing leaf area development in summer. The large LAI in pure stands led to a mutual shading, thus inducing an increased internode extension intraspecifically, which resulted in insignificant plant height differences of *C. album* in experiment 2.

In the faba bean experiment the crop emerged earlier than *C. album*. This gave the faba bean a competitive edge that restrained the weed from overgrowing. On the one hand, the constant shading by crop foliage should theoretically incite the height growth of *C. album*. On the other hand, however, the radiation deficiency reduced the dry matter production so considerably that the weed's height growth potential could not be realised. Data on plant

diameter of *C. album* in the cauliflower crops are subject to a higher variability than plant height. Therefore only a general tendency can be verified that lower plant densities produce *C. album* plants with a greater diameter suggesting that the physical space available for the individual determines its diameter. In the faba bean experiment neither plant density nor canopy composition had a marked influence on plant diameter. It is concluded that the value measured in this experiment indicates the least diameter of *C. album*. The vertical leaf area distribution of *C. album* was not modified in the cauliflower experiments. This is presumably due to competition not severe enough in the planting densities examined. An increased stem extension seems to be the initial response to changes in the spectral light quality inside a canopy.

Unlike models proposed hitherto (SPITTERS & AERTS, 1983; KROPFF, 1988; WILES & WILKERSON, 1991), the approach to simulate plant height presented here takes into account that *C. album* displays a distinct morphological plasticity to spectral changes in the canopy. From experimental data on plant height and LAI of *C. album* a model is constructed that reproduces the growth of both plant characteristics on a node level. It is assumed that the node position only defines the maximum value for internode length or LAI, but it does not alter the logistic course of progress and thus the duration of the process. This is confirmed by results found for faba bean (KASIM & DENNETT, 1986a), irrigated potatoes (JEFFERIES, 1989) and summer rape (MORRISON ET AL., 1992), where leaf position did not have a significant effect on leaf expansion duration ranging from 140 to about 300 °Cd. Consequently, the expansion duration of *C. album* leaves of 178 °Cd (Table 6) estimated by eq. 26 seems appropriate. The calculation of the 'effective' canopy LAI by setting a height threshold (eq. 30) considers leaf area of neighbouring plants, which is not in close proximity of extending internodes. This summary approach therefore also accounts for the reaction to spectral changes in reflected radiation (BALLARÉ ET AL., 1987). Since the model does not distinguish between inter- and intraspecific shading, it is likewise applicable to describe the situation in mixed stands of *C. album* and cauliflower as well as the conditions in pure stands at different densities. A close relationship between the 'effective' canopy LAI and the potential thermal stem extension rate of *C. album* could be established that integrates three dependencies: (a) between LAI and the red:far-red ratio (HOLMES & SMITH, 1977), (b) between the red:far-red ratio and the phytochrome equilibrium (SMITH & HOLMES, 1977) and (c) between the phytochrome equilibrium and the stem extension rate (SMITH, 1982). The rectangular hyperbola used asymptotically approaches a maximum which allows an extrapolation without predicting

unrealistic extension rates. Care has to be taken, however, when the shading becomes so substantial that dry matter production is reduced below the requirements for potential height growth. Although purely empirical, the introduction of the maximum specific stem length effectively restricts height development under low light conditions. The estimated parameter, however, deviate substantially from those reported by KROPFF (1993), who examined the height development of *C. album* at a maximum plant density of 22 plants m^{-2} in competition with sugar beet. The variation to the results presented here is presumably due to the higher degree of inter- and intraspecific competition in the faba bean experiment.

The model presently ignores the effect of water and nutrient availability on the morphological development of *C. album*. But in high-input vegetable production it is common practice to amply irrigate and fertilise, so that an insufficient supply of both growth factors is not likely to occur. Thus, the model provides a useful tool to more dynamically predict the plant height of *C. album* in horticultural crops.

Most of the models for crop-weed interactions proposed hitherto (SPITTERS & AERTS, 1983; KROPFF, 1988; WILES & WILKERSON, 1991) use essentially one-dimensional light transmission models, which require the simulation of plant height alone. When radiation interception is modelled in three dimensions (GRACE ET AL., 1987; RYEL ET AL., 1990; Chapter 3), it is further necessary to determine the plants' expansion over the plane. Since these 3-D approaches use rotary geometrical solids to describe the shape of plants, the diameter (or radius) of plants has to be estimated. Experimental data have shown that plant density and thus the physical space available have a significant influence on plant diameter. Combined with plant age represented by the temperature sum, a sufficiently accurate relationship could be established. It was, however, necessary to use all available data for calibration leaving no independent data set for evaluation. Nevertheless, the approach seems to be promising, because the experimental variation covers rather contrasting competitive situations.

In summary, experimental observations confirm earlier findings (MORGAN & SMITH, 1976; HUGHES & WAGNER, 1987) that *C. album* shows a distinct morphological plasticity due to a modification in the light environment. Using an estimate for the fraction of leaf area assumed to be mainly responsible for these changes, the model presented here can explain the adaptation of stem extension of *C. album* plants in response to their light environment. It therefore extends existing approaches of plant height simulation as a function of temperature

only. Restrictions of height growth due to assimilate limitations are included in the model by using the approach of the maximum specific stem length. Given that the diameter of *C. album* plants is simulated sufficiently accurate and the vertical leaf area distribution remains unchanged, it is possible to determine the plant dimensions for any time during the growing period. This should lead to a more precise quantification of radiation interception by weeds and their effects on crops due to light competition.

5. Dry matter production and partitioning of *Chenopodium album* in contrasting competitive environments

Simple models were developed to quantify dry matter production and the effects of competition on dry matter partitioning of *C. album*. After germination, *C. album* produced biomass rapidly; weeds planted at low density accumulated 20 to 30 % less dry matter than plants growing at a 2.5-fold higher density. A close correlation between the transmission of photosynthetically active radiation (PAR) and the LAI was found. Biomass production was linearly related to cumulative intercepted PAR, but a seasonal variation of the light-use efficiency could not entirely be explained. The fraction of root dry matter was unaffected by competition, whereas planting density and canopy composition slightly changed the distribution pattern between stems and leaves. With increasing competition in the cauliflower experiments, *C. album* allocated relatively more biomass to stems than to leaves; this was less evident in mixtures with faba bean. In field vegetable production with an abundant water and nutrient supply, simple allometric relationships for dry matter distribution are adequate.

5.1. Introduction

Mechanistic models on competition between crops and weeds (SPITTERS & AERTS, 1983; WILKERSON ET AL., 1990; KINIRY ET AL., 1992b; KROPFF & SPITTERS, 1992a) are generally based on crop growth models (VAN KEULEN ET AL., 1982; WILKERSON ET AL., 1983; SPITTERS ET AL., 1989; WILLIAMS ET AL., 1989) which explicitly represent the processes of radiation interception, dry matter production and distribution. Particularly the latter was identified to be inadequately simulated in crop growth modelling (DE WIT & PENNING DE VRIES, 1985; MARCELIS, 1993).

Dry matter production of plants has been investigated thoroughly in the past and many models were proposed hitherto. Precise descriptions of the biochemical processes within a leaf (EVANS & FARQUHAR, 1991; HARLEY & TENHUNEN, 1991) usually have a number of input parameter not readily to be measured in field experiments. More aggregated formulations of plant assimilation (ACOCK ET AL., 1978; CHARLES-EDWARDS, 1981) are aiming at a precise description of the summary system response. Although not able to explain details of the photosynthetic mechanism, they yield quantitatively sound predictions of canopy assimilation and are frequently incorporated into crop growth models. The calibration of these models requires experimental data on canopy gas exchange characteristics, which have already been determined for some weeds species. It is difficult, however, to obtain these parameters for all major weeds for a comprehensive model describing the complex multispecific system found in the field. An easy and sufficiently accurate approach are canopy-integrated estimates of the light-use efficiency (MONTEITH, 1977). Since data on dry matter accumulation and light

transmission are easily acquired in field experiments, the light-use efficiency of weeds can readily be estimated.

Dry matter distribution is a process hardly understood on both the cell and the whole-plant level (FARRAR, 1988). Not only are the internal variables controlling the allocation pattern far from being known, the effects of environmental factors such as temperature on these parameters are complex. As a consequence, no valid theory exists to mechanistically simulate biomass partitioning (EVANS, 1990). Thus, among the numerous approaches proposed (see review by MARCELIS, 1993) empirical descriptions prevail. Especially in weeds, time dependent partitioning coefficients are commonly used (SPITTERS & AERTS, 1983; WILKERSON ET AL., 1990; KINIRY ET AL., 1992b; KROPFF & SPITTERS, 1992a). As even these simple approaches are occasionally not completely calibrated (KROPFF & SPITTERS, 1992a), it seems necessary to inquire into formulations that should require easily obtainable data and have a potential for extrapolation.

C. album has previously been used as a competitor to sugar beet in a mechanistic crop-weed model (KROPFF & SPITTERS, 1992a;b). The photosynthetic characteristics of *C. album* were hitherto repeatedly measured showing a wide range of gas exchange rates under high irradiances (Table 8). As a typical C_3 species of the temperate zone, *C. album* is photosynthetically more efficient at low than at high temperatures compared to the C_4 weed species *Amaranthus retroflexus* L. (CHU ET AL., 1978; PEARCY ET AL., 1981). STOLLER &

Table 8. Gas exchange rates of C. album *measured under high irradiances. The original units are converted for comparability.*

CO$_2$ exchange rate	PAR	External CO$_2$-conc.		Mean air temperature		Reference
kg ha^{-1} h^{-1}	µmol m^{-2} s^{-1}	—— ppm ——		—— °C ——		
57[†]	1800	300-330		16, 22.7, 32		(1)
27.5[†]	1140[‡]	340		23		(2)
34.2[†]	1000	330		-		(3)

Reference

(1) PEARCY ET AL. (1981)   (3) STOLLER & MYERS (1989)

(2) VAN OORSCHOT & VAN LEEUWEN (1984)

[†] estimated from graph   [‡] converted with 4.56 µmol m^{-2} s^{-1} for 1 W m^{-2} [-] not available

MYERS (1989) reported that under reduced irradiance *C. album* adjusted its gas exchange, but the ratio of support tissue (roots, stems and petioles) to leaves was unaffected. Similarly, spatial restrictions in either root or shoot zone hardly altered the allocation pattern of *C. album* (MCCONNAUGHAY & BAZZAZ, 1992a;b).

PERSALL (1927) and TROUGHTON (1956) used the allometric growth formula

$$W_R = e^a \, W_{Sh}^b \quad \text{which is linearised to} \quad \ln W_R = a + b \ln W_{Sh} \tag{42}$$

to describe the root:shoot ratio. W_{Sh} and W_R are the dry weights of shoots and roots, respectively, *a* and *b* are constants. Eq. 42 implies a fixed ratio, *b*, between the relative growth rates of shoots and roots. This parameter is also called 'allometric growth coefficient' and can be considered a measure for the intensity of the differential variation between the growth of the compartments (CARADUS ET AL., 1995): if treatments have an effect on partitioning it will become evident in changes of *b*. TESCH ET AL. (1992) reported that the root:shoot balance of Douglas-fir seedlings was not changed by moderate and strong competition with a sclerophyllous shrub resulting in consistent allometric growth coefficients. Other impacts on plant growth were likewise shown to have insignificant effects on root:shoot allometry. Cowpeas (*Vigna unguiculata* L.) did not alter their distribution pattern when infected with *Striga gesneroides* (HIBBERD ET AL., 1996a). A near-isometric growth of roots and shoots in barley was neither influenced by an infection with powdery mildew nor by an elevated CO_2 concentration (HIBBERD ET AL., 1996b). Modifications of the root:shoot ratio were reported by CARADUS ET AL. (1995), where white clover cultivars responded differently to phosphorus. They concluded that these changes in allometry were due to limited nitrogen uptake with high levels of phosphorus. GEDROC ET AL. (1996) presented a significant linear allometric relationship for *C. album* plants in a high nutrient regime showing only minor deviations from linearity when the nutrient supply was reduced. These results support the assumption that root:shoot allometry gives a robust description of the distribution between above- and below-ground dry matter in a wide range of agronomic conditions. The aim of the present paper is to quantify the dry matter production and the influence of competition on dry matter allocation of *C. album* using simple functional relationships.

5.2. Model description

Dry matter production

Between measurements light transmission was interpolated. Therefore, the canopy light extinction coefficient, K, was determined first

$$\frac{I}{I_0} = T = e^{-K\,L} \quad \text{which is linearised to} \quad \ln(T) = -K\,L \tag{43}$$

where I_0 and I are the light intensities on a horizontal plane above and below a canopy, respectively, T denotes the relative light transmission and L the canopy leaf area index (MONSI & SAEKI, 1953). A sigmoid function was used to obtain interpolated values for L between harvests. The cumulative intercepted PAR, J, was then given by

$$J = \sum_{d=0}^{t} S_d \left(1 - e^{-K\,L_d}\right) \tag{44}$$

where t is the growing period in days, S_d (MJ m^{-2}) and L_d are the daily PAR and the LAI on day d, respectively. Total plant dry matter W_T and J are linearly related with the slope representing the light-use efficiency, *LUE*

$$W_T = LUE\ J \tag{45}$$

Dry matter partitioning

The partitioning of plant dry matter between shoot and root was determined by the allometric growth function (eq. 42). The intercept a and the slope b were determined by plotting root, W_R, against shoot weight, W_{Sh}, after a ln-transformation.

The allocation of shoot biomass between stems and leaves was investigated by using the approach presented by STÜTZEL & AUFHAMMER (1991a). Emanating from the concept of a primary (physiologically active) and a secondary (structural) stem component they derived a relationship between stem and leaf dry weight by

$$W_S = d\ W_L^{g/2} + f\ W_L^{g} \tag{46}$$

where W_S and W_L are stem and leaf biomass, respectively (see eq. 16 in STÜTZEL & AUFHAMMER, 1991a). The coefficients d, f and g are constants. For a detailed derivation of eq. 46 see STÜTZEL ET AL. (1988) and STÜTZEL & AUFHAMMER (1991a).

5.3. Results

Although plant density of *C. album* varied by a factor of 2 (faba bean experiment) and 2.5 (cauliflower experiments), the weeds' total biomass in pure stands at high and low density differed only by 20 to 30 % in later growth stages (Fig. 19). In cauliflower experiment 2, total biomass growth of *C. album* was promoted by increased light intensities and higher temperatures during the juvenile development. A lag of approximately 20 days between
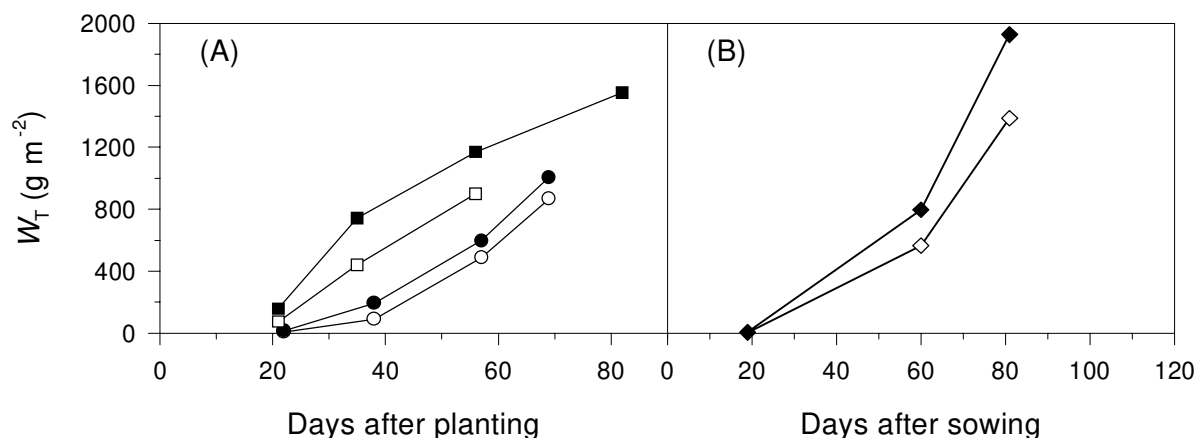

Fig. 19. Total dry weight, W_T, *of* C. album *from pure weed stands in (A) cauliflower experiment 1* ($\circ$,$\bullet$) *and experiment 2* ($\square$,$\blacksquare$) *and (B) the faba bean experiment* ($\diamond$,$\blacklozenge$). *Open and filled symbols depict low and high density plots, respectively. Due to a sampling error, data from harvest 4 in low density plots of cauliflower experiment 2 could not be evaluated.*

sowing and emergence was the reason for a late onset of competition in the mixed plots with faba bean. Data from pure stands of *C. album* in both cauliflower experiments revealed a strong linear relationship between the natural logarithm of the transmitted fraction of PAR and the leaf area index (Fig. 20). Light-use efficiency did not differ significantly between high and low density plots, but a significant difference was apparent between cauliflower experiment 1 and 2 (Fig. 21).
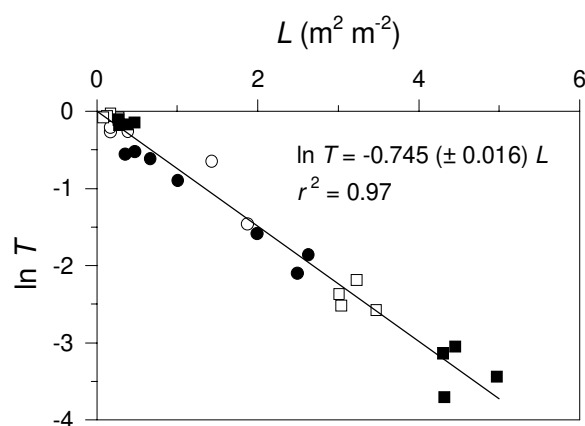
Fig. 20. Relationship between the transmission of PAR, T, *and the leaf area index,* L, *of* C. album. *Data are from pure weed stands in cauliflower experiment 1 (○,●) and experiment 2 (□,■). Open and filled symbols depict low and high density plots, respectively, and the value in parentheses denotes s.e.*
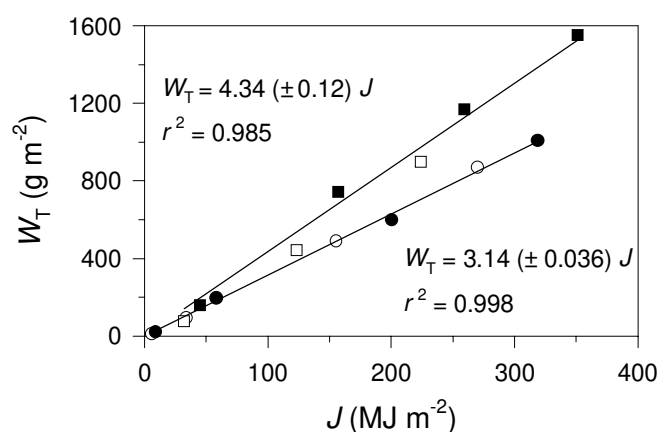

Fig. 21. Relationship between the total dry weight, W_T, *and the cumulative PAR intercepted,* J, *of* C. album. *Symbol definition corresponds with Fig. 20 and values in parentheses denote s.e.*

Allocation between roots, leaves and stems (including petioles) followed a similar trend in all environments examined (Fig. 22). The root fraction laid between 10 and 15 % throughout the growth cycle in all experiments. The leaf fraction was high in early growth stages, but the share of stem biomass increased during the growing period until about 75 % of the total dry weight consisted of stem tissue. Dry matter partitioning between root and shoot was well described by an allometric relationship (Fig. 23A, B). The coefficients obtained (Table 9) represent a near isometric growth ($b \approx 1$) and the constant root fraction ($e^a \approx 0.11$).
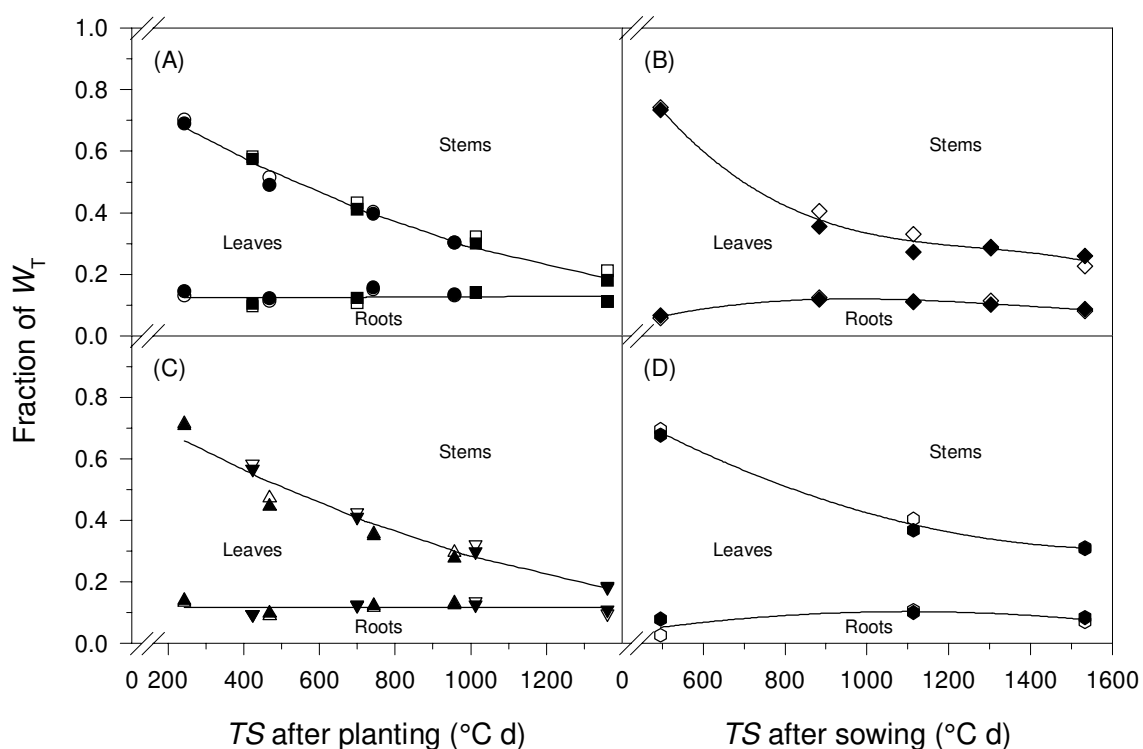
Fig. 22. Fraction of roots, leaves and stems on total dry weight, W_T, during the development of C. album. *(A) Pure stands in cauliflower experiment 1 ($\circ$, $\bullet$) and experiment 2 ($\square$, $\blacksquare$). (B) Pure stands in faba bean experiment ($\diamond$, $\blacklozenge$). (C) Mixed stands with cauliflower in experiment 1 ($\triangle$, $\blacktriangle$) and experiment 2 ($\triangledown$, $\blacktriangledown$). (D) Mixed stands with faba bean ($\ominus$, $\ominus$). Lines are polynomials to indicate the prevailing trend.*

Table 9. Equation coefficients, their corresponding standard error (s.e.) and the coefficient of determination (r^2) of the allometric relationship between shoot and root biomass: $\ln W_R = a + b \ln W_{Sh}$ *(eq. 42).*

| Experiment	Plot/density	a	s.e.	b	s.e.	r^2
Cauliflower	pure/low	-2.18	0.24	1.06	0.044	0.990
Cauliflower	pure/high	-1.72	0.29	0.99	0.054	0.983
Cauliflower	mixed/low	-1.73	0.33	1.01	0.055	0.982
Cauliflower	mixed/high	-1.63	0.30	0.96	0.051	0.984
Cauliflower	all variants	-1.85	0.14	1.01	0.025	0.983
Faba bean	all/low	-2.56	0.44	1.12	0.076	0.977
Faba bean	all/high	-2.41	0.20	1.09	0.034	0.994
Faba bean	all variants	-2.46	0.19	1.10	0.034	0.988
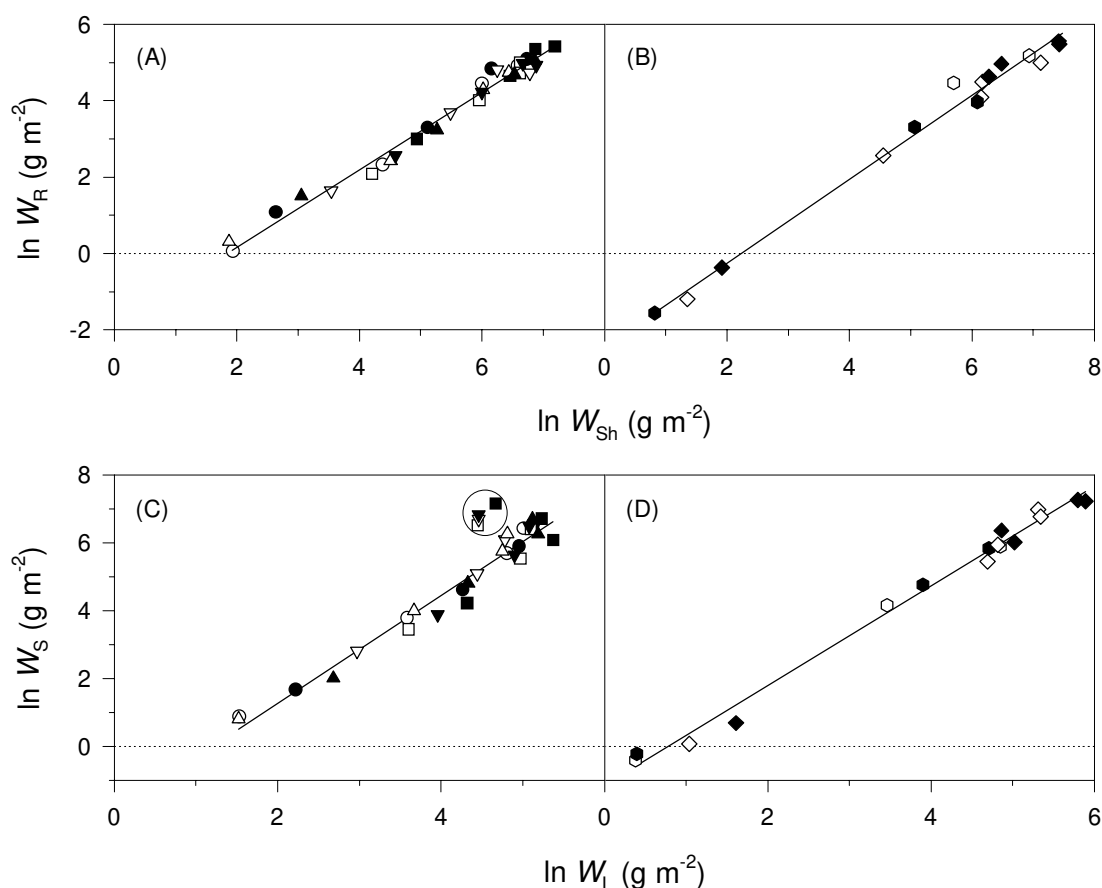
Fig. 23. Relationships between the natural logarithms of root, W_R, and shoot dry weight, W_{Sh}, (top row) and stem, W_S, and leaf dry weight, W_L, (bottom row) of C. album. *Data are from both cauliflower experiments (A and C) and the faba bean experiment (B and D). The circled data in C come from senescent plants and are omitted from the regression. For the symbol definition see legend of Fig. 22. Lines represent the linear relationship of all variants within an experiment. The coefficients and statistics of the regressions are listed in Table 9 (root:shoot) and Table 10 (stem:leaf).*

The estimation of the coefficients in eq. 46 for the distribution of shoot biomass between stem and leaves gave values for *d* not significantly different from zero. Thus, the first term in eq. 46 could be omitted and the remainder was linearised to yield

$$\ln W_S = h + g \ln W_L \qquad \text{where} \qquad h = \ln f \tag{47}$$

Fig. 23C and D show a close linear relationship between the natural logarithms of stem and leaf dry weight as predicted by eq. 47. A deviation from linearity was observed, however, during later growing stages of *C. album.* At the last harvest of cauliflower experiment 2 leaves started to senescence and drop (Fig. 23C, circled data), whereas stems continued to grow. Thus, leaves may have been sampled incompletely and were excluded from the regression analyses summarised in Table 10. In the cauliflower experiments the allometric growth

Table 10. Equation coefficients, their corresponding standard error (s.e.) and the coefficient of determination (r^2) of the allometric relationship between leaf and stem biomass: $\ln W_S = h + g \ln W_L$ *(eq. 47).*

Experiment	Plot/density	h	s.e.	g	s.e.	r^2
Cauliflower	pure low	-1.66	0.47	1.53	0.11	0.975
Cauliflower	pure high	-2.07	0.76	1.59	0.16	0.950
Cauliflower	mixed low	-1.80	0.32	1.61	0.079	0.988
Cauliflower	mixed high	-3.08	0.61	1.83	0.13	0.974
Cauliflower	all variants	-1.90	0.26	1.59	0.059	0.965
Faba bean	all/low	-1.20	0.20	1.48	0.049	0.994
Faba bean	all/high	-1.09	0.28	1.45	0.064	0.988
Faba bean	all variants	-1.14	0.16	1.47	0.038	0.991

coefficient, *g*, increased with the level of competition. This trend, however, could not be observed in the faba bean experiment, where the lowest values were found despite severe competition. The intercept and the slope of the allometric equations were linearly related: a regression analysis yielded a significant correlation between *a* and *b* from eq. 42 (Fig. 24A) as well as between *h* and *g* from eq. 47 (Fig. 24B). Values found for the stem:leaf ratio coincided with those reported for faba bean (STÜTZEL & AUFHAMMER, 1991a).
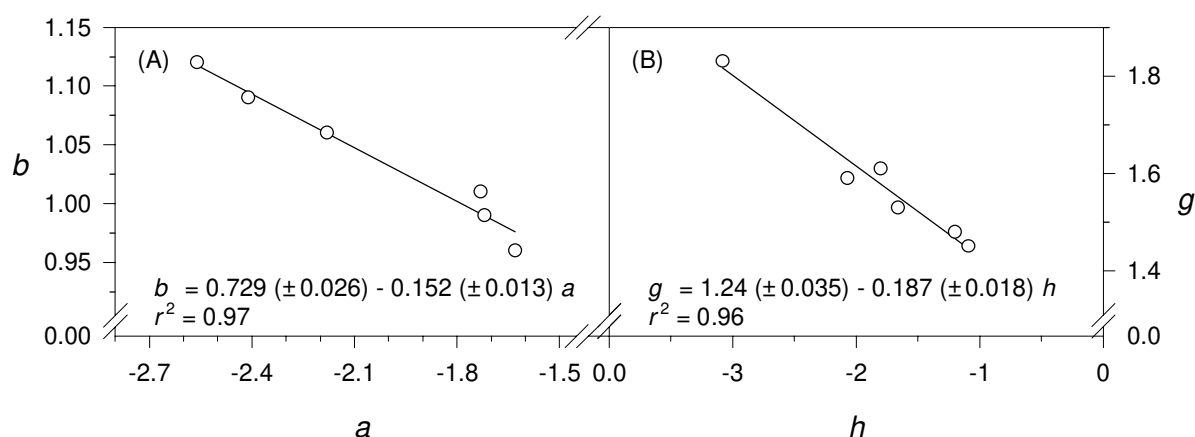

Fig. 24. Relationship between the slope and intercept of the allometric equations for the root:shoot ratio (A) and stem:leaf ratio (B). Data are from Table 9 and Table 10, values in parentheses denote s.e.

5.4. Discussion

To simulate the growth of weeds in a mixed canopy, information is necessary on the light environment of the weed plants, their dry matter production in relation to light interception and the biomass partitioning into the various organs. Especially dry matter allocated to leaves is of interest, since these are the organs mainly responsible for light interception. While a model for the light environment in crop-weed canopies is presented in Chapter 3, growth and dry matter partitioning of *C. album* are analysed here.

The concept of the light-use efficiency (MONTEITH, 1977) has been successfully applied in crop growth models of various plant species like faba bean (STÜTZEL & AUFHAMMER, 1991b), soybean (SINCLAIR & SHIRAIWA, 1993), sunflower (GIMENEZ ET AL., 1994; HALL ET AL., 1995) and vegetable crops (TEI ET AL., 1996). KINIRY ET AL. (1992b) used this approach to simulate the influence of three weed species on crop growth and derive *LUE* values for C_3 weed species ranging from 3.3 to 3.7 g MJ^{-1}. KROPFF & VAN LAAR (1993) gave an estimate of *LUE* for *C. album* amounting to 4.0 g MJ^{-1} in early and 2.5 g MJ^{-1} in later growth stages. Such a segmented relationship could not be confirmed by the results presented here. Relationships between the cumulative intercepted PAR and total dry weight in pure stands of *C. album* in both cauliflower experiments were significant. But the value of 4.3 g MJ^{-1} calculated from cauliflower experiment 2 seemed rather outside the expected range. Several variables have been determined hitherto to influence *LUE* of a plant species (Table 11). The suggestion of STÜTZEL & AUFHAMMER (1991b) to calculate *LUE* from the light extinction coefficient was not applicable, as the values for *K* in both cauliflower experiments did not differ significantly. A tangible sensitivity of *LUE* on specific leaf nitrogen (*SLN*, g N m^{-2} leaf) is only to be expected at low *SLN* (SINCLAIR & HORIE, 1989). In the present experiments, however, nitrogen was applied based on the soil analyses taken in high weed density plots in mixtures with cauliflower, thus satisfying the combined demand of crop and weed. It is therefore unlikely that the plants in pure weed stands were suboptimally supplied. The influence of the atmospheric transmissivity and hence the diffuse fraction of incident radiation on *LUE* (SINCLAIR ET AL., 1992; HAMMER & WRIGHT, 1994) are also negligible, as the values differed only slightly between the experiments. The daily global radiation averaged over the growing period was by *c.* 4 MJ m^{-2} higher in the first than in the second trial. Assuming the relationship proposed by MANRIQUE ET AL. (1991) of -0.15 (g MJ^{-1}) MJ^{-1}, this would account for a difference of ~0.6 g MJ^{-1}. The same authors quantified the temperature effects on *LUE* to -0.12 (g MJ^{-1}) °C^{-1}, although the parameter correlate only poorly ($r^2 = 0.34$). As the mean

Table 11. Possible sources of variation in light-use efficiency, LUE*, within a plant species.*

Variable	Influence on *LUE* with increasing variable value	Reference
Light extinction coefficient	Decrease	(8)
Specific leaf nitrogen (g N m^{-2})	Increase	(3) (7) (12) (13)
Fraction of diffuse radiation	Increase	(6) (10) (11) (12) (14)
Level of global radiation (MJ m^{-2})	Decrease	(1) (2) (5) (11) (12) (14)
Ambient temperature (°C)	Decrease	(5) (13)
Vapour pressure deficit (kPa)	Decrease	(4) (5) (9)

Reference:

(1)   MURATA (1981)
(2)   KASIM & DENNETT (1986b)
(3)   SINCLAIR & HORIE (1989)
(4)   STÖCKLE & KINIRY (1990)
(5)   MANRIQUE ET AL. (1991)
(6)   NORMAN & ARKEBAUER (1991)
(7)   SINCLAIR (1991)

(8)   STÜTZEL & AUFHAMMER (1991b)
(9)   KINIRY ET AL. (1992a)
(10)   SINCLAIR ET AL. (1992)
(11)   SINCLAIR & SHIRAIWA (1993)
(12)   HAMMER & WRIGHT (1994)
(13)   HAXELTINE & PRENTICE (1996)
(14)   BANGE ET AL. (1997)

temperature was higher in the second experiment by *c.* 2.5 °C, this reduces the variance explained by the irradiance level. In both trials the vapour pressure deficit (*VPD*, kPa) hardly exceeded the threshold value of 1.0 kPa, above which *LUE* is supposed to decrease (STÖCKLE & KINIRY, 1990; KINIRY ET AL., 1992a) making a major influence of *VPD* improbable. The differences in *LUE* found in the trials are not satisfactorily explicable by the variation of internal or external factors. An artefact can also not completely be ruled out: as the global radiation sensor of the on-site automatic weather station is located only 2 m above ground level, it is possible that a dust cover might have obstructed the sensor's field of vision and thus data below the genuine values have been logged. Since no comparable data are available, a light-use efficiency specific for each experiment will have to be used in the model.

A description of dry matter partitioning with allometric relationships is essentially empirical (WILSON, 1988; MARCELIS, 1993). But the constant root fraction of *C. album* in all competitive situations indicates a consistent functional relationship which tallies with published data (MCCONNAUGHAY & BAZZAZ, 1992a;b; GEDROC ET AL., 1996). The resulting

isometry of the root:shoot ratio can therefore be expected to be appropriate for a range of agronomic environments.

STÜTZEL & AUFHAMMER (1991a) showed that planting density and ontogenetic processes significantly influence dry matter partitioning between leaves and stems. With a higher degree of competition *C. album* allocated relatively more biomass to stems than to leaves, which is reflected by an increasing allometric growth coefficient in the cauliflower experiments. In the faba bean experiment the lowest coefficients were found, although competition was even stronger reducing the available space and the weight per plant of *C. album*. Fewer branches and thinner stems were the result of less dry matter distribution to stem tissue than to leaves. The influence of ontogeny on the stem:leaf ratio was obvious in cauliflower experiment 2. Since the transplantation at the 3-node stage gave *C. album* a competitive edge, only in this trial the weeds reached maturity and plants were notably senescent altering the allocation pattern. Compared to agricultural root crops, where *C. album* infestations are similarly problematic, vegetable crops usually have a shorter growing period. It is therefore not likely that *C. album* completes its whole generative cycle from emergence to maturity in crops like cauliflower. Thus, as a simplification, ontogenetic effects on biomass allocation as well as to model the partitioning into reproductive organs can be omitted. The strong linear relationships between the allometric constants indicate that dry matter distribution of *C. album* is primarily determined by one coefficient only.

In conclusion, dry matter production of *C. album* can in principle be estimated by the light-use efficiency concept, although better knowledge of the factors determining the magnitude of *LUE* is required. Under optimum water and nutrient supply the root proportion appears to be constant, irrespective of planting density. Plant density of *C. album* had an effect on the allometric relationship between stem and leaf growth. The implications to this effect will have to be examined in a simulation model.

6. A model for light competition between crops and weeds

A precise prediction of the yield losses inflicted by weeds is the basis of decisions in weed management. Hitherto, only rough estimates are available for vegetable crops which neglect the specific production situation. This study was conducted to develop a simple simulation model that estimates the yield loss by light competition as a function of environmental variables. In the model, the distribution of incoming radiation is calculated using a spatially high-resolved approach. Growth is calculated as a function of absorbed light and its utilisation. Newly produced dry matter is allocated to roots and shoots, the latter comprising vegetative and generative organs according to the developmental stage. Vegetative shoot dry matter is partitioned according to the main functions of light interception (leaves) and structural stability (stems and petioles). The resulting leaf area is distributed in the canopy according to the spatial expansion of individual plants. Calibration runs revealed uncertainties predicting the growth of *C. album* and a high sensitivity on the leaf area development. With the LAI of *C. album* as input a good correspondence between simulated and observed yield loss of cauliflower was found. Since the plant height of *C. album* is calculated as a function of leaf area, this variable has a multiple effect on light absorption. A first evaluation with an independent data set likewise gave an acceptable prediction. To reduce model complexity, a simplified version is proposed.

6.1. Introduction

To optimise weed control measures, a reliable estimate of the expected impact on crop yield is required. Hence in vegetable production 'critical periods' of weed competition were defined as the time interval during which a crop has to be kept weed-free to achieve the maximum yield (NIETO ET AL., 1968; ROBERTS, 1976). 'Critical periods' were determined empirically for a range of crops (HEWSON & ROBERTS, 1971; 1973; FRIESEN, 1979; WEAVER & TAN, 1983; WEAVER, 1984; QASEM, 1992), but this concept ignores the influence of the site-specific ecological and agronomic conditions and is therefore not an adequate method for decision support in weed control. Consequently, the effects of weeds on crop growth and yield can only be accurately quantified, if the competitive system is simulated as authentic as possible taking the specific production situation into account.

A large number of simulation models was developed to extrapolate the results of experimental field studies. These are in majority empirical regression models describing yield losses statically by a single equation based on one or more parameters such as weed density, relative leaf area or relative time of weed emergence (BAEUMER & DE WIT, 1968; WRIGHT, 1981; COUSENS, 1985; COUSENS ET AL., 1987; BRAIN & COUSENS, 1990; KROPFF & SPITTERS, 1991; LOTZ ET AL., 1992). Since the estimated parameter values often vary considerably between locations and years, the potential for extrapolation is limited. To achieve results valid more universally, resource-consuming field experiments would have to be carried out repeatedly for additional calibrations. Furthermore, the coefficients of empirical models commonly lack a

physiological basis, thus giving no insight into the causal relationships underlying crop-weed competition. Competition in the sense of process-oriented models is defined as the distribution of growth-limiting factors between species in a vegetation canopy and the efficiency of each species to use these resources for biomass production (SPITTERS, 1990). These resources comprise light, nutrients and water, which are modelled with a varying degree of detail dependent on the situation to be examined. With this approach, crucial determinants of crop-weed competition can be identified and used for the manipulation of the competitive relationships. Moreover, processes not well understood are disclosed, suggesting fields for further investigations. Most mechanistic models on competition between crops and weeds (SPITTERS & AERTS, 1983; WILKERSON ET AL., 1990; KINIRY ET AL., 1992b; KROPFF & SPITTERS, 1992a; DEBAEKE ET AL., 1997) were derived from models of crop growth in monoculture (VAN KEULEN ET AL., 1982; WILKERSON ET AL., 1983; SPITTERS ET AL., 1989; WILLIAMS ET AL., 1989). To quantify the light interception of competing species, the canopy is divided into horizontal layers in which the species have a different share of total leaf area. In principle, either the height (SPITTERS & AERTS, 1983; RIMMINGTON, 1984; SPITTERS, 1989; BARNES ET AL., 1990) or the number of layers (WILKERSON ET AL., 1990) is held constant. This approach is basically one-dimensional assuming a homogeneous leaf area distribution within a layer. To account for a horizontally heterogeneous leaf area distribution in row canopies, WILKERSON ET AL. (1990) proposed an empirical approach by calculating light interception based on a competitive factor and an 'area of influence'. The latter is defined as 'a rectangle of width equal to the rowspacing and length down to the crop row equal to the weed canopy diameter'. After validation, these models can be applied to systems in other environments (KROPFF ET AL., 1993), but are rarely used in practical weed management which is often due to a large number of parameters.

In the simulation study presented here, special attention is drawn to the competition for light in heterogeneous plant canopies. This considers the particular situation of vegetable production where (a) a range of field crops is usually planted in widely spaced rectangular patterns, thus being rather single plants than 'closed' or row canopies and (b) the competitive situation is mainly reduced to light competition due to the common practice to amply irrigate and fertilise. In this specific situation, the spatial development of competing plants and their morphological adaptation to unfavourable growth conditions strongly influences the distribution of light within the canopy. Therefore, a three-dimensional light interception model presented in Chapter 3 is extended to calculate the radiation uptake in multispecies

canopies. This improves existing approaches, because a horizontal heterogeneity of leaf area distribution and its implication on competition can explicitly be described. Close attention has been drawn to quantify the morphological plasticity of *C. album* under competition (Chapter 4) and dry matter production and distribution of *C. album* in different environments (Chapter 5). This paper gives details on (a) the principles of the model and its calibration, (b) simulation results with an independent data set and (c) a simplified model derived from the spatially high resolved approach to reduce complexity and to adapt the simulation to an intended use in decision support.

6.2. Model description

The model presented here was derived from a crop growth simulation for faba bean (STÜTZEL, 1995a;b), which calculates plant growth based on the photosynthetically active radiation. The calculation of the canopy light absorption profile is based on the leaf area distribution in three dimensions. From the absorbed light and the efficiency of its use, the total growth rate of the competing species is estimated. The biomass produced is partitioned into the various plant organs. From the leaf dry weight and the specific leaf area, the LAI is calculated, which is distributed in the canopy according to plant positions and dimensions. Developmental processes such as vernalisation and ontogeny are modelled as a function of ambient temperature.

The light absorption submodel (Chapter 3) is extended to mixed stands and calculates a daily total of absorbed radiation, I_a (eq. 21), for each species. The increase of total plant biomass, W_T, is calculated as a function of I_a and the light-use efficiency, *LUE* (MONTEITH, 1977)

$$\frac{\mathrm{d}W_T}{\mathrm{d}t} = I_a \; LUE \tag{48}$$

Throughout an experiment the light-use efficiency is a constant parameter for *C. album*, but considerable variation between experiments was observed (Chapter 5). In cauliflower, *LUE* is defined as a function of light intensity to explain seasonal variations as well as dry matter losses due to competition. A log-normal function was used to describe this relationship

$$LUE = -LUE_{min} + e_1 \; \mathrm{e}^{-0.5\left(\frac{\ln\left(I_{0,c}/I_{0,LUE\,max}\right)}{e_2}\right)^2} \tag{49}$$

where LUE_{min} is the minimum LUE, $I_{0,c}$ is the light intensity on a horizontal plane above the cauliflower crop, $I_{0,\,LUE\,max}$ is the light intensity where LUE maximises, and e_1 and e_2 are constants. If I_0 is the incoming light intensity and $I_{a,t}$ denotes the total light absorption of the canopy, the light intensity above species S, $I_{0,c,S}$, amounts to

$$I_{0,c,S} = I_0 - \left(I_{a,t} - I_{a,H_S} \right) \tag{50}$$

where I_{a,H_S} is the canopy light absorption from the height of species S down to ground level. In the case of a monospecific canopy $I_{0,c}$ equals I_0, in mixtures the term in parentheses represents the light absorption by species with leaf area between the top of the canopy and the top of the species under consideration. Newly produced biomass is allocated to root, W_R, and shoot dry matter, W_{Sh}, using the allometric growth equation (Chapter 5, p. 53, eq. 42). As shown by KAGE & STÜTZEL (1999, eq. 18), the growth rates of plant organs growing allometrically are obtained by

$$\frac{dW_{Sh}}{dt} = \frac{dW_T}{dt} \frac{1}{1 + e^a\, b\, W_{Sh}^{b-1}} \quad \text{and} \quad \frac{dW_R}{dt} = \frac{dW_T}{dt} - \frac{dW_{Sh}}{dt} \tag{51}$$

For cauliflower, the shoot dry matter is allocated to vegetative, W_V, and generative organs, W_G, but only after curd initiation (KAGE & STÜTZEL, 1999). They proposed that during the generative phase the fraction of curd growth rate to shoot growth rate increases logistically. On the transition from the exponential to the linear phase of the logistic function, the sink strength of the curd becomes substantial. At this point it is assumed that a fraction of the vegetative shoot dry weight is reallocated to the curd. The generative growth rate is then

$$\frac{dW_G}{dt} = \begin{cases} f\, \dfrac{dW_{Sh}}{dt} & \text{if} \quad f \le 0.1 \\[2ex] f\, \dfrac{dW_{Sh}}{dt} + r_t\, T_{av}\, W_v & \text{if} \quad f > 0.1 \end{cases} \tag{52}$$

where f is a logistic growth function (see eq. 21 in KAGE & STÜTZEL, 1999) and r_t is the translocation rate. For the distribution of vegetative shoot dry matter into stems, W_S, and leaves, W_L, the approach of STÜTZEL ET AL. (1988) and STÜTZEL & AUFHAMMER (1991a) is used, which mainly assumes an allometric growth. Thus, in analogy to eq. 51, the growth rates of leaves and stem are obtained by

$$\frac{\mathrm{d}W_{\mathrm{L}}}{\mathrm{d}t} = \frac{\mathrm{d}W_{\mathrm{V}}}{\mathrm{d}t} \frac{1}{1+\mathrm{e}^{h}\, g\, W_{\mathrm{L}}^{\mathrm{g}\text{-}1}} \quad \text{and} \quad \frac{\mathrm{d}W_{\mathrm{S}}}{\mathrm{d}t} = \frac{\mathrm{d}W_{\mathrm{V}}}{\mathrm{d}t} - \frac{\mathrm{d}W_{\mathrm{L}}}{\mathrm{d}t} \tag{53}$$

where h and g are constants. Under low light conditions eq. 49 may become negative. Since stems and roots are less physiologically active, these losses are solely attributed to leaf dry weight and all other growth rates are set to zero. It is furthermore assumed that the leaf area index, L, is directly linked to leaf dry weight by

$$\frac{\mathrm{d}L}{\mathrm{d}t} = \begin{cases} \dfrac{\mathrm{d}W_{\mathrm{L}}}{\mathrm{d}t}\, SLA & \text{if} \quad \dfrac{\mathrm{d}W_{\mathrm{L}}}{\mathrm{d}t} > 0 \\[2ex] \dfrac{\mathrm{d}W_{\mathrm{L}}}{\mathrm{d}t}\, 0.5\, \dfrac{L}{W_{\mathrm{L}}} & \text{if} \quad \dfrac{\mathrm{d}W_{\mathrm{L}}}{\mathrm{d}t} \le 0 \end{cases} \tag{54}$$

where SLA is the specific leaf area of newly formed leaves. Eq. 54 also implies that per unit dry weight loss, leaf area is decreasing only by half the actual leaf area ratio. SLA is a constant input parameter for *C. album*, but in cauliflower it is made a function of the light environment quantified by ALT (pers. comm., 1999)

$$SLA = 0.059\, I_{0,\mathrm{c,av}}^{-0.85} \tag{55}$$

where $I_{0,\mathrm{c,av}}$ is $I_{0,\mathrm{c}}$ as a running average of five days. This relationship takes into account that leaves become thinner under low light conditions.

Developmental processes. Vernalisation and flower initiation in cauliflower are modelled by a modified approach of WIEBE (1979), as presented by KAGE & STÜTZEL (1999). The spatial expansion of cauliflower plants is calculated as hyperbolic functions of stem dry weight for plant height, H, and vegetative shoot dry weight for plant diameter, D. Plant dimensions, however, are not allowed to be less than the initial values H_0 and D_0 at transplanting, thus

$$H = \max\left(\frac{H_{\max}\, W_{\mathrm{S}}}{h_1 + W_{\mathrm{S}}}, H_0\right) \quad \text{and} \quad D = \max\left(\frac{D_{\max}\, W_{\mathrm{V}}}{d_1 + W_{\mathrm{V}}}, D_0\right) \tag{56}$$

where $H_{\max}$ and $D_{\max}$ denote the maximum height and diameter, respectively, and h_1 and d_1 are constants. Plant height of *C. album* is simulated dependent on the competitive environment (Chapter 4), thus incorporating the response of *C. album* to spectral changes in the canopy.

All plants in the model were assumed to have an ellipsoidal foliage envelope and the cube edge length was set to 0.01 m (see Chapter 3). The latitude of the experimental site (52°15' N) was input in the model as well as the north-south alignment of the field.

Crop canopies usually have a plant pattern defined by a repetitious basic unit. This basic unit is specific for each treatment and is modelled accordingly by (a) its boundaries in west-east (*x*-axis) and south-north (*y*-axis) direction and (b) the number and position of each species under consideration (Fig. 25). In the 1994 experiment, where *C. album* was sown by hand, the weed plants were randomly distributed and the plant density corresponds with the number of plants actually emerged (see Chapter 2, p. 9, Table 1). For the 1995 cauliflower experiments, the planting patterns of *C. album* were reproduced.
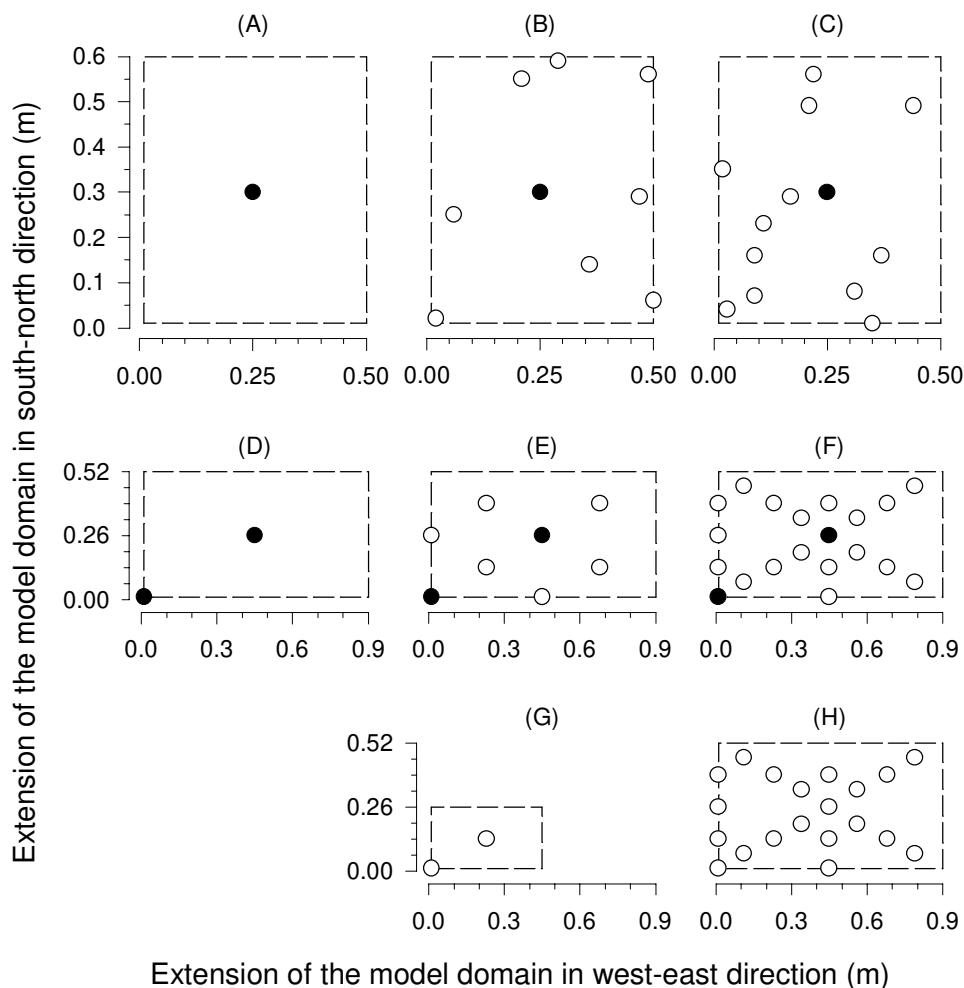

Fig. 25. Distribution of cauliflower (●) and C. album *plants (○) in the field experiments as reproduced in the model. The top and the middle row represent the mixed stands of the cauliflower experiments in 1994 (A-C) and 1995 (D-F), respectively. The bottom row shows the pure weed plots in the 1995 trials (G-H). The columns from left to right represent weed-free, low and high weed planting densities.*

Run control. The model runs start at the planting date of cauliflower. *C. album* is initiated at the three-node stage, i.e. at the weed planting date in 1995. This stage was reached in the 1994 experiments about 300 °Cd after sowing. The simulation is terminated when the crop has reached harvest time, which is determined by a specified curd diameter in cauliflower. For those treatments where curds did not reach a marketable size, the model is stopped at the day of the final harvest.

Model simplification. To reduce complexity, the detailed model was compared to a modified version of the light interception module XASSNM of SUCROS87 (SPITTERS, 1989, p. 387-392), which stratifies the canopy into a number of horizontal leaf layers amounting to one layer per 0.01 m canopy height. For each competing species the absorption of diffuse and direct radiation by sunlit and shaded leaves is calculated per layer. Within a layer, a homogenous leaf area distribution is assumed, whereas in the vertical dimension a parabolic density function is used. Summation over all layers yields the total light absorption of each species.

The modification used here applies to the light extinction coefficient for diffuse radiation. Instead of using a constant value, the absorption of solar rays from selected elevation angles in a layer is calculated and a Gaussian integration procedure (GOUDRIAAN, 1986) is used for integration over the hemisphere. Five points, *p*, are selected at defined distances, d_{5p}, from the central point of the integration range of the solar elevation angle *β*. The absorption of radiation originating at these solar heights $β_p$ is calculated and weighted, w_{5p}. For the distances and weights for the Gaussian integration see Chapter 3 (p. 25, Table 3). The solar elevation angles are determined by

$$\beta_p = \frac{\pi}{2}\left(0.5 + d_{5p}\right) \quad \text{for} \quad 0 < \beta \le \frac{\pi}{2} \quad \text{with} \quad p = [1..5] \tag{57}$$

The light extinction coefficient to be used for integrating the absorption of diffuse radiation, K_a, is (GOUDRIAAN, 1977, eq. 2.41)

$$K_a = \frac{O_{av}}{\sin\beta_p}\sqrt{1-\sigma} \tag{58}$$

where O_{av} is the average projection of leaves, which is 0.5 for a spherical leaf angle distribution and σ is the scattering coefficient amounting to 0.2 for visible light. According to

the Gauss integration the relative absorption of diffuse radiation, $F_{a,f}$, is then the weighted sum of all rays considered

$$F_{a,f} = \pi^2 \sum_{p=1}^{5} I_p \left(1 - e^{-K_a L_{LY}}\right) \sin \beta_p \, \cos \beta_p \, w_{5p} \tag{59}$$

where I_p is the relative light intensity of the selected solar ray, which equals $1/\pi$ for each solid angle above the canopy and L_{LY} is the total leaf area in layer LY. Multiplication by $\sin \beta_p$ considers the fraction of radiation effective on a horizontal plane and the factor $\cos \beta_p$ is needed when integrating the solid angles over the hemisphere. Since the light absorption of canopy with a horizontally homogeneous leaf area distribution is insensitive to changes of the solar azimuth angle, the weighted sum has finally to be multiplied with the integration range of both solar angles ($2\pi \cdot \pi/2 = \pi^2$). Calculating the absorption of diffuse radiation in a layer with the above procedure yields a value that is dependent on the leaf area (GOUDRIAAN, 1977) and on the depth in the canopy. Subsequently, the 'effective' diffuse light extinction K_f is calculated, which is needed to realise the relative absorption of diffuse radiation given by eq. 59, thus

$$F_{a,f} = 1 - e^{-K_f L_{LY}} \tag{60}$$

which can be rewritten to

$$K_f = \frac{-\ln\left(1 - F_{a,f}\right)}{L_{LY}} \tag{61}$$

Eq. 59 estimates the fraction of absorbed diffuse radiation in relation to the light intensity above the canopy. If the absorption is calculated based on the light intensity above a layer, $I_{0,LY}$, eq. 61 is modified by

$$K_{f,LY} = \frac{-\ln\left(1 - F_{a,f}/I_{0,LY}\right)}{L_{LY}} \tag{62}$$

yielding the 'effective' diffuse light extinction coefficient in a layer $K_{f,LY}$, which is used in the routines of XASSMN.

6.3. Results and discussion

Unless stated otherwise all calibration data were taken from the experiments conducted in 1995, whereas the model was evaluated with data from the trial in 1994.

Model calibration

Cauliflower. In the second trial in 1995, the impact of *C. album* on the growth of cauliflower was so substantial that the crops' standing biomass decreased. This dry weight reduction starting only few weeks after planting may be attributed to both respiratory losses and to an accelerated senescence and abscission (SPITTERS ET AL., 1989) due to stress from low light conditions. Although senescent leaves were sampled, it cannot be ruled out that part of the biomass shed was already degraded by the time of subsequent harvests. Since no detailed respiration measurements were made, a quantification of the total biomass loss and thus the gross dry weight produced was not possible. Applying the light-use efficiency of cauliflower estimated from weed-free plots to simulate growth of weed-infested cauliflower led to a considerable overestimation. To overcome these problems, the net standing biomass is simulated instead of gross dry weights. Furthermore, the light-use efficiency revealed the same tendency also found in *C. album* (Chapter 5). Presumably due to a lower level of global radiation, the light-use efficiency was higher in the second compared to the first experiment. As a provisional procedure, a log-normal function was used (eq. 49) to describe the relationship between the light intensity and light-use efficiency (Fig. 26). The properties of this function type include (a) a negative function value at low light intensities and after reaching a maximum (b) a gradual negative slope at high light intensities. Thus both the degree of competition as well as the general growing conditions could be integrated in one relationship. A similar response is obtained by integrating a single-leaf photosynthesis approach (ACOCK ET AL., 1978) over the canopy and the diurnal course. The losses predicted by such an integration, however, are solely due to respiration, whereas the dry matter reduction estimated by eq. 49 additionally comprises senescence and abscission. The parameters of the log-normal function were not estimated directly, because the equation needs the light intensity above the cauliflower canopy (eq. 50), which can only be precisely predicted by the model itself. Due to the large number of calculations in the model the execution time easily exceeds several hours for one simulation run. The parameters were therefore adjusted by eye in repeated model runs with measured LAI and plant height of both species as input until a good correspondence between the simulation output and measured
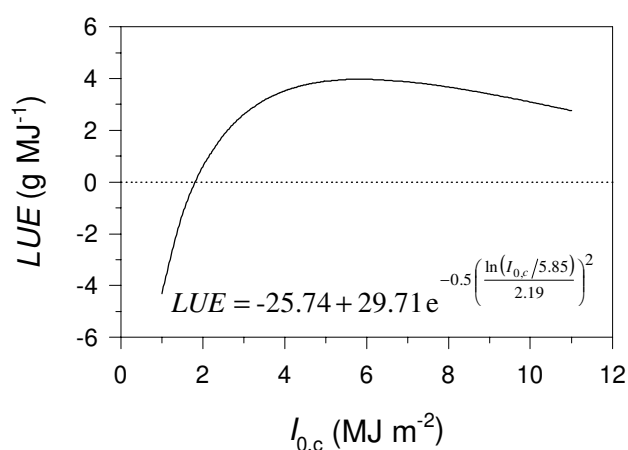
Fig. 26. Relationship between the light-use efficiency, LUE*, of cauliflower and the light intensity above the cauliflower canopy,* $I_{0,c}$.

data was found. Evidently, this procedure is only a stopgap until further information exists on the production and degradation of cauliflower biomass under reduced light conditions.

The relationship between the specific leaf area of newly formed cauliflower leaves and the radiation environment was established from field experiments with shaded and unshaded plants (ALT, 1999, pers. comm.). If the radiation above the canopy drops below about 2 MJ m^{-2}, eq. 55 will predict an unrealistically high specific leaf area. But this relationship applies to newly produced leaf dry matter only, which is given when a positive light-use efficiency is predicted, i.e. at light intensities above *c.* 1.8 MJ m^{-2} (Fig. 26).

Although growing under contrasting competitive environments, the dry matter distribution between roots and shoot (Fig. 27A) as well as stem and leaves (Fig. 27B) was hardly altered resulting in robust allometric relationships. It seems that cauliflower has a relatively constant allocation pattern throughout vegetative and generative growth stages and does not respond to light competition by significantly changing dry matter distribution. Similarly accurate were the predictions of plant dimension as functions of dry weight (Fig. 28). Since a tall plant is susceptible to wind and rainfall, it has to be supported by an appropriately sized stem, which is mainly responsible for the plant's stability. The lateral expansion on the other hand is primarily determined by leaves for the lack of side shoots and branches in cauliflower. By these simple relationships a link between the spatial expansion and growth could be established.
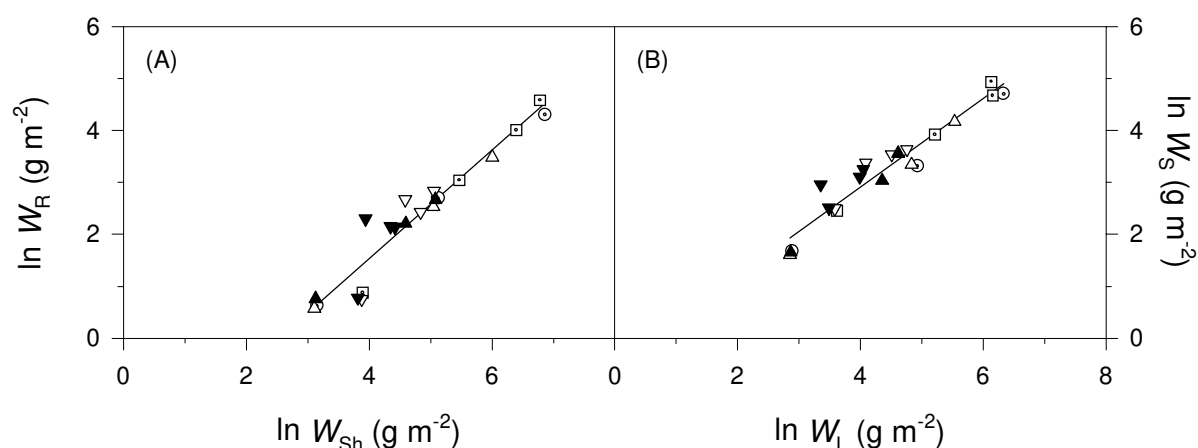
Fig. 27. Relationships between the natural logarithms of (A) root, W_R, and shoot dry weight, W_{Sh}, and (B) stem, W_S, and leaf dry weight, W_L, of cauliflower. Symbols denote data are from weed-free ($\odot$ exp. 1, $\boxdot$ exp. 2), low ($\triangle$ exp. 1, $\triangledown$ exp. 2) and high ($\blacktriangle$ exp. 1, $\blacktriangledown$ exp. 2) weed density cauliflower plots. The regressions are

$$(A) \quad \ln W_R = -2.67 \,(\pm 0.34) + 1.05 \,(\pm 0.069) \ln W_{Sh} \quad (r^2 = 0.92)$$

$$(B) \quad \ln W_S = -0.53 \,(\pm 0.25) + 0.86 \,(\pm 0.056) \ln W_L \quad (r^2 = 0.93)$$

Chenopodium album. The model was run with the dry matter production and distribution parameters given in Chapter 5. For roots and shoot the allometric growth coefficient was constant throughout. Although the partitioning coefficient increased slightly with the plant density of the canopy, the accuracy of the simulation was not enhanced compared to the summary relationship calculated for all treatments. Since this general function could explain more than 96 % of the variation found (see Chapter 5, p. 59, Table 10), its parameters were used to simulate the stem:leaf ratio in *C. album* throughout. The specific leaf area of *C. album* was estimated by a linear regression between the area and weight of leaves (Fig. 29). Regressions calculated separately for all treatments yielded insignificantly different values for *SLA*. The estimated value is slightly higher than the 0.0231 m^2 g^{-1} reported for *C. album* by KROPFF & SPITTERS (1992a). All parameters used in the model are summarised in Table 12.
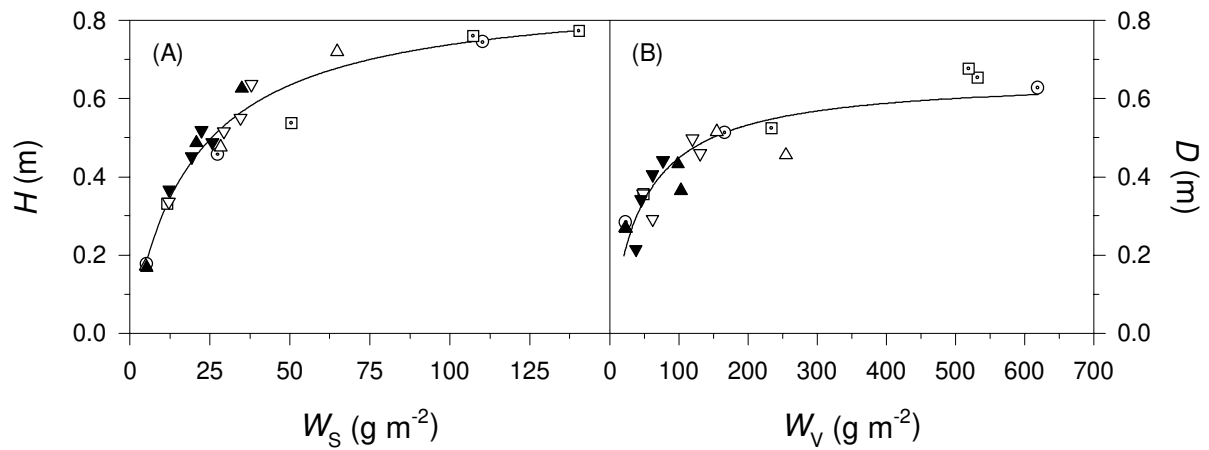
Fig. 28. (A) Relationship between plant height, H, *and stem dry weight,* W_S, *and (B) plant diameter,* D, *and vegetative shoot dry weight,* W_V, *of cauliflower. For the symbol definition see legend of Fig. 27. The regressions are*

$$(A) \quad H = \frac{0.882 \, (\pm 0.033) \, W_S}{19.49 \, (\pm 2.0) + W_S} \quad (r^2 = 0.96)$$

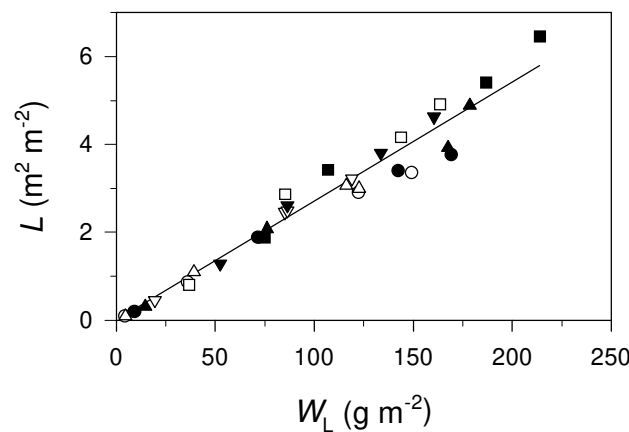$$(B) \quad D = \frac{0.656 \, (\pm 0.32) \, W_V}{46.31 \, (\pm 7.6) + W_V} \quad (r^2 = 0.84)$$

Fig. 29. Relationship between leaf area index, L, *and leaf dry weight,* W_L, *of* C. album. *Symbols represent data are from pure weed stands (○, ● exp. 1, □, ■ exp. 2) and mixed stands with cauliflower (△, ▲ exp. 1, ▽, ▼ exp. 2). Open and filled symbols denote low and high weed density plots, respectively. The regression is defined by*

$$L = 0.0271 \, (\pm 0.00054) \, W_L \quad (r^2 = 0.96)$$

- 74 -

Table 12. Overview of the parameter for cauliflower and C. album *used in the model.*

Parameter	Symb.	Unit	Cauliflower			*C. album*		
			1994	1995 exp. 1	1995 exp. 2	1994	1995 exp. 1	1995 exp. 2
Day of planting / sowing		d	108	114	199	109	123	201
			—— for all trials ——					
Curd diameter at harvest		mm		200		-	-	-
Day of final harvest		d		-		171	191	282
Light-use efficiency	*LUE*	g MJ^{-1}		Fig. 26		3.5	3.14	4.34
						—— for all trials ——		
Specific leaf area	*SLA*	m^2 g^{-1}		eq. 55			Fig. 29	
Root-shoot allometry	*a*	-		Fig. 27A			-2.13	
	b	-					1.06	
Stem-leaf allometry	*h*	-		Fig. 27B			-1.42	
	g	-					1.52	
Translocation rate	r_t	°C^{-1}		0.0005			-	
Plant height	*H*	m		Fig. 28A			see Chapter 4	
Plant diameter	*D*	m		Fig. 28B			see Chapter 4	

Simulation results. In weed-free cauliflower plots, total dry matter production and leaf area growth was simulated as well as plant height and the size of the marketable organ (Fig. 30). Calculation of plant height with eq. 56 resulted in a distinct lag in height growth after transplanting. This lasted longer in spring than in summer due to a slower growth early in the year and may be interpreted as the transplanting shock. Data show that plant height development was even further delayed in the first experiment. Since this effect is probably due to low temperatures not considered in the model, plant height is overestimated.

Calibration runs showed that it was not possible to correctly model the effects found in weed-infested cauliflower plots, if the leaf area development of *C. album* was simulated. Predictions of yield losses were satisfactory only if the LAI of *C. album* was given as input. With this prerequisite, total dry weight of cauliflower was slightly overestimated in the first experiment, whereas the breakdown of the crop in the second trial was adequately reproduced. This is due to a more accurate simulation of plant height of cauliflower in the summer compared to the spring experiment. The size of the marketable organ was calculated sufficiently precise in all
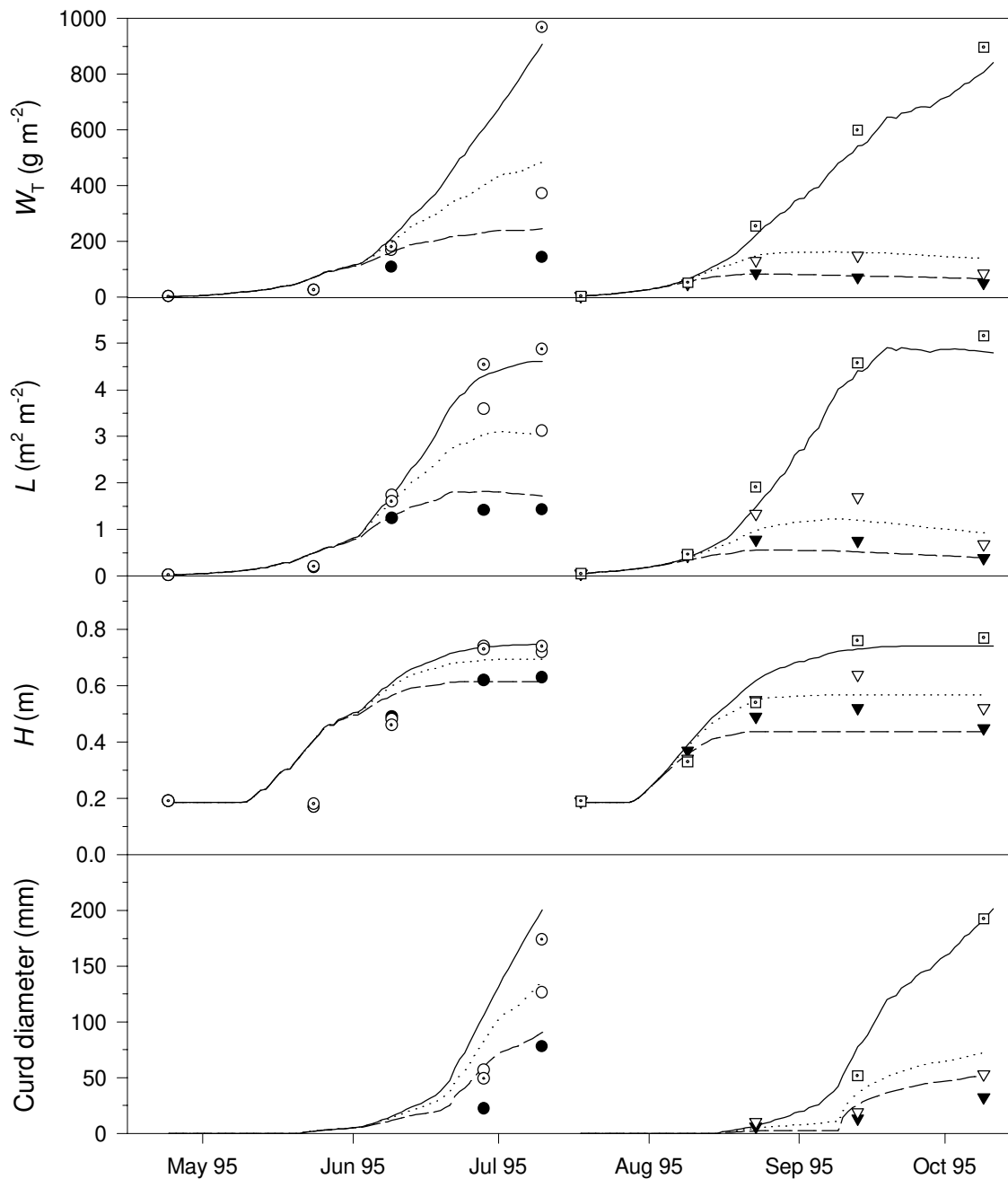
Fig. 30. Simulated (lines) and observed (symbols) total dry weight, W_T, leaf area index, L, plant height, H, and curd diameter of cauliflower. Data are from weed-free (⊙ exp. 1, ⊡ exp. 2, solid line), low (△ exp. 1,▽ exp. 2, dotted line) and high (▲ exp. 1,▼ exp. 2, dashed line) weed density cauliflower plots.

treatments. In the weed-infested plots of experiment 2, the curd dry weight and diameter increased with a decreasing total growth rate. This describes the attempt to initiate, maintain and develop an inflorescence even under most unfavourable growing conditions, which can be explained by retranslocation of dry weight from vegetative to generative plant organs.

C. album obviously had a different impact on cauliflower in the two experiments. An identical weed density resulted in a greater yield loss in the second compared to the first trial, due to a more vigorous growth of *C. album*. Even with the LAI as input, growth of *C. album* was
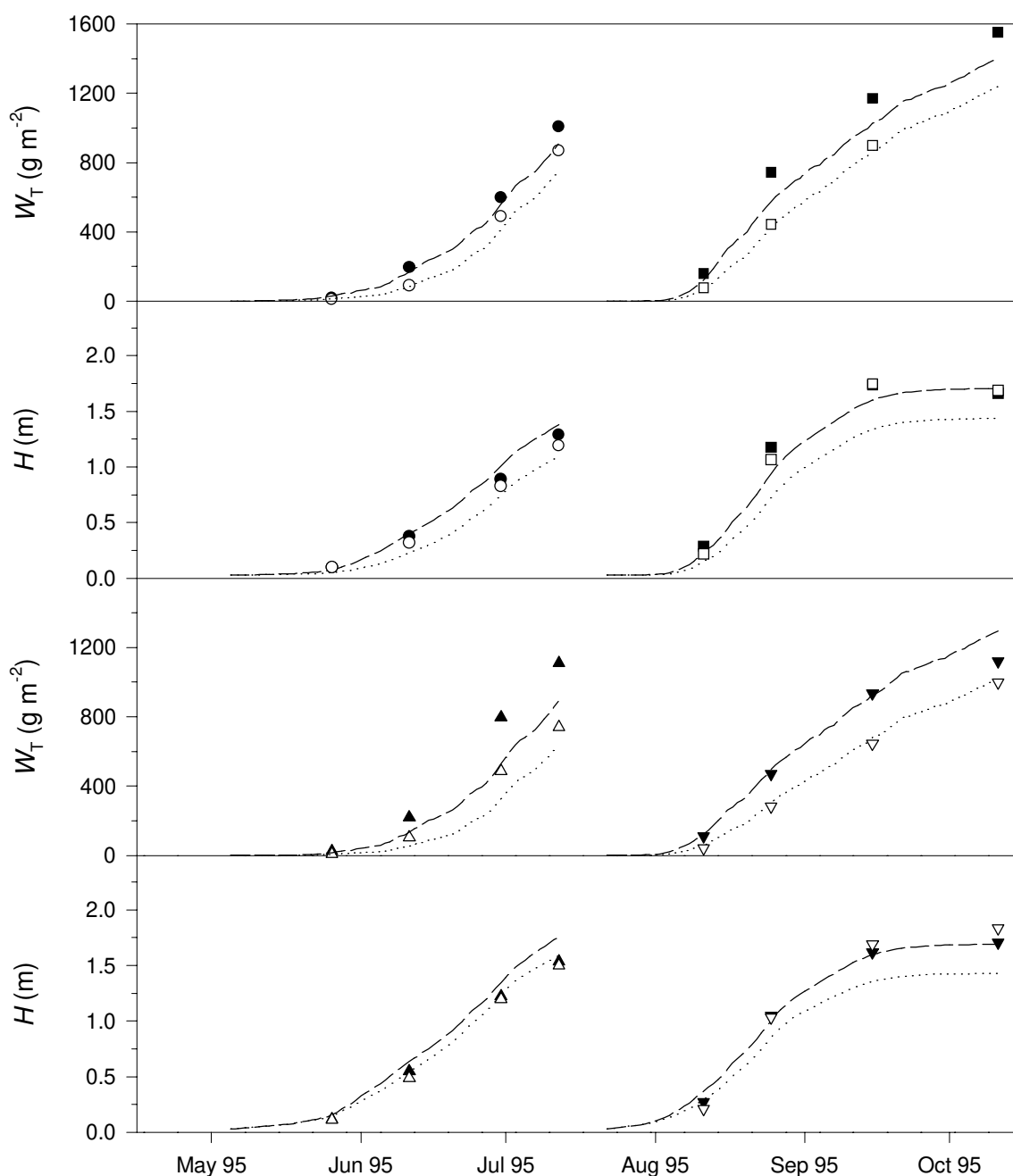

Fig. 31. Simulated (lines) and observed (symbols) total dry weight, W_T*, and plant height,* H, *of* C. album. *Data are from pure weed stands (top rows,* ○,● *exp. 1,* □,■ *exp. 2) and mixed stands with cauliflower (bottom rows,* △,▲ *exp. 1,* ▽,▼ *exp. 2). Open and filled symbols denote low (dotted line) and high (dashed line) weed density plots, respectively.*

nevertheless underestimated in experiment 1, whereas simulation results are better in the second trial (Fig. 31). This indicates some problems calculating the light-use efficiency of *C. album* (Chapter 5), where the light extinction coefficient may be too large and light interception is thus overestimated. Plant height development of *C. album*, being a function LAI (Chapter 4), was acceptably reproduced by the model. An underestimated total growth of *C. album* has a feedback on leaf area development and consequently on plant height as well, both mainly determining the outcome of light competition. Hence, the model produces an unrealistic low impact on cauliflower in the first experiment, if the LAI of *C. album* is simulated dynamically. This high sensitivity on the leaf area development will have to be reconsidered in future model improvements.

Model evaluation

The late emergence of *C. album* due to low spring temperatures and a long juvenile phase resulted in a delayed onset of competition in the 1994 cauliflower experiment (Fig. 32). Only minor differences between both weed densities were found, which are adequately reproduced by the model with respect to total dry weight and leaf area index of cauliflower. Although,

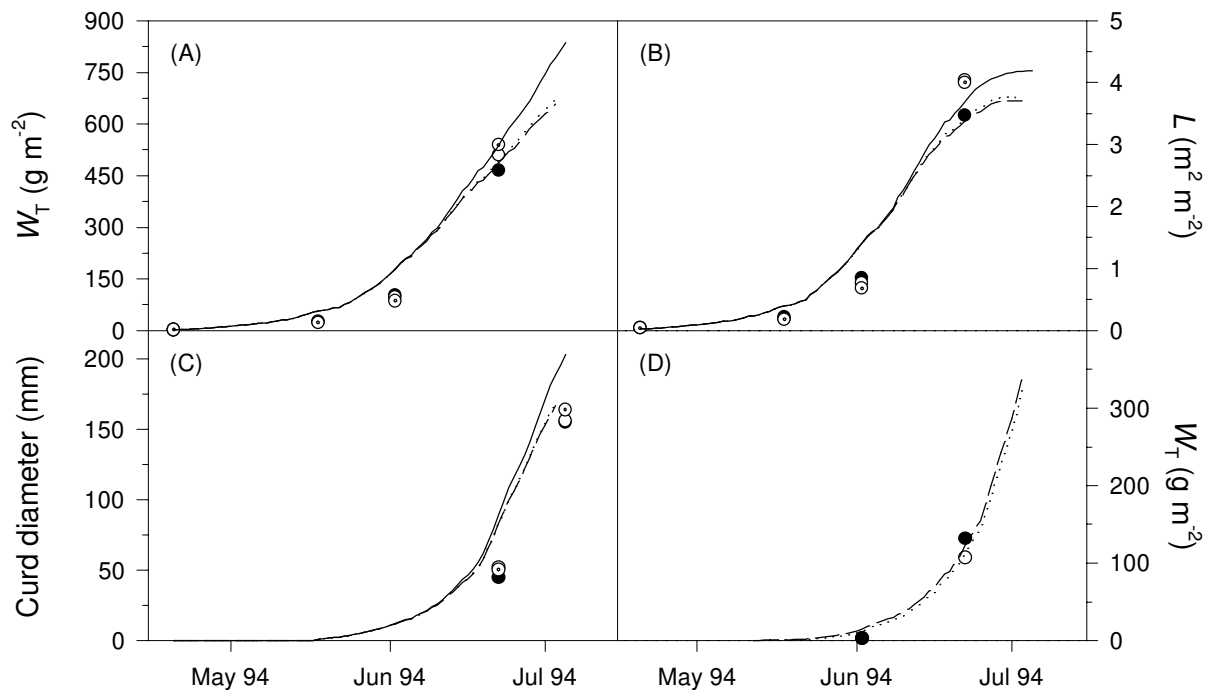*Fig. 32. Simulated (lines) and observed (symbols) data from the 1994 cauliflower experiment used for evaluation. Symbols denote weed-free (⊙, solid line), low (○, dotted line) and high (●, dashed line) weed density cauliflower plots. (A-C) Total dry weight, W_T, leaf area index, L, and curd diameter of cauliflower, respectively, and (D) total dry weight, W_T, of C. album.*

curd growth is slightly overestimated, the model correctly terminated the calculations at the measured harvest date. Dry matter production of *C. album* was also simulated appropriately using an average light-use efficiency of 3.5 g MJ^{-1} and calculating the leaf area development dynamically. These results give a first indication to the applicability of the relationships and assumptions used. The model is able to predict the reduced curd yield of cauliflower by late weed infestations. It thus reproduces the high competitiveness of this crop with regard to light interception. It has to be noted, however, that the 1994 cauliflower data set is incomplete making a further evaluation necessary.

Model simplification

At the outset of model simplification, a comparison between the complex and the simplified model under identical conditions was made. Assuming a 'closed canopy' situation, both models were run to simulate the weed-free cauliflower plots of the 1995 experiments. Apart from numerical deviations, the relationship between the light absorption calculated by the complex model and by the simple model was very close (slope = 1.0001, r^2 > 0.999). Having thus eliminated systematic errors, the same experimental treatments were calculated, this time considering the heterogeneous canopy structure in the complex model. The calculated absorption rates between both models diverged most in early growth stages when the clumping of leaf area is evident. The relative groundcover *rgc*, i.e. the fraction of shaded ground with the sun directly overhead, was taken as a measure for this clumping. Assuming that plants are solids of rotation and that a value of 1.0 is not exceeded, the relative ground cover is approximated by

$$rgc = \min\left(D^2 \frac{\pi}{4} PD, 1.0 \right) \tag{63}$$

where *D* is the plant diameter and *PD* is the planting density. This is then related to the deviation between the complex and the simplified model by

$$\frac{I_{abs, complex}}{I_{abs, simple}} = c_1 + c_2 \left(1 - e^{-c_3 \, rgc} \right) \tag{64}$$

where c_1 is the minimum value, c_2 and c_3 are constants. The parameters were estimated using the weed-free plots of both cauliflower experiments in 1995 (Fig. 33). For the simulation of mixed canopies, the relative ground cover of all species is summed. Furthermore, the
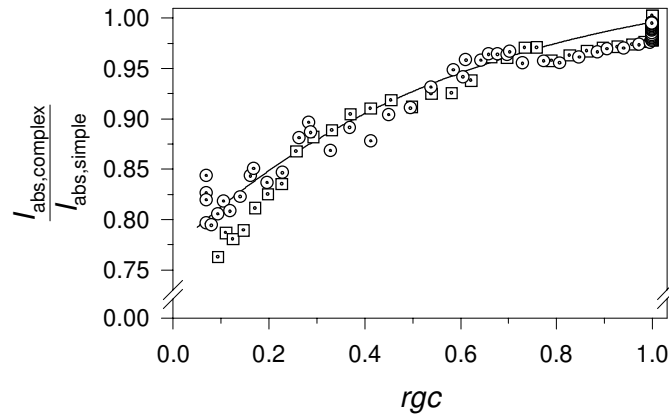
Fig. 33. Relationship between the deviation in the calculation of light absorption between complex and simplified model and the relative ground cover, rgc. *Symbols denote simulated light absorption from weed-free cauliflower plots from experiment 1 ($\odot$) and experiment 2 ($\boxdot$). The regression is*

$$\frac{I_{\text{abs, complex}}}{I_{\text{abs, simple}}} = 0.77 \left(\pm 0.0053\right) + 0.28 \left(\pm 0.007\right)\left(1 - e^{-1.65\,(\pm 0.15)\,rgc}\right) \qquad (r^2 = 0.96)$$

calculation of $I_{0,c}$ (eq. 50) had to be modified, since the light absorption of the taller species is overestimated if a homogeneously distributed leaf area is assumed. As an approximation, the leaf area in the upper layer is supposed to have an average relative ground cover of 50 per cent. Eq. 64 then yields a value of *c.* 0.93, thus eq. 50 is modified to

$$I_{0,c,S} = I_0 - 0.93\left(I_{\text{abs,t}} - I_{\text{abs},H_S}\right) \tag{65}$$

The relationships in eqs. 64 and 65 were evaluated by simulation of mixed stands. A comparison of simulation results in different competitive environments from both models reveal a good correspondence (Table 13). The variation between the models increases, however, with canopy heterogeneity. In cauliflower experiment 2, the crop was suppressed to such an extent that the plants stayed comparatively small leading to a continuously heterogeneous canopy. In other variants, the canopy structure approaches homogeneity in the course of time and the error made by the simplified model is less significant for the final result. Shown by a scenario calculation for one day, a reduction in weed density and thus a higher spatial heterogeneity of the canopy leads to an increased deviation of the simplified model (Table 14). The deviation is reduced by introduction of eq. 64, but it does not completely account for the variation. Furthermore, the weed densities used in the cauliflower experiments led to a substantial yield reduction up to a complete loss. Therefore, much lower weed densities will be of particular interest in vegetable production. In this case, the complex model will give more accurate information on the light distribution between crop and weeds.

Table 13. Comparison of the cumulative light absorption and total dry weight of cauliflower in the 1995 experiments between the complex (CM) and the simplified model (SM). The relative deviation between the models is also given.

Experiment /Variant	Cumulative light absorption			Total dry weight		
	CM	SM	SM/CM	CM	SM	SM/CM
	—— MJ m^{-2} ——		%	—— g m^{-2} ——		%
1 / weed-free	326.7	328.8	101	907.5	910.4	100
1 / low weed density	147.0	143.8	98	486.2	474.8	98
1 / high weed density	83.0	89.4	108	245.5	261.5	107
2 / weed-free	253.8	254.7	100	842.6	845.7	100
2 / low weed density	66.9	69.7	104	138.8	145.4	105
2 / high weed density	31.5	42.6	135	65.2	83.3	128

Table 14. Sensitivity analysis for the simplified model. Scenario 1 represents the situation in a low weed density plot in the 1995 cauliflower experiments (Fig. 25, plot H), in scenario 2 and 3 the weed density was reduced to one half and one sixth, respectively. Shown are the fractions of absorbed radiation by cauliflower (cau) and C. album *(che) as calculated by the complex model and the simple model. For the latter, results are given before (uncorrected) and after (corrected) modification by eq. 64. Calculations were made for day 152 (1 June) at 50 per cent diffuse radiation.*

	Scenario 1		Scenario 2		Scenario 3	
	cau	che	cau	che	cau	che
Plant density (m^{-2})	4.27	12.82	4.27	6.41	4.27	2.14
Plant height (m)	0.4	0.4	0.4	0.4	0.4	0.4
Plant diameter (m)	0.33	0.17	0.33	0.17	0.33	0.17
LAI (m m^{-2})	1.0	0.70	1.0	0.35	1.0	0.117
Relative ground cover	0.657		0.511		0.414	
Fraction of absorbed radiation (deviation from complex model)						
Complex model	0.342	0.278	0.367	0.143	0.386	0.049
	(100)	(100)	(100)	(100)	(100)	(100)
Uncorrected simple model	0.395	0.277	0.441	0.155	0.478	0.056
	(116)	(99)	(120)	(108)	(124)	(113)
Corrected simple model	0.378	0.264	0.410	0.144	0.434	0.051
	(110)	(95)	(112)	(100)	(112)	(103)

- 81 -

In summary, simulation results encourage the use of a three-dimensional light interception model when the leaf area is not homogeneously distributed in the canopy. Even if a mainly one-dimensional approach is modified by a correction factor, deviations still persist due to the complex system of interactions between the spatial leaf area distribution of competing species and the radiation environment. The present findings suggest a closer look at dry matter production and losses under low light conditions in cauliflower and also indicate uncertainties in the quantification of growth processes in *C. album*. Nevertheless, the model proposes to be an effective tool to gain insight into the mechanisms of light competition and thus support decision-making in weed-control management.

7. Final discussion

The objective of this study was to analyse the processes of competition for light and to quantify the relationships by simple mathematical formulations. These formulations should then be integrated into a mechanistic simulation model. Comparison of the model output to observational data should evaluate (a) the – abstracted – conception of crop-weed interactions, (b) the hypotheses made for processes not well understood and (c) the implications of simplifying assumptions, which were necessary to reduce system complexity. This evaluation of the approaches used are discussed here in the general context.

To describe the distribution of light in a heterogeneously structured canopy, the three-dimensional approach used here seems appropriate. In horticultural crops, this detailed model has been shown to be advantageous to approaches with a lower spatial resolution. For the monospecific case, i.e. a cauliflower crop growing under potential conditions, the output of the model was successfully reproduced by a modified version of an existing one-dimensional light interception model. In a mixed stand, the interactions between species are much more complex and the simplified model was not able to account for all effects of spatial heterogeneity on radiation distribution in the canopy. It can be concluded that the detailed approach can be used to derive simplified models, which may give a first approximation in the quantification of light interception in heterogeneous canopies.

As a first step to quantify the morphological plasticity of a weed species in response to shading, a simple approach was proposed to calculate plant height growth as a function of leaf area. Sufficiently accurate relationships could be established, but as a consequence the resulting competition model was highly sensitive on the development of canopy foliage. The strong correlation between leaf area distribution and the competitiveness of a species is exactly what is observed in the field, but it requires a precise description of leaf area development in a model. Nevertheless, the results indicate that it is feasible to examine the behaviour of shade-avoiding species not only as seedlings or in controlled environments (MORGAN & SMITH, 1981; HUGHES & WAGNER, 1987) but in later growth stages in the field as well. The response could be quantified dependent on the optical properties of plant leaves by simulating the absorption in different regions of the red waveband. Extinction coefficients for this waveband can be derived from literature (MONTEITH & UNSWORTH, 1990) and integrated into the light interception model. Plant height could then be explicitly simulated

dependent on the red:far-red ratio, which may reduce the high sensitivity of the competition model on leaf area development.

Modelling biomass production with the summary approach of the light-use efficiency assumes a constant proportionality between assimilation and respiration processes. The relationship between cumulative intercepted PAR and total dry weight can be accurately quantified using readily obtainable parameter. However, the present results indicate that the light-use efficiency (a) might be affected by external variables such as the level of global radiation and (b) is reduced by the degree of shading. Under extreme low-light conditions plants still intercept radiation, but this energy is used – and sometimes is not sufficient – to maintain the plant's vital functions. In this situation the ratio between carbon uptake and respiratory losses is presumably altered. It is concluded that the light-use efficiency does not remain constant in all radiation environments, thus an extension of this concept seems necessary to use it in models for light competition.

Dry matter partitioning between plant organs is commonly simulated by descriptive relationships, as it is in the present work. But the assumption of allometric growth between roots and shoot as well as stem and leaves resulted here in a sufficiently accurate description of carbon allocation for both *C. album* and cauliflower. Since a universally valid theory with a greater explanatory value is lacking, the presented approach offers a robust description of dry matter partitioning and is readily calibrated. The problems in calculating the leaf area development in *C. album* that were revealed in the competition model are primarily attributed to an erroneous estimation of dry matter production and only to a lesser extend to the partitioning coefficients.

The objective of this study was to quantify the impact of weed competition on crop yield. Since it is impossible to separate the effects of multiple causes and their interactions simultaneously, several abstractions and simplifications to the complex situation found in the field were made. In the following discussion these limitations will be considered and possible solutions are indicated.

The exclusive analysis of light competition in the crop-weed system is evidently a major simplification. Significant deviations between measured and simulated yield are to be expected if extreme water and nutrient limitations occurred in the field and the model is based on radiation and temperature only. But under potential growing conditions it has been shown

that the amount of intercepted radiation limits crop production in the temperate zone (MONTEITH, 1981). Since it is presently common practice to amply fertilise and irrigate in intensive vegetable production in northern Europe, the situation examined in the present work may be called an 'important special case'. An extension of the model, however, will be necessary if it is to be adapted to low-input production implying that the crop will increasingly compete with weeds for nutrients and water. This situation is encountered in production regions where fertiliser and/or irrigation water is scarce. But it may also apply to agricultural systems without source limitations if the utilisation of fertiliser or water is restricted by law. Several competition models have been proposed that additionally quantify the effects of water and/or nutrient competition, but with much less detail compared to the light interception and utilisation submodels. (GRAF ET AL., 1990; KINIRY ET AL., 1992; KROPFF & VAN LAAR, 1993). Since the general approach is similar, the model proposed by KROPFF & VAN LAAR (1993) is outlined here.

A limited availability of water is assumed to have a direct effect on the potential growth rate, $(\mathrm{d}W/\mathrm{d}t)_\mathrm{p}$ (g m^{-2} d^{-1}, Chapter 6, eq. 48, p. 65), that is achieved without limitations. The reduction in growth rate due to drought is assumed to be proportional to the reduction in the transpiration rate (VAN KEULEN, 1975). The actual growth rate, $(\mathrm{d}W/\mathrm{d}t)_\mathrm{a}$, is thus calculated by

$$\left(\frac{\mathrm{d}W}{\mathrm{d}t}\right)_\mathrm{a} = \left(\frac{\mathrm{d}W}{\mathrm{d}t}\right)_\mathrm{p} \frac{T_\mathrm{a}}{T_\mathrm{p}} \tag{66}$$

where T_a and T_p (mm d^{-1}) are the actual and the potential transpiration rate. A modified Penman-Monteith-equation (MONTEITH, 1965) is used to calculate T_a and the estimation of T_p is based on the soil moisture content.

Likewise, the effect of nitrogen competition on the potential growth rate is simulated; similar approaches are followed for other nutrients. All mineral nitrogen – soil-borne or fertilised – that is present in the rooting zone is assumed to be available for uptake by plants ('supply', A, kg N ha^{-1}). The potential rate of N uptake by a vegetation ('demand', D, kg N ha^{-1} d^{-1}) is calculated using the actual and maximum nitrogen amount. The actual nitrogen uptake, U (kg N ha^{-1} d^{-1}), is estimated by

$$U = \min(D, A) \tag{67}$$

The potential growth rate is linearly reduced if the nitrogen content in the biomass, W, decreases below a critical threshold value

$$\left(\frac{\mathrm{d}W}{\mathrm{d}t}\right)_a = \left(\frac{\mathrm{d}W}{\mathrm{d}t}\right)_p \frac{NC_a - NC_{\min}}{NC_{cr} - NC_{\min}} \quad \text{with} \quad NC_a = \frac{W}{U} \tag{68}$$

where NC_a, $NC_{\min}$ and NC_{cr} are the actual, minimum and critical nitrogen contents, respectively. If two or more species compete for the available N supply, the uptake rate of species i is related to its share in the total root system

$$U_i = \frac{l_i}{\Sigma l} \Sigma U \quad \text{with} \quad U_i \leq D_t \tag{69}$$

where ΣU is the uptake summed over all species, D_i is the demand of species i and l (m ha^{-1}) is the effective root length.

These simple approaches do not use complex models for soil processes, but give some insight into the nature of water and nutrient limitations in mixed canopies. Due to the direct effect on the potential growth rate, they could easily be incorporated into the model presented here. Despite their simplicity, however, further experimental work to calibrate the necessary parameter will be required.

If the range of weed species is to be extended, an easy calibration of a competition model is increasingly important. Simple and summary relationships should be preferably used that are at best derived from a detailed description of the underlying processes. KINIRY ET AL. (1992) have shown that a versatile mechanistic competition model which was mainly calibrated using literature data can give reasonably accurate results.

So far, the model considers short-term effects of weed competition allowing at most tactical decisions. A more strategic model for weed management (e.g. WILES ET AL., 1996) would additionally include (a) a database module with details of control measures with respect to timing and efficacy and (b) a simulation module that estimates weed population dynamics and seedbank processes. The development and calibration of models for population dynamics, however, is a particularly laborious task since critical gaps in the knowledge of these systems as well as a considerable regional variation in weed biology and ecology were found (SCHWEIZER ET AL., 1993). Although the main system components are identified (Fig. 34) the
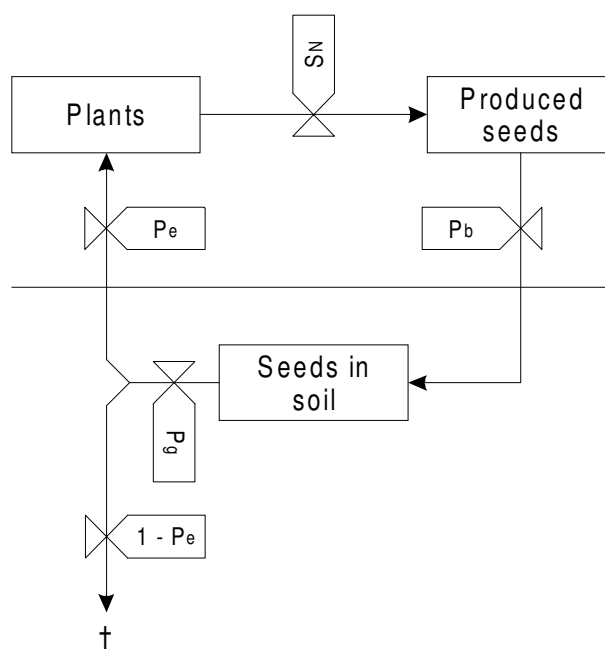
Fig. 34. Schematic representation of the population dynamics of an annual weed. The boxes represent state variables (ha^{-1}), P_e, P_b and P_g are the transition probabilities for seedling emergence, seed burial and exhaustion, respectively (yr^{-1}) and S_N denotes the number of seeds produced per plant (SPITTERS, 1989).

measurements of the seedbank in the soil and the quantification of the transition probabilities are difficult. All system components are highly dependent on a number of external variables such as soil management, weed control measures and climate. The influence of crop rotation, for instance, on weed seed bank was examined by JORDAN ET AL. (1995). But even with a focus on a single influential variable, many parameter values were hypothetical due to limited knowledge on the relevant aspects. They state that if their model is applied to a complex cropping system, the parameter estimation for an accurate prediction would require an undue research effort.

This short digest does not raise a claim of completeness, but shows exemplary how the model could be extended beyond the scope of the crop-weed system defined here. It furthermore gives an idea how a more realistic description of the situation in the field may be achieved and where future work is necessary. A study on light competition between crops and weeds can never be conclusive. But it may lead to a better understanding of the underlying mechanisms and to a more precise prediction of system responses, an objective science is concerned with.

8. References

Acock, B., D.A. Charles-Edwards, D.J. Fitter, D.W. Hand, L.J. Ludwig, J.W. Wilson & A.C. Withers. 1978. The contribution of leaves from different levels within a tomato crop to canopy net photosynthesis: an experimental examination of two canopy models. Journal of Experimental Botany 29:815-827.

Baeumer, K. & C.T. de Wit. 1968. Competitive interference of plant species in monocultures and mixed stands. Netherlands Journal of Agricultural Science 16:103-122.

Ballaré, C.L., R.A. Sánchez, A.L. Scopel, J.J. Casal & C.M. Ghersa. 1987. Early detection of neighbour plants by phytochrome perception of spectral changes in reflected sunlight. Plant, Cell and Environment 10:551-557.

Ballaré, C.L., A.L. Scopel & R.A. Sánchez. 1995. Plant photomorphogenesis in canopies, crop growth, and yield. HortScience 30:1172-1191.

Bange, M.P., G.L. Hammer & K.G. Rickert. 1997. Effect of radiation environment on radiation use efficiency and growth of sunflower. Crop Science 37:1208-1214.

Barnes, P.W., W. Beyschlag, R. Ryel, S.D. Flint & M.M. Caldwell. 1990. Plant competition for light analyzed with a multispecies canopy model. II. Influence of canopy structure in mixtures and monocultures of wheat and wild oat. Oecologia 82:560-566.

Beyschlag, W., R.J. Ryel & M.M. Caldwell. 1995. Photosynthesis of vascular plants: assessing canopy photosynthesis by means of simulation models. *In* E.D. Schulze & M.M. Caldwell (eds.) Ecophysiology of photosynthesis, 409-430. Springer-Verlag, Berlin Heidelberg New York.

Brain, P. & R.D. Cousens. 1990. The effect of weed distribution on prediction of yield loss. Journal of Applied Ecology 27:735-742.

Caradus, J.R., A.D. Mackay, J. Dunlop & J. van den Bosch. 1995. Relationships between shoot and root characteristics of white clover cultivars differing in response to phosphorus. Journal of Plant Nutrition 18:2707-2722.

Charles-Edwards, D.A. 1981. The mathematics of photosynthesis and productivity. Academic Press, London.

Charles-Edwards, D.A. & M.R. Thorpe. 1976. Interception of diffuse and direct-beam radiation by a hedgerow apple orchard. Annals of Botany 40:603-613.

Chu, C., P.M. Ludford, J.L. Ozbun & R.D. Sweet. 1978. Effects of temperature and competition on the establishment and growth of redroot pigweed and common lambsquarters. Crop Science 18:308-310.

Cousens, R.D. 1985. An empirical model relating crop yield to weed and crop density and a statistical comparison to other models. Journal of Agricultural Science 105:513-521.

Cousens, R.D., P. Brain, J.T. O'Donovan & A. O'Sullivan. 1987. The use of biologically realistic equations to describe the effects of weed density and relative time of emergence on crop yield. Weed Science 35:720-725.

de Castro, F. & N. Fetcher. 1998. Three dimensional model of the interception of light by a canopy. Agricultural and Forest Meteorology 90:215-233.

de Wit, C.T. 1965. Photosynthesis of leaf canopies. Pudoc, Wageningen, 57 p.

de Wit, C.T. & F.W.T. Penning de Vries. 1985. Predictive models in agricultural production. Philosophical Transactions of the Royal Society B 310:309-315.

Debaeke, P., J.P. Caussanel, J.R. Kiniry, B. Kafiz & G. Mondragon. 1997. Modelling crop:weed interactions in wheat with ALMANAC. Weed Research 37:325-341.

Dennett, M.D., J. Elston & J.R. Milford. 1979. The effect of temperature on the growth of individual leaves of *Vicia faba* L. in the field. Annals of Botany 43:197-208.

Downs, R.J., S.B. Hendricks & H.A. Borthwick. 1957. Photoreversible control of elongation of Pinto beans and other plants under normal conditions of growth. Botanical Gazette 118:199-208.

Duncan, W.G., R.S. Loomis, W.A. Williams & R. Hanau. 1967. A model for simulating photosynthesis in plant communities. Hilgardia 38:181-205.

Evans, J.R. & G.D. Farquhar. 1991. Modeling canopy photosynthesis from the biochemistry of the C3 Chloroplast. *In* K.J. Boote & R.S. Loomis (eds.) Modeling crop photosynthesis - from biochemistry to canopy, 1-15. CSSA Special Publication Number 19, Crop Science Society of America, Inc., American Society of Agronomy, Inc., Madison, Wisconsin

Evans, L.T. 1990. Assimilation, allocation, explanation, extrapolation. *In* R. Rabbinge, J. Goudriaan, H. van Keulen, F.W.T. Penning de Vries & H.H. van Laar (eds.) Theoretical production ecology: reflections and prospects. 34th ed, 77-87. Pudoc, Wageningen.

Farrar, J.F. 1988. Temperature and the partitioning and translocation of carbon. *In* F.P. Long & F.I. Woodward (eds.) Plants and Temperature, 203-235. Company of Biologists Ltd., Cambridge

Fiveland, T.J. 1974. The competition between swedes or carrots and annual weeds. Meldinger fra Norges Landbrukshogskole 53:1-15.

Friesen, G.H. 1979. Weed interference in transplanted tomatoes (*Lycopersicon esculentum*). Weed Science 27:11-13.

Gallant, A.R. 1987. Nonlinear statistical models. XII ed. John Wiley & Sons, New York, 610 p.

Gedroc, J.J., K.D.M. McConnaughay & J.S. Coleman. 1996. Plasticity in root/shoot partitioning: optimal, ontogenetic, or both? Functional Ecology 10:44-50.

Gijzen, H. & J. Goudriaan. 1989. A flexible and explanatory model of light distribution and photosynthesis in row crops. Agricultural and Forest Meteorology 48:1-20.

Gimenez, C., D.J. Connor & F. Rueda. 1994. Canopy development, photosynthesis and radiation-use efficiency in sunflower in response to nitrogen. Field Crops Research 38: 15-27.

Goel, N.S. 1988. Models of vegetation canopy reflectance and their use in the estimation of biophysical parameters from reflectance data. Remote Sensing Reviews 4:1-213.

Goudriaan, J. 1977. Crop micrometeorology: a simulation study. Pudoc, Wageningen, 249 p.

Goudriaan, J. 1986. A simple and fast numerical method for the computation of daily totals of crop photosynthesis. Agricultural and Forest Meteorology 38:249-254.

Goudriaan, J. 1988. The bare bones of leaf-angle distribution in radiation models for canopy photosynthesis and energy exchange. Agricultural and Forest Meteorology 43:155-169.

Goudriaan, J. & H.H. van Laar. 1994. Modelling potential crop growth processes. Kluwer Academic Publishers, Dordrecht / Boston / London, 238 p.

Grace, J.C., P.G. Jarvis & J.M. Norman. 1987. Modelling the interception of solar radiant energy in intensively managed stands. New Zealand Journal of Forestry Science 17: 193-209.

Graf, B., A.P. Gutierrez, O. Rakotobe, P. Zahner & V. Delucchi. 1990. A simulation model for the dynamics of rice growth and development: Part II - The competition with weeds for nitrogen and light. Agricultural Systems 32:367-392.

Hall, A.J., D.J. Connor & V.O. Sadras. 1995. Radiation-use efficiency of sunflower crops - effects of specific leaf nitrogen and ontogeny. Field Crops Research 41:65-77.

Hammer, G.L. & G.C. Wright. 1994. A theoretical analysis of nitrogen and radiation effects on radiation use efficiency in peanut. Australian Journal of Agricultural Research 45: 575-589.

Harley, P.C. & J.D. Tenhunen. 1991. Modeling the photosynthetic response of C3 leaves to environmental factors. *In* K.J. Boote & R.S. Loomis (eds.) Modeling crop photosynthesis - from biochemistry to canopy, 17-40. CSSA Special Publication Number 19, Crop Science Society of America, Inc., American Society of Agronomy, Inc., Madison, Wisconsin

Haxeltine, A. & I.C. Prentice. 1996. A general model for the light-use efficiency of primary production. Functional Ecology 10:551-561.

Hendricks, S.B., V.K. Toole & H.A. Borthwick. 1959. Photocontrol of plant development by the simultaneous excitation of two interconvertible pigments. III. Control of seed germination and axis elongation. Botanical Gazette 121:1-8.

Hewson, R.T. & H.A. Roberts. 1971. The effect of removal at different times on the yield of bulb onions. Journal of Horticultural Science 46:471-483.

Hewson, R.T. & H.A. Roberts. 1973. Effects of weed competition for different periods on the growth and yield of red beet. Journal of Horticultural Science 48:281-292.

Hibberd, J.M., W.P. Quick, M.C. Press & J.D. Scholes. 1996a. The influence of the parasitic angiosperm *Striga gesnerioides* on the growth and photosynthesis of its host, *Vigna unguiculata*. Journal of Experimental Botany 47:507-512.

Hibberd, J.M., R. Whitbread & J.F. Farrar. 1996b. Effect of 700 μmol mol^{-1} CO_2 and infection with powdery mildew on the growth and carbon partitioning of barley. New Phytologist 134:309-315.

Holmes, M.G. & H. Smith. 1977. The function of phytochrome in the natural environment. II. The influence of vegetation canopies on the spectral energy distribution of natural daylight. Photochemistry and Photobiology 25:539-545.

Hughes, J.E. & E. Wagner. 1987. Photomorphogenesis in *Chenopodium album*. Effects of supplementary far-red light on the kinetics of stem extension. Planta 172:131-138.

Jackson, J.E. & J.W. Palmer. 1972. Interception of light by model hedgerow orchards in relation to latitude, time of year and hedgerow configuration and orientation. Journal of Applied Ecology 9:341-357.

Jackson, J.E. & J.W. Palmer. 1979. A simple model of light transmission and interception by discontinuous canopies. Annals of Botany 44:381-383.

Jefferies, R.A. 1989. Water-stress and leaf growth in field-grown crops of potato (*Solanum tuberosum* L.). Journal of Experimental Botany 40:1375-1381.

Joenje, W. & M.J. Kropff. 1987. Relative time of emergence, leaf area development and plant height as major factors in crop-weed competition. British Crop Protection Conference 3, 971-978.

Jordan, N., D.A. Mortensen, D.M. Prenzlow & K.C. Cox. 1995. Simulation analysis of crop rotation effects on weed seedbanks. American Journal of Botany 82:390-398.

Kage, H. & H. Stützel. 1999. A simple empirical model for predicting development and dry matter partitioning in cauliflower (*Brassica oleracea* L. *botrytis*). Scientia Horticulturae 80:19-38.

Kasim, K. & M.D. Dennett. 1986a. Effects of shading and plant density on leaf growth of *Vicia faba*. Annals of Applied Biology 109:627-638.

Kasim, K. & M.D. Dennett. 1986b. Radiation absorption and growth of *Vicia faba* under shade at two densities. Annals of Applied Biology 109:639-650.

Kimes, D.S. 1991. Radiative transfer in homogeneous and heterogeneous vegetation canopies. *In* R.B. Myneni & J. Ross (eds.) Photo-vegetation interactions. Application in optical remote sensing and plant ecology, 339-388. Springer-Verlag, Berlin.

Kiniry, J.R., R. Blanchet, J.R. Williams, V. Texier, C.A. Jones & M. Cabelguenne. 1992a. Sunflower simulation with the EPIC and ALMANAC models. Field Crops Research:403-423.

Kiniry, J.R., J.R. Williams, P.W. Gassman & P. Debaeke. 1992b. A general, process-oriented model for two competing plant species. Transactions of the ASAE 35:801-810.

Kropff, M.J. 1986. Simulation of crop weed competition. Weed control in vegetable production: proceedings of a meeting of the EC Experts' Group, 73-83.

Kropff, M.J. 1988. Modelling the effects of weeds on crop production. Weed Research 28:465-471.

Kropff, M.J. 1993. Mechanisms of competition for light. *In* M.J. Kropff & H.H. van Laar (eds.) Modelling crop-weed interactions, 33-61. CAB International

Kropff, M.J. & L.A.P. Lotz. 1992. Optimization of weed management systems: the role of ecological models of interplant competition. Weed Technology 6:462-470.

Kropff, M.J., L.A.P. Lotz & S.E. Weaver. 1993. Practical applications. *In* M.J. Kropff & H.H. van Laar (eds.) Modelling crop-weed interactions, 83-104. CAB International

Kropff, M.J. & C.J.T. Spitters. 1991. A simple model of crop loss by weed competition from early observations of relative leaf area of the weeds. Weed Research 31:97-105.

Kropff, M.J. & C.J.T. Spitters. 1992a. An eco-physiological model for interspecific competition, applied to the influence of *Chenopodium album* L. on sugar beet. I. Model description and parameterization. Weed Research 32:437-450.

Kropff, M.J. & C.J.T. Spitters. 1992b. An eco-physiological model for interspecific competition, applied to the influence of *Chenopodium album* L. on sugar beet. II. Model evaluation. Weed Research 32:451-463.

Kropff, M.J. & H.H. van Laar. 1993a. Eco-physiological characterization of the species. *In* M.J. Kropff & H.H. van Laar (eds.) Modelling crop-weed interactions, 83-104. CAB International

Kropff, M.J. & H.H. van Laar. 1993b. Modelling crop-weed interactions, CAB International, 274 p.

Lawson, H.M. 1972. Weed competition in transplanted spring cabbage. Weed Research 12:254-267.

Lotz, L.A.P., M.J. Kropff, B. Bos & J. Wallinga. 1992. Prediction of yield loss based on relative leaf cover of weeds. Proceedings 1st International Weed Control Congress 2, 290-296.

Mann, J.E., G.L. Curry, D.W. DeMichele & D.N. Baker. 1980. Light penetration in a row-crop with random plant spacing. Agronomy Journal 72:131-142.

Manrique, L.A., J.R. Kiniry, T. Hodges & D.S. Axness. 1991. Dry matter production and radiation interception of potato. Crop Science 31:1044-1049.

Marcelis, L.F.M. 1993. Simulation of biomass allocation in greenhouse crops - a review. Acta Horticulturae 328:49-67.

Marquart, D.W. 1963. An algorithm for least squares estimation of non-linear parameters. Journal of the Society for Industrial and Applied Mathematics 11:431-441.

McConnaughay, K.D.M. & F.A. Bazzaz. 1992a. The occupation and fragmentation of space: consequences of neighbouring roots. Functional Ecology 6:704-710.

McConnaughay, K.D.M. & F.A. Bazzaz. 1992b. The occupation and fragmentation of space: consequences of neighbouring shoots. Functional Ecology 6:711-718.

Meijer, G. 1958. Influence of light on the elongation of gherkin seedlings. Acta Botanica Neerlandica 7:614-620.

Milford, G.F.J., T.O. Pocock & J. Riley. 1985a. An analysis of leaf growth in sugar beet. I. Leaf appearance and expansion in relation to temperature under controlled conditions. Annals of Applied Biology 106:163-172.

Milford, G.F.J., T.O. Pocock & J. Riley. 1985b. An analysis of leaf growth in sugar beet. II. Leaf appearance in field crops. Annals of Applied Biology 106:173-185.

Monsi, M. & T. Saeki. 1953. Über den Lichtfaktor in den Pflanzengesellschaften und seine Bedeutung für die Stoffproduktion. Japanese Journal of Botany 14:22-52.

Monteith, J.L. 1965. Evaporation and environment. Proceedings Symposium Society of Experimental Biology 19, 205-234.

Monteith, J.L. 1977. Climate and the efficiency of crop production in Britain. Philosophical Transactions of the Royal Society B 281:277-294.

Monteith, J.L. 1981. Does light limit crop production? *In* C. Johnson (ed.) Physiological processes limiting plant productivity, 23-38. Pitman, London.

Monteith, J.L. & M.H. Unsworth. 1990. Environmental physics. 2nd ed. Edward Arnold, 241 p.

Morgan, D.C., T. O'Brian & H. Smith. 1980. Rapid photomodulation of stem extension in light-grown *Sinapis alba* L. Planta 150:95-101.

Morgan, D.C. & H. Smith. 1976. Linear relationship between phytochrome equilibrium and growth in plants under simulated natural radiation. Nature 262:210-212.

Morgan, D.C. & H. Smith. 1978. The relationship between phytochrome equilibrium and development in light-grown *Chenopodium album* L. Planta 142:187-193.

Morgan, D.C. & H. Smith. 1981. Control of development in *Chenopodium album* L. by shadelight: the effect of light quantity (total fluence rate) and light quality (red:far-red ratio). New Phytologist 88:239-248.

Morrison, M.J., D.W. Stewart & P.B.E. McVetty. 1992. Maximum area, expansion rate and duration of summer rape leaves. Canadian Journal of Plant Science 72:117-126.

Murata, Y. 1981. Dependence of potential productivity and efficiency for solar energy utilization on leaf photosynthetic capacity in crop species. Japanese Journal of Crop Science 50:223-232.

Myneni, R.B., A. Marshak, Y. Knyazikhin & G. Asrar. 1991. Discrete ordinate method for photon transport in leaf canopies. *In* R.B. Myneni & J. Ross (eds.) Photo-vegetation interactions. Application in optical remote sensing and plant ecology, 339-388. Springer-Verlag, Berlin.

Nieto, J.H., M.A. Brondo & J.T. Gonzales. 1968. Critical periods of the crop growth cycle for competition from weeds. Pest articles and news summaries. Section C 14:159-166.

Norman, J.M. 1979. Modeling the complete crop canopy. *In* B.J. Barfield & J.F. Gerber (eds.) Modification of the aerial environment of crops, ASAE Monograph 2, 249-277

Norman, J.M. & T.J. Arkebauer. 1991. Predicting canopy photosynthesis and light-use efficiency from leaf characteristics. *In* K.J. Boote & R.S. Loomis (eds.) Modeling crop photosynthesis - from biochemistry to canopy, 75-94. CSSA Special Publication Number 19, Crop Science Society of America, Inc., American Society of Agronomy, Inc., Madison, Wisconsin

Norman, J.M. & J.M. Welles. 1983. Radiative transfer in an array of canopies. Agronomy Journal 75:481-488.

Pearcy, R.W., N. Tumosa & K. Williams. 1981. Relationships between growth, photosynthesis and competitive interactions for a C_3 and a C_4 plant. Oecologia 48: 371-376.

Pereira, A.R. & R.H. Shaw. 1980. A numerical experiment on the mean wind structure inside canopies of vegetation. Agricultural and Forest Meteorology 22:308-318.

Persall, W.H. 1927. Growth studies. VI. On the relative sizes of growing plant organs. Annals of Botany 41:549-556.

Qasem, J.R. 1992. Pigweed (*Amaranthus ssp.*) interference in transplanted tomato (*Lycopersicon esculentum*). Journal of Horticultural Science 67:421-427.

Rimmington, G.M. 1984. A model of the effect of interspecies competition for light on dry-matter production. Australian Journal of Plant Physiology 11:277-286.

Roberts, H.A. 1976. Weed competition in vegetable crops. Annals of Applied Biology 83:321-324.

Ryel, R.J., P.W. Barnes, W. Beyschlag, M.M. Caldwell & S.D. Flint. 1990. Plant competition for light analyzed with a multispecies canopy model. I. Model development and influence of enhanced UV-B conditions on photosynthesis in mixed wheat and wild oat canopies. Oecologia 82:304-310.

Ryel, R.J., W. Beyschlag & M.M. Caldwell. 1993. Foliage orientation and carbon gain in two tussock grasses as assessed with a net canopy gas exchange model. Functional Ecology 7:115-124.

SAS/STAT. 1990. User's Guide, Version 6.

Schweizer, E.E., D.W. Lybecker, L.J. Wiles & P. Westra. 1993. Bioeconomic weed management models in crop production. *In* D.R. Buxton, R. Schibles, R.A. Forsberg, B.L. Blad, K.H. Asay, G.M. Paulsen & R.F. Wilson (eds.) International Crop Science I, 103-107. Crop Science Society of America, Madison, Wisconsin.

Sinclair, T.R. 1991. Canopy carbon assimilation and crop radiation-use efficiency dependence on leaf nitrogen content. *In* K.J. Boote & R.S. Loomis (eds.) Modeling crop photosynthesis - from biochemistry to canopy, 95-107. CSSA Special Publication Number 19, Crop Science Society of America, Inc., American Society of Agronomy, Inc., Madison, Wisconsin

Sinclair, T.R. & T. Horie. 1989. Leaf nitrogen, photosynthesis, and crop radiation use efficiency: a review. Crop Science 29:90-98.

Sinclair, T.R. & T. Shiraiwa. 1993. Soybean radiation-use efficiency as influenced by nonuniform specific leaf nitrogen distribution and diffuse radiation. Crop Science 33: 808-812.

Sinclair, T.R., T. Shiraiwa & G.L. Hammer. 1992. Variation in crop radiation-use efficiency with increased diffuse radiation. Crop Science 32:1281-1284.

Smith, H. 1982. Light quality, photoperception, and plant strategy. Annual Review of Plant Physiology 33:481-518.

Smith, H. 1986. The perception of light quality. *In* R.E. Kendrick & G.H.M. Kronenberg (eds.) Photomorphogenesis in Plants, 187-217. Nijhoff, Dordrecht.

Smith, H., J.J. Casal & G.M. Jackson. 1990. Reflection signals and the perception by phytochrome of the proximity of neighbouring vegetation. Plant, Cell and Environment 13:73-78.

Smith, H. & M.G. Holmes. 1977. The function of phytochrome in the natural environment. III. Measurement and calculation of phytochrome photoequilibria. Photochemistry and Photobiology 25:547-550.

Smith, H. & G.C. Whitelam. 1997. The shade avoidance syndrome: multiple responses mediated by multiple phytochromes. Plant, Cell and Environment 20:840-844.

Spitters, C.J.T. 1984. A simple simulation model for crop-weed competition. Proceedings 7th International Symposium on Weed Biology, Ecology and Systematics, 355-366.

Spitters, C.J.T. 1989. Weeds: population dynamics, germination and competition. *In* R. Rabbinge, S.A. Ward & H.H. van Laar (eds.) Simulation and system management in crop protection. 32nd ed, 182-216, 332-346, 379-392. Pudoc, Wageningen.

Spitters, C.J.T. 1990. On descriptive and mechanistic models for inter-plant competition, with particular reference to crop-weed interaction. *In* R. Rabbinge, J. Goudriaan, H. van Keulen, F.W.T. Penning de Vries & H.H. van Laar (eds.) Theoretical production ecology: reflections and prospects. 34th ed, 217-236. Pudoc, Wageningen.

Spitters, C.J.T. & R. Aerts. 1983. Simulation of competition for light and water in crop-weed associations. Aspects of Applied Biology 4:467-483.

Spitters, C.J.T., H.A.J.M. Toussaint & J. Goudriaan. 1986. Separating the diffuse and direct component of global radiation and its implications for modeling canopy photosynthesis. Part I. Components of incoming radiation. Agricultural and Forest Meteorology 38: 217-229.

Spitters, C.J.T., H. van Keulen & D.W.G. van Kraalingen. 1989. A simple and universal crop growth simulator: SUCROS87. *In* R. Rabbinge, S.A. Ward & H.H. van Laar (eds.) Simulation and system management in crop protection. 32nd ed, 147-181. Pudoc, Wageningen.

Squire, G.R. 1989. Response to temperature in a stand of pearl millet. 9. Expansion processes. Journal of Experimental Botany 40:1383-1389.

Stewart, D.W. & L.M. Dwyer. 1994. Appearance time, expansion rate and expansion duration for leaves in field-grown maize (*Zea mays* L.). Canadian Journal of Plant Science 74: 31-36.

Stöckle, C.O. & J.R. Kiniry. 1990. Variability in crop radiation-use efficiency associated with vapor pressure deficit. Field Crops Research 25:171-181.

Stoller, E.W. & A. Myers. 1989. Response of soybeans (*Glycine max*) and four broadleaf weeds to reduced irradiance. Weed Science 37:570-574.

Stützel, H. 1995a. A simple model for simulation of growth and development in faba beans (*Vicia faba* L.) 1. Model description. European Journal of Agronomy 4:175-185.

Stützel, H. 1995b. A simple model for simulation of growth and development in faba beans (*Vicia faba* L.) 2. Model evaluation and application for the assessment of sowing date effects. European Journal of Agronomy 4:187-195.

Stützel, H. & W. Aufhammer. 1991a. Dry matter partitioning in a determinate and indeterminate cultivar of *Vicia faba* L. under contrasting plant distributions and densities. Annals of Botany 67:487-495.

Stützel, H. & W. Aufhammer. 1991b. Light interception and utilization of determinate and indeterminate cultivars of *Vicia faba* L. under contrasting plant distributions and population densities. Journal of Agricultural Science 116:395-407.

Stützel, H., D.A. Charles-Edwards & D.F. Beech. 1988. A model of partitioning of new above-ground dry matter. Annals of Botany 61:481-487.

Szeicz, G. 1974. Solar radiation for plant growth. Journal of Applied Ecology 11:617-636.

Tei, F., A. Scaife & D.P. Aikman. 1996. Growth of lettuce, onion, and red beet. 1. Growth analysis light interception and radiation use efficiency. Annals of Botany 78:633-643.

Tesch, S.D., E.J. Korpela & S.D. Hobbs. 1992. Effects of sclerophyllous shrub competition on root and shoot development and biomass partitioning of Douglas-fir seedlings. Canadian Journal of Forest Research 23:1415-1426.

Thornley, J.H.M. 1976. Mathematical models in plant physiology. Academic Press, London, 318 p.

Thornley, J.H.M., D.W. Hand & J. Warren Wilson. 1992. Modelling light absorption and canopy net photosynthesis of glasshouse row crops and application to cucumber. Journal of Experimental Botany 43:383-391.

Thornley, J.H.M. & I.R. Johnson. 1990. Plant and crop modelling. Oxford University Press, New York.

Troughton, A. 1956. Studies on the growth of young grass plants with special reference to the relationship between root and shoot systems. Journal of the British Grassland Society 6: 56-65.

van Keulen, H. 1975. Simulation of water use and herbage growth in arid regions. Simulation Monographs, Pudoc, Wageningen, 176 pp.

van Keulen, H., F.W.T. Penning de Vries & E.M. Drees. 1982. A summary model for crop growth. *In* F.W.T. Penning de Vries & H.H. van Laar (eds.) Simulation of plant growth and crop production, 87-97. Pudoc, Wageningen.

van Oorschot, J.L.P. & P.H. van Leeuwen. 1984. Comparison of the photosynthetic capacity between intact leaves of triazine-resistant and -susceptible biotypes of six weed species. Zeitschrift für Naturforschung 39c:440-442.

Walker, A. 1997. ModelMaker. Version 3.0.3. Cherwell Scientific, Oxford, UK.

Wang, Y.P. & P.G. Jarvis. 1990. Description and validation of an array model - MAESTRO. Agricultural and Forest Meteorology 51:257-280.

Weaver, S.E. 1984. Critical period of weed competition in three vegetable crops in relation to management practices. Weed Research 24:317-325.

Weaver, S.E. & C.S. Tan. 1983. Critical period of weed interference in transplanted tomatoes (*Lycopersicon esculentum*): growth analysis. Weed Science 31:476-481.

Welles, J.M. & J.M. Norman. 1991. Instrument for indirect measurement of canopy architecture. Agronomy Journal 83:818-825.

Whitfield, D.M. 1986. A simple model of light penetration into row crops. Agricultural and Forest Meteorology 36:297-315.

Wiebe, H.J. 1979. Short term forecasting of the market supply of vegetables, especially cauliflower. Acta Horticulturae 97:399-409.

Wiles, L.J., R.P. King, E.E. Schweizer, D.W. Lybecker & S.M. Swinton. 1996. GWM: General weed management model. Agricultural Systems 50:355-376.

Wiles, L.J. & G.G. Wilkerson. 1991. Modelling competition for light between soybean and broadleaf weeds. Agricultural Systems 35:37-51.

Wilkerson, G.G., J.W. Jones, K.J. Boote, K.T. Ingram & J.W. Mishoe. 1983. Modeling soybean growth for crop management. Transactions of the ASAE 26:63-73.

Wilkerson, G.G., J.W. Jones, H.D. Coble & J.L. Gunsolus. 1990. SOYWEED: a simulation model of soybean and common cocklebur growth and competition. Agronomy Journal 82:1003-1010.

Williams, J.R., C.A. Jones, J.R. Kiniry & D.A. Spanel. 1989. The EPIC crop growth model. Transactions of the ASAE 32:497-511.

Williams, M. 1996. A three-dimensional model of forest development and competition. Ecological Modelling 89:73-98.

Wilson, J.B. 1988. A review of evidence on the control of shoot:root ratio, in relation to models. Annals of Botany 61:433-449.

Wright, A.J. 1981. The analysis of yield-density relationships in binary mixtures using inverse polynomials. Journal of Agricultural Science 96:561-567.

Curriculum vitae

University studies:	1987-1989	Agriculture, University of Bonn
	1990-1993	Agronomy, University of Hohenheim Title of student thesis: 'Modelling the interspecific competition for light in faba bean' (in German)
Doctorate:	1993-1998	Research assistant, Institute for Vegetable and Fruit Crops, University of Hanover

Acknowledgements

First of all, I wish to thank Prof. Dr. H. Stützel for making this work possible. I have learned a lot from his critical advice in both experimental and theoretical studies and his guidance into scientific work.

I am especially grateful to Mr. N. Hacke for his outstanding commitment to the field experiments and to Mr. C. Alt and Dr. H. Kage for trying to teach me and my PC some mathematics.

To name only few does not mean to depreciate the contribution of all members of the Institute for Vegetable and Fruit Crops to this work. Since I always found a helping hand, I am indebted to them all.

Last but not least, very special thanks go to my wife for her immense patience.